Analysis of pion nucleon scattering at high energies

Rajkumar Roychoudhury

ANALYSIS OF PION NUCLEON SCATTERING

AT

HIGH ENERGIES

ANALYSIS OF PION NUCLEON SCATTERING

AT

HIGH ENERGIES

Thesis submitted to the

University of Durham

by

Rajkumar Roychoudhury, M.Sc. (Calcutta)

For the Degree of Doctor of Philosophy

Department of Physics
University of Durham

December, 1969

To

My Parents

Abstract

A phenomenological analysis of Pion Nucleon scattering data at high and intermediate energies and at all angles has been undertaken.

At high energies say above 5 GeV/c the differential cross sections are strongly peaked in the forward and backward directions and these peaks can be adequately explained by a small number of leading Regge poles in t channel (for the forward peak) and u channel (for the backward peak). In this work new Regge fits are performed to all available recent high energy data, to obtain the Regge parameters.

Below 5 GeV/c down up to 2 GeV/c the forward and backward peaks are still very conspicuous and can still be explained by the Regge poles used in the high energy fits. So it is thought to be convenient to define an amplitude $F_p(s,t,u)$ which is the difference between the total and the Regge amplitudes. A parametric form of this amplitude (viz, F_s) was taken to fit all data between 2 to 5 GeV/c simultaneously, while the parameters of the Regge Amplitudes are held fixed to their values obtained from high energy fits.

First all π^+ p scattering data were fitted to get $I = 3/2$ amplitude then π^- p and charge exchange data were fitted to obtain $I = 1/2$ amplitudes.

Two different ways of parameterising F_s (s,t,u) have been attempted. The first was based on the direct channel Regge pole model with Khuri modification, and the second was of a simpler and less sophisticated phenomenological form, the amplitudes being expressed as a power series in Cos θ (θ being scattering angle) with energy dependent coefficients, the second method was found particularly successful in the present work.

Partial Wave projections of both $T = {}^1/2$ and $T = {}^3/2$ amplitudes were made and the phase shifts were obtained for both the isospin amplitudes. Possibilities of the existence of resonances in the energy region 2 to 5 GeV are discussed.

ACKNOWLEDGEMENTS

It is a pleasure to express my thanks to my supervisor Professor B.H. Bransden for suggesting the problem and his friendly guidance throughout this work. I should also like to thank Dr. R. Perrin (at present of Loughborough University of Technology) for his continued support and help.

I am very grateful to Mrs. J. Lincoln for typing the thesis.

I should like to thank also the Government of West Bengal for the award of the state scholarship 1966, enabling me to carry out this research.

PREFACE

Part of the work reported here has been done in collaboration with Dr. R. Perrin and Professor B.H. Bransden and is published (Durham University preprint, to be published in Nuclear Physics).

No part of the work presented here has previously been submitted for a degree in this or any other University.

CONTENTS

Introduction

The elementary particle interactions are usually divided into four rather well seperated classes viz.

(i) Gravitational interaction

(ii) Electromagnetic interaction

(iii) Weak interaction

(iv) Strong interaction

the first one i.e. the Gravitational interaction is the weakest of all the four listed above and is represented by a potential inversely proportional to the distance between two interacting bodies.

However only the last three are relevant in the discussion of scatterings and decays of elementary particles and we shall describe them briefly in the following:

(a) Electromagnetic interaction: this is caused by the charges and the magnetic moments of the particles and this is the only interaction apart from the gravitational interaction for which there is a complete theory.

However it is understood that properties of nuclear interactions cannot be explained in terms of the electromagnetic forces, since the nuclear forces are known to operate only over a very short range and even between a charged

particle and a neutral one (for example the charged proton and the neutron in the nucleus.)

The measure of strength of the electromagnetic interaction is provided by the fine structure constant

$$\alpha = e^2/\hbar c = 1/137.$$

(b) Weak interaction: (the nomenclature is due to its weakness compared with the other two). Weak interaction is the one which is responsible for the decay properties of the unstable particles. (except π^0 , Σ^0 , which decay by electromagnetic interaction; $\pi^0 \sim 2\gamma$, $\Sigma^0 \sim \pi + \gamma$). Its strength is represented by a coupling constant $G \sim 10^{-49}$ erg cm^3.

(c) Strong interaction: this interaction connects all the baryons through the virtual emissions and reabsorptions of mesons according to the Yukawa process $N^* \longrightarrow N + \pi$ and is mainly responsible for nuclear forces. Its coupling constant is of the order of unity.

Strong interaction also accounts for very fast decay rates, such as the decay $N^* \longleftrightarrow N + \pi$

In 1935 Yukawa[1] developed a theory of nuclear forces. The most important experimental feature of these forces is that they have a range i.e. they decrease very rapidly when the interacting particles are at a distance greater than about 10^{-13} cm. The nuclear potential proposed by

Yukawa was in the form

$$V(r) \sim g \frac{e^{-kr}}{r}$$

where k is the reciprocal of the length which can be assumed to represent the range of nuclear forces.

Yukawa also postulated, as the quantum of nuclear forces a particle with mass about $m = \hbar/rc$ where r is the range of nuclear forces. In 1935 Anderson et al[2] discovered in cosmic ray, particles with mass about that of Yukawa particles. But it turned out that the particles were not the same as postulated by Yakawa. Because, though they had the right mass, they did not interact appreciably with nucleus; these particles came to be known as muons. Later in 1947 Lattes, Occhialini and Powell[3] found out particles in cosmic rays which were identified with Yukawa particles. These strongly interacting particles with zero spin and mass about 139.59 MeV are known as pi-mesons or simply pions. Since then numerous particles have been discovered experimentally. Many of them were first found in cosmic rays and large accelerating machines made it possible to generate these particles for detailed study and investigation.

Attempts have been made to classify these particles in various ways, making some particles more elementary than others or to derive all particles from quarks[4] which are

thought to be the building stone of all hadrons (i.e. strongly interacting particles).

Phenomenologically one may consider four families of particles in order of increasing rest mass.

1. Photon: which is a boson of spin 1

2. Leptons: containing fermions of spin $^1/_2$ lighter than proton (such as electron) they are subject to electromagnetic and weak interactions but not to strong interaction.

3. Mesons: it consists of bosons of spin 0 . These are heavier than the leptons, lighter than the proton and subject to all the three ((a) to (c)) types of interactions.

4. Baryons: this class comprised the proton, the neutron and heavier fermions. They are subject to all three types of interactions. Those which are heavier than the neutron are called hyperons.

The pions which fall in class 3 are very important in the study of nuclear and particle physics, because they are the particles which are responsible for the forces that bind proton and neutron together in a nucleus. In particular pion - nucleon interaction is of fundamental importance in the understanding of strong interactions, and has been studied extensively both theoretically and

experimentally. A large number of experimental data exist for elastic pion - nucleon scattering processes, which we also analyse phenomenologically in this work.

It would be convenient for our discussion to divide the Pion - nucleon scattering in to three energy regions (the energy in this case is the pion laboratory energy)

1) from zero to about 2 GeV/c
2) from 2 GeV/c to about 5 GeV/c
3) for energies higher than about 5 GeV/c

the reasons for choosing these energy regions will be clear from the following.

The partial wave structure of the elastic pion nucleon scattering has been studied by phase-shift analysis of the scattering data in the first energy region[4] and discloses a structure in which many of the partial waves can be represented as a conventional Breight-Wigner resonance of the type $f_\ell \sim \frac{g}{s - s_0 + i\Gamma}$ with a smoothly varying background.

In the third energy region the cross sections are slowly decreasing functions of the energy and do not show any appreciable structures. This is the region where rather sharp peaks are present in both the forward and backward angular regions. Regge exchanges in cross channels explain

these peaks rather nicely[5].

In fact only a few number of Regge trajectories are required to describe the high energy pion - nucleon scattering data.

But the energy region (2), where conventional phase shift analysis become increasingly difficult due to paucity of data and also because of the presence of high angular momentum states, will be our main point of interest.

This energy region is the so called intermediate region where the forward and the backward peaks are still conspicuous and can be explained by the same Regge poles employed in the high energy region.

In our phenomenological analysis of pion - nucleon scattering it was found to be convenient to define an amplitude $F_p(s,t,u)$ which is the difference between the exact amplitude say $F(s,t,u)$ and the Regge amplitude denoted by $F_R(s,t,u)$,

$$F_p(s,t,u) = F(s,t,u) - F_R(s,t,u)$$

the Regge parameters required to construct $F_R(s,t,u)$ were fixed by fitting the high energy pion - nucleon scattering data and $F_p(s,t,u)$ was parameterised to fit all the data in the 2nd energy region, keeping the Regge parameters fixed at their high energy values.

This procedure is consistent with the generalised interference model[6], but independent of any dynamical idea, the success of decomposition depending on whether a suitable parameterisation of F_p (s,t,u) could be found.

Two different ways of parameterising F_p(s,t,u) have been tried. One is based on the modified direct channel Regge formalism as proposed by Khuri[7] and the other is of a simple form, the amplitude F_p(s,t,u) being expressed as a power series in cos θ (θ being the scattering angle) with energy dependent coefficients. Both these procedures are described in detail in this work. The parameters for $T = {}^3/_2$ (T denoting the isospin) were first obtained by fitting all the $\pi^+ p$ data and then the parameters for $T = {}^1/_2$ amplitude were fixed by fitting $\pi^- p$ and charge exchange data.

Partial wave amplitudes for both the isospin amplitudes were obtained by the usual method and they were studied for possible resonance structures.

CHAPTER I

KINEMATICS

KINEMATICS

Introduction:

In this chapter we shall study the Kinematics of pion - nucleon scattering, including the analyticity of the pion - nucleon amplitude. We shall also present the relevant formulae.

1. Kinematics and Lorentz invariant description of the

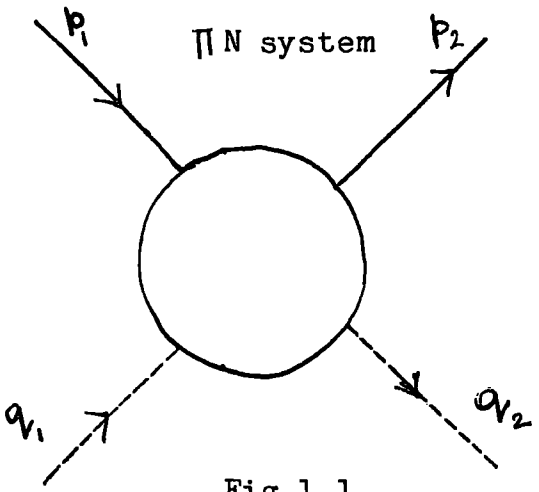

Fig.1.1

Let p_1, $p_2(q_1, q_2)$ be the momenta of the incoming and outgoing nucleon (pion) respectively.

We use the convention $p_i^2 = -m^2$, $q_i^2 = -\mu_i^2$, $i = 1,2$ (where m, μ are the masses of the nucleon and the pion respectively) throughout this work unless otherwise stated.

We neglect the mass differences among the three charge states of pion and between the two states of nucleon.

The following table gives the masses and other properties of pion and nucleon

(* natural units are used $\hbar = c = 1$)

TABLE 1

	Symbol	Mass (MeV)	Spin	Parity	Isospin	Strangeness	Baryon No.
Mesons	π^+	139.6	0	-1	(1,1)	0	0
	π^0				(1,0)	0	0
	π^-				(1,-1)	0	0
Nucleons	p	938.21	$1/2$		$(1/2, 1/2)$	0	1
	n		$1/2$		$(1/2, -1/2)$	0	1

By the law of conservation of total momentum we get (see Fig.1.1)

$$p_1 + q_1 = p_2 + q_2 \qquad (1.1)$$

So there will be only three independent vectors which determine the kinematics of the process. We choose the combination

$$\begin{aligned} P &= {}^1/_2 (p_1 + p_2) \quad Q = {}^1/_2 (q_1 + q_2) \\ K &= {}^1/_2 (p_2 - p_1) \quad = -{}^1/_2 (q_1 - q_2) \end{aligned} \qquad (1.2)$$

With these vectors one can form the invariants

(with the help of the results $p_i^2 = -m^2$, $q_i^2 = -\mu_i^2$)

$$K^2 = -\frac{1}{4}(p_2 - p_1)^2 = -\frac{1}{4}t, \quad P^2 = -m^2 - K^2, \quad Q^2 = -\mu^2 - K^2 \tag{1.3}$$

Also we get $P.Q. = -\nu = -\frac{s-u}{4}$

$P.K = Q.K = 0$

where s,t,u are the usual Mandelstam variables defined in the following way

$$\begin{aligned} s &= -(p_1 + q_1)^2 \\ u &= -(p_2 - q_1)^2 \\ t &= -(q_1 - q_2)^2 \end{aligned} \tag{1.4}$$

We can see from (1.3) that there are only two independent invariant quantities.

It is easy to check from (1.4) that

$$s + t + u = 2(m^2 + \mu^2) \tag{1.5}$$

In the centre of mass frame where

$$\vec{p_1} + \vec{q_1} = 0 = \vec{p_2} + \vec{q_2} \tag{1.6}$$

and hence $|\vec{p_1}| = |\vec{q_1}| = q$ say

we can write

$$s = w^2$$

$$t = 2q^2 (1 - \cos\theta)$$

$$u = \left[(w + m)^2 - \mu^2\right] \left[(w - m)^2 - \mu^2\right] / (4 w^2) \qquad (1.7)$$

where q = c.m. momentum

$w = (m^2 + q^2)^{1/2} + (\mu^2 + q^2)^{1/2}$ = total energy in the centre of mass system.

θ = scattering angle in the centre of mass system

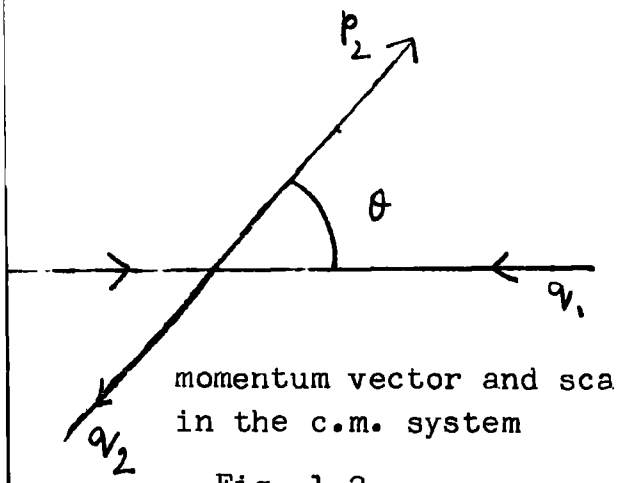

momentum vector and scattering angle in the c.m. system

Fig. 1.2

The S matrix for elastic pion nucleon scattering can be written in the form

$$S_{fi} = \delta_{fi} - i(2\pi)^4 \delta^4(p_2 + q_2 - p_1 - q_1) \times \left(\frac{m^2}{4E_1 E_2 W_1 W_2} \right)^{1/2} \bar{U}_2 T U_1 \qquad (1.8)$$

where $E_i = (\vec{p}_i^{\,2} + m^2)^{1/2}$

$$W_i = (\vec{q}_i^{\,2} + \mu^2)^{1/2} \qquad (1.9)$$

and E_1, W_1 (E_2, W_2) are the energies of the initial (final) nucleon and pion respectively. U_1 and U_2 are the Dirac spinors for the initial and final states respectively.

The amplitude T is a Lorentz scalar and we write T in terms of the invariant amplitudes A, B as follows

$$T = -A(s,u,t) + i (\gamma \cdot Q) B(s,u,t) \qquad (1.10)$$

where $Q_\mu = \frac{1}{2}(q_1 + q_2)_\mu$ and γ^μ are the Dirac matrices

A and B are invariant scalar functions.

A is independent of the nucleon spin and B is associated with nucleon spin flip through the term $(\gamma \cdot Q)$

2. Isospin analysis and crossing

The scalar invariant amplitudes A and B are still

matrices in the I space. The pion and the nucleon having isospin 1 and $^1/_2$ respectively can form states with the total isospin $I = {}^1/_2$ and $I = {}^3/_2$

So if isospin invariance is assumed π - N scattering will be completely described by four invariant functions, two for each isospin. Let the pion and nucleon isospin vectors be $\vec{t}$ and $\vec{\tau}/_2$ respectively.

The total isospin vector of a state composed of a pion and a nucleon is represented by

$$\vec{I} = \frac{1}{2}\vec{\tau} + \vec{t} \qquad (1.11)$$

where $\vec{\tau}$'s are the Pauli matrices and $\vec{t}$'s are spin one rotation matrices given by

$$t_1 = \frac{1}{\sqrt{2}}\begin{pmatrix} 0 & -1 & 0 \\ -1 & 0 & 0 \\ 0 & 1 & 0 \end{pmatrix}, \quad t_2 = \frac{1}{\sqrt{2}}\begin{pmatrix} 0 & i & 0 \\ -i & 0 & -i \\ 0 & i & 0 \end{pmatrix} \quad t_3 = \begin{pmatrix} 1 & 0 & 0 \\ 0 & 0 & 0 \\ 0 & 0 & -1 \end{pmatrix} \qquad (1.12)$$

here $i = \sqrt{-1}$

From $|\pi^+\rangle$, $|\pi^0\rangle$ and $|\pi^-\rangle$ states we form $|\pi_\alpha\rangle$ ($\alpha = 1,2,3$) states which behave like the components of a cartesian vector in the pion isospace

$$|\pi_1\rangle = \frac{1}{\sqrt{2}}\left(|\pi^+\rangle + |\pi^-\rangle\right), \quad |\pi_2\rangle = -\frac{i}{\sqrt{2}}\left(|\pi^+\rangle - |\pi^-\rangle\right)$$
$$|\pi_3\rangle = |\pi^0\rangle \qquad (1.13)$$

it may be shown from (1.12) and (1.13) that

$$\langle \pi_\alpha | t_\beta | \pi_\gamma \rangle = i \epsilon_{\alpha\beta\gamma} \qquad (1.14)$$

where $\epsilon_{\alpha\beta\gamma}$ is an antisymmetric tensor, defined as follows

$\epsilon_{\alpha\beta\gamma} = 0$ if any two of α, β, γ are equal

$= 1$ if α, β, γ are all unequal and in cyclic order

$= -1$ if α, β, γ are all unequal but not in cyclic order

Now $\vec{I}^2$ has eigen values $1/2\ (1/2 + 1)\ (= 3/4)$ and $3/2\ (3/2 + 1)\ (= 15/4)$, so from (1.11)

$$\begin{aligned} \vec{\tau}.\vec{t} &= -2 \quad \text{for } I = 1/2 \\ \vec{\tau}.\vec{t} &= +1 \quad \text{for } I = 3/2 \end{aligned} \qquad (1.15)$$

Now with the help of the isospin projection operator

$$P_{1/2} = \frac{1}{3}(1 - \vec{\tau}\cdot\vec{t}), \quad P_{3/2} = \frac{1}{3}(2 + \vec{\tau}.\vec{t}) \qquad (1.16)$$

We write the total amplitude as

$$T_{\beta\alpha} = \langle N' \pi_\beta | \left[P_{1/2}\ T^{1/2} + P_{3/2}\ T^{3/2} \right] | \pi_\alpha N \rangle \qquad (1.17)$$

where α, β denote the initial and final pion states respectively.

With the help of (1.14) it may be shown that

$$T_{\beta\alpha} = \langle N' | \left\{ \delta_{\alpha\beta} T^{+} + \frac{1}{2} [\tau_\beta, \tau_\alpha] \; T^{-} \right\} | N \rangle \qquad (1.18)$$

where

$$T^{+} = \frac{T^{1/2} + T^{3/2}}{3}$$

$$T^{-} = \frac{T^{1/2} - T^{3/2}}{3} \qquad (1.19)$$

to derive (1.18) the result $[\tau_\beta, \tau_\alpha] = i \epsilon_{\beta\alpha\gamma} \tau_\gamma$ (1.20)

has been used.

Now inverting equation (1.13) we get

$$|\pi^{+}\rangle = \frac{|\pi_1\rangle + i |\pi_2\rangle}{\sqrt{2}}$$

$$|\pi^{-}\rangle = \frac{|\pi_1\rangle - i |\pi_2\rangle}{\sqrt{2}} \qquad (1.21)$$

and from (1.14), (1.16) and (1.17) we obtain

$$T(\pi^{\pm} p \to \pi^{\pm} p) = \langle \pi^{+} p | T | \pi^{+} p \rangle = T_{+} = T^{3/2}$$

$$T(\pi^{-} p \to \pi^{-} p) = \langle \pi^{-} p | T | \pi^{-} p \rangle = T_{-} = (T^{3/2} + 2T^{1/2})/3 \qquad (1.22)$$

$$T(\pi^{-} p \to \pi^{0} n) = \langle \pi_3 | T | \pi_3 \rangle = T_{c.e.} = \frac{\sqrt{2}}{3} (T^{3/2} - T^{1/2})$$

Crossing symmetry (see Fig.1.4) can be written in terms of the matrix elements of T

$$\langle p_2, q_2 | T^{+} | p_1, q_1 \rangle = \langle p_2, -q_1 | T^{-} | p, -q_2 \rangle \qquad (1.23)$$

i.e. under the exchange $q_1 \longleftrightarrow -q_2$, we have

$s \longleftrightarrow u, \quad t \longrightarrow t.$

Also since A and B are independent amplitudes crossing symmetry applies separately to A and ($\gamma . Q$)B and under crossing ($\gamma . Q$) $\longrightarrow -($ $\gamma . Q$) (1.24)

Defining new amplitudes

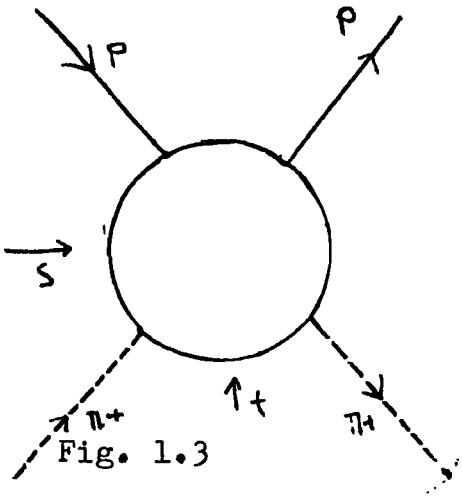

Fig. 1.3

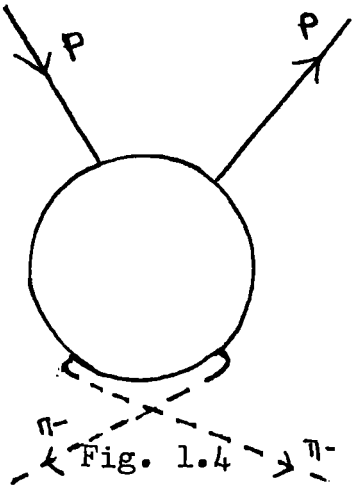

Fig. 1.4

$$A^+ = \frac{1}{2}(A_- + A_+),$$
$$A^- = \frac{1}{2}(A_- - A_+),$$
$$B^+ = \frac{1}{2}(B_- + B_+),$$
$$B^- = \frac{1}{2}(B_- - B_+) \qquad (1.25)$$

($A^{\pm}$, $B^{\pm}$ are related to $T^{\pm}_{-}$).

We can see that crossing gives [8]

$$A^{\pm}_{-}(s,u,t) = \pm A^{\pm}_{-}(u,s,t)$$
$$B^{\pm}_{-}(s,u,t) = \mp B^{\pm}_{-}(u,s,t) \qquad (1.26)$$

Also from the amplitudes A^+, B^+, the amplitudes for the eigen states of the isospin can be written in the form (see (1.19))

$$A^{1}/2 = A^{+} + 2A^{-}, \quad A^{3}/2 = A^{+} - A^{-} \qquad (1.27)$$

identical relations hold for the B amplitudes.

We see that the reaction described by Fig. 1.3 in the s channel is the elastic scattering

$$\pi^{+} + p \rightarrow \pi^{+} + p$$

For the t channel it becomes

$$\pi^{+} + \pi^{-} \rightarrow p + \bar{p}$$

and for the crossed or u channel the reaction described by Fig. (1.4) is

$$\pi^{-} + p \rightarrow \pi^{-} + p \text{ as implied by (1.23)}$$

So, the variables for the s,t and u channels exchange their roles as shown in table below.

TABLE 2

	s-ch	t-ch	u-ch
Energy variable	s	t	u
Momentum variable	t	s	t
Cross-momentum variable	u	u	s

3. Partial Wave Analysis

Equation (1.8) gives the differential cross section (in the c.m. system)

$$\frac{d\sigma}{d\Omega} = \left(\frac{m}{4\pi W}\right)^2 \sum \left| \bar{U}_2 \, T \, U_1 \right|^2 \qquad (1.28)$$

where $\sum$ denotes the sum over the final spin states and the average over the initial spin states.

We can also write:

$$\frac{d\sigma}{d\Omega} = \sum \left| \langle f \mid m \mid i \rangle \right|^2 \qquad (1.29)$$

where $|i\rangle$ and $|f\rangle$ are Pauli spinors for the initial and final nucleon spin states. The usual convention to relate M to T is

$$\langle f \mid M \mid i \rangle = -\frac{M}{4\pi W} \bar{U}_2 \, T \, U_1 \qquad (1.30)$$

if we write M in terms of the π-N helicity amplitudes[9] f_1 and f_2 then

$$M = f_1(\theta) + \frac{(\vec{\sigma}\cdot\vec{q}_1)(\vec{\sigma}\cdot\vec{q}_2)}{q^2} f_2(\theta) \qquad (1.31)$$

$\vec{\sigma}$ is the nucleon spin, $\vec{q}_1$, $\vec{q}_2$ the initial and final pion momenta respectively.

$$\text{and} \quad \frac{d\sigma}{d\Omega} = \sum_{\text{spin}} \left| \langle f \mid f_1 + \frac{(\vec{\sigma}\cdot\vec{q}_1)(\vec{\sigma}\cdot\vec{q}_2)}{q^2} f_2 \mid i \rangle \right|^2 \qquad (1.32)$$

in c.m. system

Using (1.30), (1.31) and (1.10)

f_1 and f_2 can be expressed in terms of A & B

$$f_1 = \frac{E + m}{8\pi W}\left[A + (W - m) B\right]$$

$$f_2 = \frac{E - m}{8\pi W}\left[- A + (W + m) B\right] \qquad (1.33)$$

Inverting (1.33) we get

$$A = 4\pi\left[\frac{W + m}{E + m} f_1 - \frac{(W - m)}{E - m} f_2\right]$$

$$B = 4\pi\left[\frac{1}{E + m} f_1 + \frac{1}{E - m} f_2\right] \qquad (1.34)$$

where $E = (m^2 + q^2)^{1/2}$ = Energy of the nucleon in the c.m. system.

The partial wave amplitudes $f_{l \pm}$ corresponding to total angular momentum $j = l \pm 1/2$ are expressed in terms of the phase shift $\delta_{l \pm}$ by

$$f_{l \pm} = \frac{\exp(2i\delta_{l \pm}) - 1}{2iq} \qquad (1.35)$$

where $\delta_{l \pm}$ may be complex.

The helicity amplitudes can be expressed in terms of the partial wave amplitudes by[10]

$$f_1(\theta) = \sum_{l=0}^{\infty} \left(f_{l+} P'_{l+1}(x) - f_{l-} P'_{l-1}(x)\right)$$

$$f_2(\theta) = \sum_{l=1}^{\infty} \left(f_{l-} - f_{l+}\right) P'_l(x) \qquad (1.36)$$

where $x = \cos\theta$, $P_\ell(x)$ is the Legendre polynomial and $P'_\ell(x) = \frac{d}{dx} P_\ell(x)$. Using the orthogonality relations of Legendre polynomials equation (1.36) can be inverted to get $f_{\ell\pm}$

$$f_{\ell\pm} = \frac{1}{2}\int_{-1}^{1} dx\,[f_1 P_\ell(x) + f_2 P_{\ell\pm1}(x)] \qquad (1.37)$$

3.1 MacDowell symmetry.[11]

From equation (1.33) replacing W by -W we get

$$f_1(-W) = \frac{-E+m}{-2W}\left[A + (-W-m)B\right]$$

$$= -\frac{E-m}{2W}\left[-A + (W+m)B\right]$$

(using $E(-W) = -E(W)$)

$$= -f_2(W) \qquad (1.38)$$

Now from (1.37)

$$f_{\ell\pm}(W) = \frac{1}{2}\int_{-1}^{1}(f_1 P_\ell(x) + f_2 P_{\ell\pm1}(x))\,dx$$

$$\therefore\quad f_{\ell\pm}(-W) = \frac{1}{2}\int_{-1}^{1}(f_1(-W)P_\ell(x) + f_2(-W)P_{\ell\pm1}(x))\,dx$$

$$= -\frac{1}{2}\int_{-1}^{1}[f_2(W)P_\ell(x) + f_1(W)P_{\ell\pm1}(x)]\,dx$$

(Using Equation 1.38)

Hence $f^{+}_{\ell}(W) = -\ f^{-}_{\ell+1}(-W)$ (1.39)

which is the so called MacDowell symmetry.

4. Mandelstam Representation.

The fundamental principle of the theory to work with is that A, B are analytic functions of the variables s, t, and u except for singularities associated with the three channels, that is, the boundary values of A and B describe the physical processes that can be obtained by any interchange of the legs of Fig. 1.3.

According to Mandelstam[12], the amplitudes $A^{\pm}$ and $B^{\pm}$ (referred as A^i, i = 1,2,3,4) have a representation of the form

$$A^{\pm}_{i}(s,u,t) = \frac{R^{i}_{s}}{m^2-s} + \frac{R^{i}_{u}}{m^2-u} + \frac{1}{\pi^2}\int_{(m+\mu)^2}^{\infty} ds' \int_{(m+\mu^2)}^{\infty} du' \frac{\rho^{i}_{12}(s',u')}{(s'-s)(u'-u)}$$

$$+ \frac{1}{\pi^2}\int_{(m+\mu)^2}^{\infty} ds' \int_{4\mu^2}^{\infty} dt' \frac{\rho^{i}_{13}(s',t')}{(s'-s)(t'-t)}$$

$$+ \frac{1}{\pi^2}\int_{(m+\mu)^2}^{\infty} du' \int_{4\mu^2}^{\infty} dt' \frac{\rho^{i}_{23}(u',t')}{(u'-u)(t'-t)} \qquad (1.40)$$

We can write equation (1.40) as one dimensional representation at fixed s

$$A^i(s,u,t) = \frac{R_s^i}{m^2-s} + \frac{R_u^i}{m^2-u} + \frac{1}{\pi}\int_{4\mu^2}^{\infty} dt' \frac{A_3^i(s,t')}{t'-t} + \frac{1}{\pi}\int_{(m+\mu)^2}^{\infty} du' \frac{A_2^i(s,u')}{u'-u} \tag{1.41}$$

where

$$A_3^i(s,t') = \frac{1}{\pi}\int_{(m+\mu)^2}^{\infty} ds' \frac{\rho_{13}^i(s',t')}{s'-s} - \frac{1}{\pi}\int_{-\infty}^{(m-\mu)^2-t'} ds' \frac{\rho_{23}^i(s',t')}{s'-s}$$

$$A_2^i(s,u') = \frac{1}{\pi}\int_{(m+\mu)^2}^{\infty} ds' \frac{\rho_{12}^i(s',u')}{s'-s} - \frac{1}{\pi}\int_{-\infty}^{2m^2-2\mu^2-u'} ds' \frac{\rho_{23}^i(s',u')}{s'-s} \tag{1.42}$$

The double spectral functions ρ^i_{jk} are real and do not extend up to boundaries except asymptotically. Fig. 1.5 shows the s,t,u diagram for πp process. The shaded

portions showing the physical region for the particular process indicated there. These are the non zero regions of the double spectral functions.

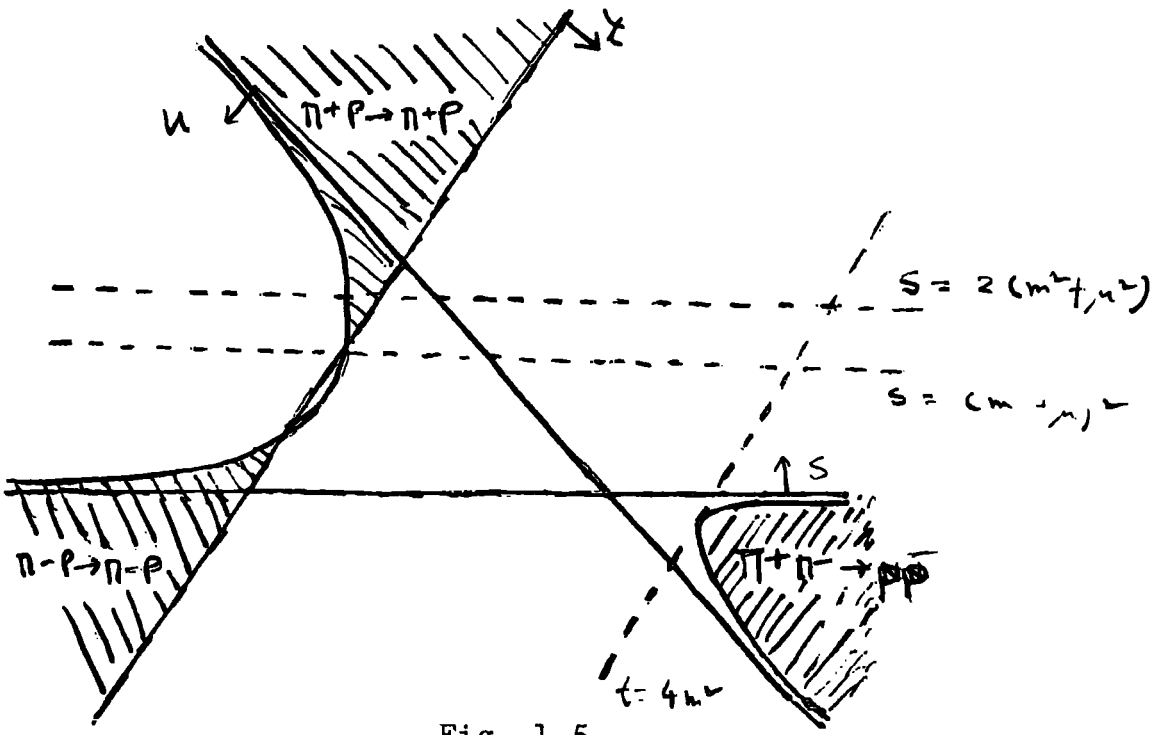

Fig. 1.5

Now we can deduce the analytic proporties of the partial wave amplitude.

defining

$$A^{i}_{\ell}(s) = \int_{-1}^{1} P_{\ell}(x)\, A^{i}(s, t(s,x), u(s,x))\, dx \qquad (1.43)$$

We get, using (1.41)

$$A_\ell^i(s) = R_s^i \int_{-1}^{1} \frac{P_\ell(x)\,dx}{m^2 - s} + R_u^i \int_{-1}^{1} \frac{P_\ell(x)\,dx}{m^2 - [2m^2 + 2\mu^2 - s + 2q^2(1-x)]}$$

$$+ \frac{1}{\pi} \int_{4\mu^2}^{\infty} dt'\, A_3^i(s,t') \int_{-1}^{1} \frac{P_\ell(x)\,dx}{t' + 2q^2(1-x)}$$

$$+ \frac{1}{\pi} \int_{(m+\mu)^2}^{\infty} du'\, A_2^i(s,u') \int_{-1}^{1} \frac{P_\ell(x)\,dx}{u' - [2m^2 + 2\mu^2 - s + 2q^2(1-x)]} \qquad (1.44)$$

where in the 2nd term and the 4th term of the R.H.S. of (1.44) we have replaced u by the expression

$$u = 2m^2 + 2\mu^2 - s + 2q^2(1 - x)$$

here $x = \cos\theta$ and q = c.m. momentum as defined in section 1.

5. Singularities of $A_\ell^{\,i}(s)$

(1) The denominators on the R.H.S. of equation (1.44) can vanish and thus give rise to branch cuts.

(2) $A_3^{\,i}(s,t')$ and $A_2^{\,i}(s,u')$ have singularities of their own.

Both $A_2^{\,i}$ and $A_3^{\,i}$ have a branch cut from

$s = (m+\mu)^2$ to ∞ i.e. in $W(=\sqrt{s}$)plane it is

$$-\infty \leq W \leq -(m+\mu)$$

and $$(m+\mu) \leq W \leq \infty$$

this branch cut corresponds to physical region for π - N scattering in s channel and would be called "the physical cut".

The 2nd integral for each term appears to give a branch cut for negative s.

That actually this is not so can be shown in the following way.

The second terms of A_2 and A_3 contribute to A_l^i as

$$-\frac{1}{\pi^2}\int_{4\mu^2}^{\infty} dt' \int_{-\infty}^{(m-\mu)^2-t'} \frac{ds' f_{23}(s',t')}{s'-s} \int_{-1}^{1} \frac{P_l(x)\,dx}{t'+2q^2(1-x)}$$

$$-\frac{1}{\pi^2}\int_{(m+\mu)^2}^{\infty} du' \int_{-\infty}^{2m^2-2\mu^2-u'} \frac{ds' f_{23}(s',t')}{s'-s} \int_{-1}^{1} \frac{P_l(x)\,dx}{u'-[2m^2+2\mu^2-s+2q^2(1-x)]}$$

if the orders of the integration are interchanged in the s', t', u' integrations and the variable of the integration there after changed to

$$t' = 2m^2 + 2\mu^2 - s' - u' \text{ in the 2nd integral}$$

(where by)

$$u' = (m+\mu)^2 \longrightarrow 2m^2 - 2\mu^2 - u' \rightleftharpoons (m-\mu)^2 - 4\mu^2$$

$$t' = 4\mu^2 \longrightarrow (m-\mu)^2 - t' \rightleftharpoons (m-\mu)^2 - 4\mu^2$$

we get

the contribution of A_2 and A_3 to A_ℓ^i as

$$-\frac{1}{\pi^2}\int_{-\infty}^{(m-\mu)^2-4\mu^2} ds' \int_{4\mu^2}^{(m-\mu)^2-s'} dt' \frac{\rho_{23}(s',t')}{s'-s} \cdot \int_{-1}^{1} P_\ell(x)\,dx \times$$

$$\times \left[\frac{1}{t'+2q^2(1-x)} + \frac{1}{s-2q^2(1-x)-t'-s'} \right]$$

this gives a term $(s' - s)$ in the numerator and hence cancels the effect of $s' - s$ in the denominator.

Next we consider the branch cuts in the plane from the vanishing of the denominator.

(i) Single nucleon term.

$$A_\ell^i(s)^N = R_s^i \int_{-1}^{1} \frac{P_\ell(x)\,dx}{m^2 - s} + R_u^i \int_{-1}^{1} \frac{P_\ell(x)\,dx}{m^2 - [2m^2 + 2\mu^2 - s + 2q^2(1-x)]}$$

(1.45)

(a) the first term has poles at

$$W = \pm m \quad \text{if} \quad \ell = 0$$

(b) the 2nd term has a branch cut for

$$-(m^2+2\mu^2)^{1/2} \le W \le -(m^2-\mu^2)/m$$

$$(m^2-\mu^2)/m \le W \le (m^2+2\mu^2)^{1/2}$$

as well as from 0 to $i\infty$ and 0 to $-i\infty$
(i.e. along the whole vertical axis)

(ii) "crossed π-N cut", denoting this contribution by A_ℓ^{ix} (s) we have

$$A_\ell^i(s)^x = \frac{1}{\pi}\int_{(m+\mu)^2}^{\infty} du' A_2^i(s,u') \int_{-1}^{1} \frac{P_\ell(x)\,dx}{[u'-(2m^2+2\mu^2 - s + 2q^2(1-x))]} \qquad (1.46)$$

this term has a branch cut for

$$-(m-\mu) \leq W \leq (m+\mu)$$

also from $-i\infty$ to $+i\infty$

(iii) 'π-π' cut in t channel
it is associated with the scattering in t channel.
This cut is from $t = 4\mu^2$ to $t = \infty$
which corresponds to a cut in W plane along the circle

$$|W| = (m^2 - \mu^2)^{1/2}$$

and also from $-i\infty$ to $+i\infty$

Fig 1.6 shows in detail the singularities of the partial wave amplitude in W plane

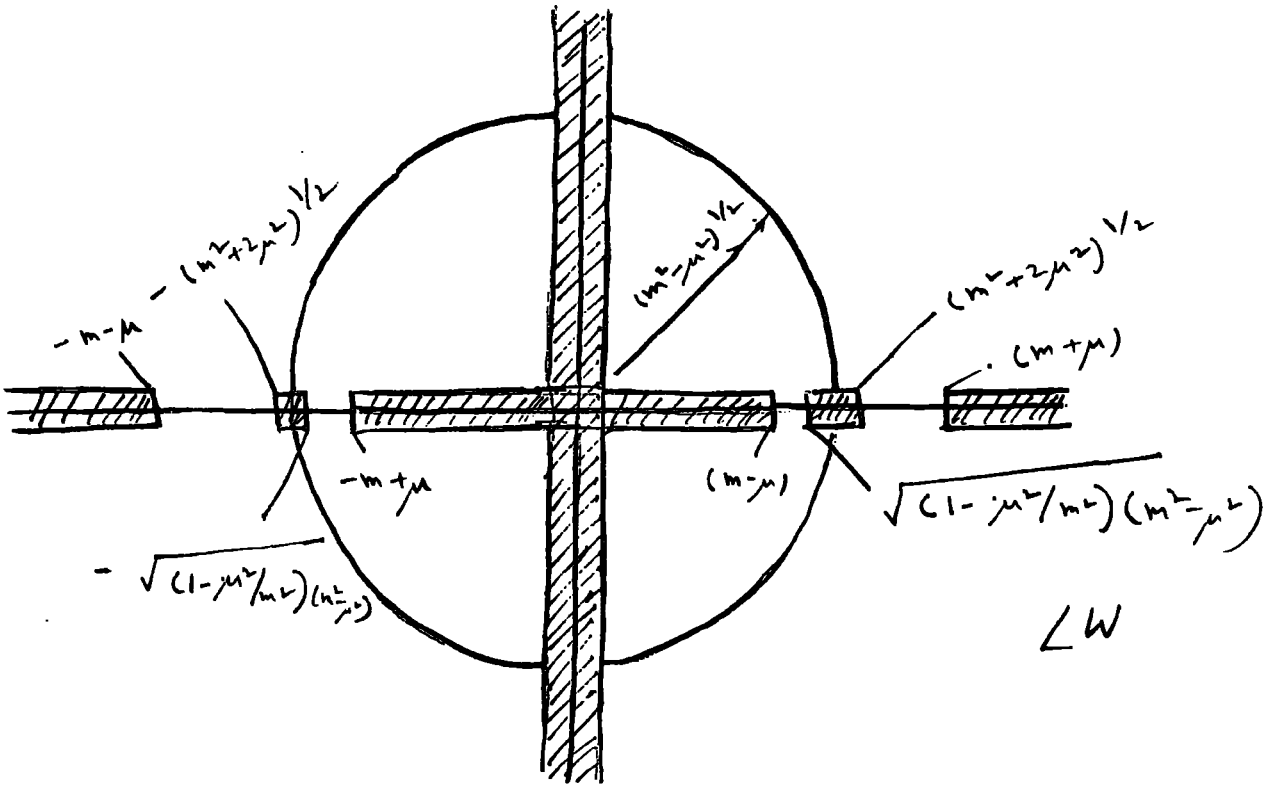

Fig. 1.6

6. Coulomb Scattering and Notations

To take proper account of coulomb scattering the amplitudes f_1 and f_2 must be modified before constructing the cross sections that are to be compared with experiment. To do this we follow Roper[13] et al. to construct coulomb amplitudes.

We define spin flip and non spin flip amplitudes as

$$f = f_1 + f_2 \cos\theta$$
$$g = f_2 \qquad (1.47)$$

and we form modified amplitudes *

$$\bar{f}(\theta) = f_c(\theta) + f(\theta)$$
$$\bar{g}(\theta) = g_c(\theta) + g(\theta) \qquad (1.48)$$

also
$$\bar{f}^{\pm}(\theta) = f_c^{\pm}(\theta) + F^{\pm}(\theta)$$
$$\bar{g}^{\pm}(\theta) = g_c^{\pm}(\theta) + g^{\pm}(\theta) \qquad (1.49)$$

where $+(-)$ indicates $\pi^+ p$ $(\pi^- p)$ elastic scattering and the subscript c denotes the coulomb contribution.

Now

$$f_c^{\pm}(\theta) = f_{rem}^{\pm}(\theta) + f_{coul}^{\pm}(\theta) - f_{coul_2}^{\pm}(\theta)$$
$$g_c^{\pm}(\theta) = g_{rem}^{\pm}(\theta) + g_{coul}^{\pm}(\theta) - g_{coul_2}^{\pm}(\theta) \qquad (1.50)$$

where $f_{rem}^{\pm}(\theta)$, $g_{rem}^{\pm}(\theta)$ are relativistic electromagnetic amplitude to the first order in α $(\alpha = e^2/\hbar c = 1/137)$ given by

$$\left[* \quad f_c^{c.E} = 0 \qquad g_c^{c.E} = 0 \right]$$

$$f^{\pm}_{rem}(\theta) = \mp \frac{\alpha \lambda}{2W(1-\cos\theta)} \left[\frac{W-\bar{m}}{p_0-\bar{m}} + \frac{W+\bar{m}}{p_0+\bar{m}} \cos\theta \right.$$

$$\left. - (\mu_p - 1) \frac{q_0}{\bar{m}} (1-\cos\theta) - (\mu_p - 1) \frac{(p_0-\bar{m})}{2\bar{m}} \sin^2\theta \right]$$

$$g^{\pm}_{rem}(\theta) = \frac{\pm \alpha \lambda}{2W(1-\cos\theta)} \left[\frac{W+\bar{m}}{p_0+\bar{m}} + (\mu_p - 1) \frac{W+q_0+\bar{m}}{\bar{m}} \right.$$

$$\left. + (\mu_p - 1) \frac{(p_0-\bar{m})}{2\bar{m}} \cos\theta \right]$$

(1.51)

where

$q_0 = (k^2 + 1)^{1/2}$ = pion total energy in c.m.

$W = q_0 + p_0$ = total energy in c.m. system

$p_0 = (k^2 + \bar{m}^2)^{1/2}$ = nucleon total energy in c.m.

} in pion mass unit

θ = c.m. scattering angle

$\bar{m}$ = nucleon mass in terms of pion mass unit

= 6.7212

k = pion c.m. momentum.

μ_p = proton magnetic moment in nucleon magnetons = 2.7275

$f^{\pm}_{coul}(\theta)$, ( ), $g^{\pm}_{coul}$ ( ) are non-relativistic coulomb amplitudes correct to all orders in α.

$$f^{\pm}_{coul}(\theta) = \frac{\mp \alpha \lambda (q_0 p_0 + k^2)}{k^2 W (1-\cos\theta)} \exp\left[\mp \frac{i\alpha(q_0 p_0 + k^2)}{kW} \times \right.$$

$$\left. \times \ln\left(\frac{1-\cos\theta}{2}\right) \right]$$

$$g^{\pm}_{coul}(\theta) = 0 \qquad (1.52)$$

and finally $f^{\pm}_{coul}(\theta)$, $g^{\pm}_{coul}(\theta)$ are non-relativistic coulomb amplitudes to first order in α

$$f^{\pm}_{coul}(\theta) = \mp \frac{\alpha \lambda (q_0 P_0 + k^2)}{k^2 W (1 - \cos\theta)}$$

$$g^{\pm}_{coul}(\theta) = 0 \qquad (1.53)$$

the differential cross section of an unpolarised beam of pions is finally given by

$$\frac{d\sigma}{d\Omega} = \left| |\bar{f}(\theta)|^2 + \sin^2\theta \, |\bar{g}(\theta)|^2 \right| \qquad (1.54)$$

and the polarization $p(\theta)$ produced is

$$P(\theta) = \frac{2\sin\theta \, \mathrm{Im}(\bar{f}(\theta) \, \bar{g}(\theta^*))}{\frac{d\sigma}{d\Omega}} \qquad (1.55)$$

($\bar{g}^*(\theta)$ is the complex conjugate of $\bar{g}(\theta)$)

The total cross section data being coulomb corrected, the total cross section will be given by (using optical theorem)

$$\sigma_{tot} = 4\pi (\mathrm{Im} f(0))/q \qquad (1.56)$$

The above formulas were actually used to construct total cross sections, differential cross sections and the polarizations to compare with the experimental results.

CHAPTER II

REGGE POLE FORMALISM

REGGE POLE FORMALISM

Introduction:

In this chapter we shall discuss the basic principles of Sommerfield Watson transformation, Regge poles and the Khuri - modification to Regge amplitude. We shall also discuss briefly the idea of finite energy sum rule.
To see how the typical Regge pole contribution is obtained we shall start with spinless particles.

In Chapter III we shall generalise this to the case of a pion - nucleon scattering.

1. Analytical continuation in complex plane.

Now in a non-relativistic spinless example the scattering amplitude can be written as

$$f(z,s) = \sum_{l=0}^{\infty} (2l+1)\, a_l(s)\, P_l(z) \qquad (2.1)$$

where $a_l(s)$ is the partial wave amplitude, s is the mandelstam variable as defined before.

$P_l(z)$ are Legendre polynomials and $z = \cos\theta$,

θ being the c.m. angle.

Now we can analytically continue both ($a_l(s)$ and $P_l(z)$) in complex l plane.

For $a_l(s)$ we do this with the help of Carlson's theorem[14] i.e. we define an analytic function $a(l,s)$ which satisfies for some L

i) $a(\ell, s) = a_\ell(s)$, $\ell = +\nu 2$ integer $\geq L$

ii) $a(\ell, s) = O(e^{\lambda|\ell|})$, $\ell \to \infty$ in $\mathrm{Re}\,\ell \geq L$ with $\lambda < \pi$

iii) $a(\ell, s)$ is holomorphic in $\mathrm{Re}\,\ell \geq L$

Now an $a(\ell, s)$ satisfying the above conditions certainly exists[15] for potential scattering problems and for those relativistic problems in which mandelstam representation is satisfied.

From Carlson's theorem we know that if an $a(\ell, s)$ exists it must be unique. Now given an $a(\ell, s)$ satisfying (i), (ii) and (iii) the summation in Equation (2.1) can be changed into a contour integral[16] (with the help of Cauchy's theorem)

$$f(s, z) = \frac{i}{2}\int_{C_1} \frac{(2\ell + 1)}{\sin \pi \ell}\, a(\ell, s)\, P(\ell, -z)\, d\ell \qquad (2.2)$$

the contour C_1 is shown in Fig.(2.1) $< L$

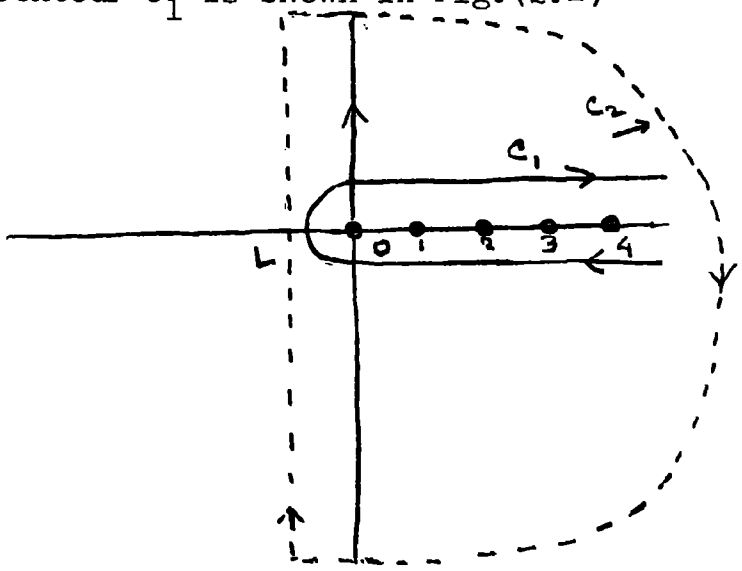

Fig.(2.1)

c_1 is so chosen as to include the positive integers and zero but to avoid any singularities of $a(\ell, s)$, the integrand has poles at each integer n due to the vanishing of $\sin\pi\ell$ at $\ell = n$.

Picking up the contributions of these poles,

(the residue of a pole at $\ell = n$ is

$$\frac{2\pi i\, P_n(-z)\, a(n,s)\,(2n+1)}{(-1)^n \pi} = 2i P_n(z)\, a(n,s)(2n+1)\Big)$$

with the help of Cauchy's theorem, we get back equation (2.1).

Now we can deform c_1 continuously into countour c_2 with a line parallel to the imaginary axis at $\mathrm{Re}\{\ell\} = L_2$ and a semicircle at ∞.

Provided $L_2 > L$ $(> -1/2)$ no singularities of $a(\ell, s)$ will be encountered in this displacement and $P_\ell(z)$ has no singularities as a function of ℓ for $\mathrm{Re}\{\ell\} \geq -1/2$

Hence $$\int_{c_1} = \int_{c_2}$$

Again the partial wave amplitude behaves at large ℓ as follows[17]

$$a_\ell(s) \underset{\ell\to\infty}{\sim} f(s)\quad e^{-\ell\,\zeta(z_n)}$$

where

$$\zeta(z) = \log(z + \sqrt{z^2-1}),\ z_n > 1 \qquad (2.3)$$

this behaviour of $a_\ell(s)$ and the fact that

$$\left|\frac{P_\ell(-z)}{\sin\pi\ell}\right| < \left|\frac{\ell^{-1/2}\exp\{|\mathrm{Im}\,\theta|\,\mathrm{Re}\,\ell + (\pi - \mathrm{Re}\,\theta)|\mathrm{Im}\,\ell|\}}{\exp(\pi|\mathrm{Im}\,\ell|)}\right|$$

enable us to throw away the contribution of the integral from the semicircle.

Now if we move the line parallel to the imaginary axis towards left i.e. when the relation $L_2 > L$ no longer holds the singularities of $a(\ell, s)$ shall appear within the new contour c_3.

Since $P_\alpha(z) \sim z^{|\alpha+\frac{1}{2}|-\frac{1}{2}}$. for large z

we can minimise the contribution coming from the vertical path of integration by taking c_3 as a line parallel to the imaginary axis at Re $\{\ell\} = -1/2$ and a semicircle at ∞.

Assuming the singularities of $a(\ell, s)$ thus encountered in c_3 are poles at $\ell = \alpha_i(s)$, with residue $\beta_i(s)$, $i = 1, 2 \cdots$

so that $a(\ell, s) \sim \sum_i \frac{\beta_i(s)}{\ell - \alpha_i(s)}$ (2.4)

we can evaluate the integral in (2.2) by covering the poles with extra loops in c_3 as shown in Fig.2.2

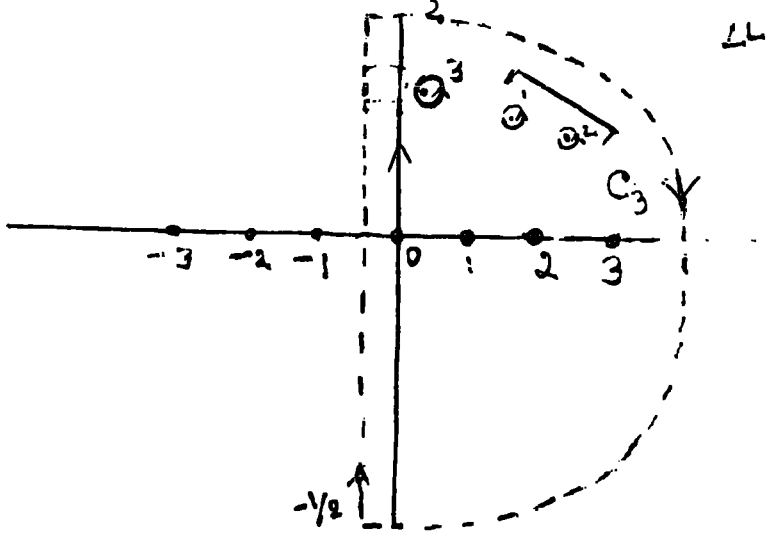

Fig. 2.2

$$f(s,z) = \frac{1}{2}\int_{-1/2+i\infty}^{-1/2+i\infty} \frac{(2l+1)\,a(l,s)}{\sin\pi l}\, P(-l,-z)\,dl - \sum_i \pi\,\frac{(2\alpha_i+1)}{\sin\pi\alpha_i}\,\beta_i\,P(\alpha_i,z) \qquad (2.5)$$

2. Regge Poles

The poles of $a(l, s)$ given by (2.4) are termed as "Regge poles". They were discovered mathematically in non-relativistic potential scattering [18]. The contribution of a typical Regge pole to the scattering amplitude is, as can be seen from the 2nd term on r.h.s of Equation (2.5),

$$f(s,z) \sim -\frac{\pi(2\alpha_i+1)}{\sin\pi\alpha_i}\,\beta_i\,P(\alpha_i,-z) \qquad (2.6)$$

We shall see later that the limit $z \to \infty$ is most important in high energy Regge amplitude.

In this limit $P(\alpha, z) \sim z^{\alpha}$ for $\mathrm{Re}\,\alpha > -1/2$

Hence Regge poles with Re α $-1/2$ dominates over the background integral and the leading Regge pole i.e. One with the largest Re α dominates overall.

For $L < -1/2$ $P(\alpha, z) \sim z^{-\alpha-1}$ and the b.g. integral

becomes very small for large z.

Mandelstam[19] showed that equation (2.5) can be re-set and the background integral term can be pushed further to the left by using Legendre function of the 2nd kind $Q_\ell(z)$ i.e. the Regge pole terms would have $\frac{P_\alpha(-z)}{\sin\pi\alpha}$ replaced by $-\frac{Q_{-\alpha-1}(-z)}{\pi\cot\pi\alpha}$ and behave like z^α as before. For $\mathrm{Re}\,\alpha > -1/2$ either P_α or $Q_{-\alpha-1}$ can be used but for cases in which $\mathrm{Re}\,\alpha < -1/2$ only $Q_{-\alpha-1}$ form makes sense.

3. Signature[20]

We generally expect $a_\ell(s)$ to have two different continuations in complex ℓ plane for L even or odd, so as to take care of the exchange forces which could make the dynamics of even and odd states differ we split $f(s,z)$ into even and odd parts.

We define

$$f_\pm(s,z) = \sum_\ell (2\ell+1)\, a_\ell{}^\pm(s)\, P_\ell(z) \qquad (2.7)$$

and the actual amplitude

$$f(s,z) = 1/2\,\big[f_+(s,z) + f_+(s,-z) + f_-(s,z) - f_-(s,-z)\big] \qquad (2.8)$$

Thus we can see that even part of $f(s,z)$ equals to the even part of $f_+(s,z)$ and the odd part of $f(s,z)$

equals to the odd part of $f_-(s,z)$. The two amplitude f_+ and f_- are called the even and odd 'signature' amplitudes, respectively and they will have in general quite different Regge poles at $\ell = \alpha^{\pm}(s)$.

The $\pm$ sign define the signature of the trajectory $\alpha^{\pm}$.

Now we make separate S.W. transformation for even and odd parts and recombine them to get the contribution of a single Regge pole at $\ell = \alpha^{\pm}$ to $f(s,z)$

$$f(s,z) = -\pi \frac{(2\alpha_\pm + 1)}{2 \sin \pi \alpha_\pm} \beta_\pm \left[P_{\alpha_\pm}(-z) \pm P_{\alpha_\pm}(z) \right] \tag{2.9}$$

or taking the large z behaviour of $P_\alpha(z)$

$$f(z) \sim -\pi \frac{(2\alpha_\pm + 1)}{\sin \pi \alpha_\pm} \beta_\pm \frac{\Gamma(\alpha)}{2} \left[e^{-i\pi\alpha_\pm} \pm 1 \right] z^{\alpha_\pm} \tag{2.10}$$

where we have used $P_\alpha(z) \sim \Gamma(\alpha) z^\alpha$, $\mathrm{Re}\,\alpha > -1/2$

and $P_\alpha(-z)^\alpha = e^{-i\pi\alpha} z^\alpha$, the choice of the phase in this case[21] (i.e. $e^{-i\pi\alpha}$ instead of $e^{i\pi\alpha}$) is the one suggested by the analyticity in the upper half of the complex u plane. If there are no exchange forces we get degenerate pairs of Regge trajectories with opposite signatures and get back Equation (2.6).

Now suppose for some values of s say $s = s_0$

$\alpha_\pm(s_0) = L_{0\pm}$ is an integer

We then have in the neighbourhood of s_0

$$\sin\pi\alpha(s) = \cos\pi\alpha(s_0)\,\pi\alpha'(s_0)(s-s_0) + \cdots \tag{2.11}$$

so that such a pole contribution to f(z) for s near s_0 is

$$f(s,z) \sim -\frac{(2L_0^{\pm}+1)}{\alpha'_{\pm}(s_0)}\beta_{\pm}(s_0)\frac{1}{2}\left[1\pm(-1)^{L_0^{\pm}}\right]\frac{P_{L_0^{\pm}}(z)}{s-s_0} \tag{2.12}$$

and that if the pole is of even(odd) signature and $L_{0\pm}$ is even(odd) integer

$$f(s,z) \sim \text{const.}\ \frac{P_{L_0^{\pm}}(z)}{s-s_0}$$

but if the pole is of wrong signature there is no such term, the zero in thedeminator is compensated by the zero in the numerator coming from $\left[1 \pm (-1)^{L_0^{\pm}}\right]$

Hence when a Regge trajectory passes through an integer it gives a contribution to the amplitude like a bound state of the corresponding angular momentum if and only if the trajectory has the correct signature.

4. Resonance and Bound States.

If for* $s < s_0$, $\alpha(s)$ goes through integer value and has the appropriate signature it will lead to a bound state in the amplitude with the angular momentum equal to the integer value and at that corresponding energy.

On the other hand if for $s > s_0$ it passes close to an

(* Here $s_0 = (m+\mu)^2$)

integer i.e. if say

$$\begin{aligned} \mathrm{Re}\,\alpha(s) &= L + y \qquad |y| < 1 \\ \mathrm{Im}\,\alpha(s) &< < 1 \end{aligned} \tag{2.13}$$

where L is an integer, y is a function of s

$$\begin{aligned} \sin \pi \alpha &= \sin \pi (L + y + i\,\mathrm{Im}\,\alpha) \\ &\simeq (-1)^L \pi (y + i\,\mathrm{Im}\,\alpha) \end{aligned} \tag{2.14}$$

Let $\mathrm{Re}\,\alpha(s_R) = L$ (2.15)

then $y \simeq (s - s_R)\ \mathrm{Re}\,\alpha'(s_R)$

where $\mathrm{Re}\,\alpha'(s_R) = \left.\frac{d}{ds}\,\mathrm{Re}\,\alpha(s)\right|_{s=s_R}$

and $\mathrm{Im}\,\alpha \sim \mathrm{Im}\,\alpha(S_R)$

Hence from (2.11)

$$f(s,z) \simeq -\frac{(2L+1)}{2}\,\beta\,(1 \pm (-1)^L)\,\frac{1}{\mathrm{Re}\,\alpha'(s_R)}\,\frac{P_L(z)}{s - s_R + \frac{i\,\mathrm{Im}\,\alpha(s_R)}{\mathrm{Re}\,\alpha'(s_R)}} \tag{2.16}$$

Equation (2.16) corresponds to a Breit-Wigner resonance of mass $\sqrt{s_R}$ and width

$$\Gamma = \frac{\mathrm{Im}\,\alpha(s_R)}{\sqrt{s_R}\,\mathrm{Re}\,\alpha'(s_R)} \tag{2.17}$$

5. Asymptotic Regge behaviour

We have said before that the limit $\cos\theta \to \infty$ is very important in Regge analysis. We shall see now why

this is so.

Let us consider high energy equal mass scattering

$$a + b \longrightarrow c + d$$

where $m_a = m_b = m_c = m_d$ (m denotes the mass)

$= m$ say.

If s,t,u are the usual Mandelstam variables then t represents the square of the centre of mass energy in t channel $\bar{a} + c \longrightarrow b + \bar{d}$

u represents the square of the c.m. energy in u channel

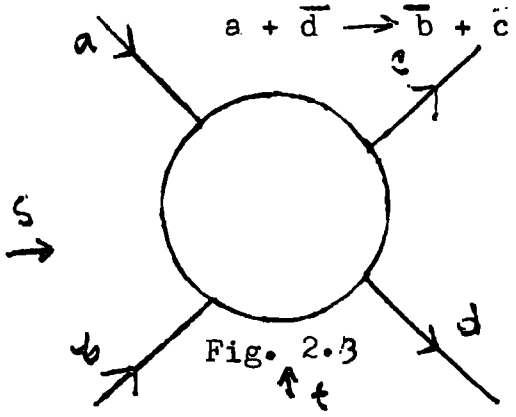

Fig. 2.3

Now it is always possible to find a single invariant amplitude which represents s,t and u channel processes, their physical regions however correspond to different ranges of s,t, and u. This being demonstrated clearly in the Mandelstam representation (Equation 1. 40)

Now for equal mass scattering if q_n and θ_n, in channel n (n = s,t,u) are c.m. momenta and angle then

$$s = 4\,(m^2 + q^2{}_s) = -\,2q_s{}^2\,(1 + \cos\theta_t)$$

$$t = 4(m^2 + q_t^2) = -2q_s^2(1 - \cos\theta_s)$$
$$u = 4(m^2 + q_u^2) = -2q_s^2(1 + \cos\theta_s) \qquad (2.18)$$

where

$$\cos\theta_t = \frac{s - 2m^2 + t/2}{2m^2 - t/2}$$
$$\cos\theta_u = 1 + \frac{2(4m^2 - s - u)}{u - 4m^2} \qquad (2.19)$$

Hence the high energy small angle region in the s channel corresponds in the t channel to an unphysical region with large $\cos\theta_t$ and $\cos\theta_u$ respectively.

So we can no doubt apply the asymptotic Regge behaviour

$$P_\alpha(z) \underset{z\to\infty}{\sim} z^\alpha \qquad (2.20)$$

in both t channel and u channel.

But this is not so for unequal mass scattering, though $\cos\theta_t$ is still large for high energy forward scattering. The kinematic limitations on Regge asymptotics have been discussed by Atkinson and Barger[22]. We shall confine our discussions to the pion - nucleon scattering where $m_a = m_c$, $m_b = m_d$ but $m_a \neq m_b$, writing $m_a = m_b = m$, and $m_b = m_d = \mu$ we have in this case

$$\cos\theta_t = (s + p_t^2 + q_t^2) / 2p_t q_t$$

with

$$p_t^2 = (t - 4m^2)/4$$
$$q_t^2 = (t - 4\mu^2)/4 \qquad (2.21)$$

more explicitely

$$\cos\theta_t = \frac{2(4_s + 2_t - 4(m^2 + \mu^2)}{(t - 4m^2)^{1/2}(t - 4\mu^2)^{1/2}} \qquad (2.22)$$

Hence the high energy small angle region in the s channel still corresponds in the t channel to an unphysical region with large $\cos\theta_t$.

But, as we shall see, life is not so easy in u channel. The u channel Regge asymptotic behaviour does not appear to be an obvious fact.

In u channel

$$\cos\theta_u = 1 - \frac{2u(s - 2(m^2+\mu^2) + 4)}{(u^2 - 2(m^2+\mu^2)(u+(m^2-\mu^2)^2)} \qquad (2.23)$$

which gives $\cos\theta_u = -1$ when $\cos\theta_s = -1$

i.e. the exact backward direction in s channel gives a finite value of $\cos\theta_u$ which is not unphysical. Also $\cos\theta_u$ is bounded by unity for all s in the backward cone defined by[23]

$$0 \leq \mu \leq \mu_B \left(= \frac{(m^2-\mu^2)^2}{s}\right) \qquad (2.24)$$

Hence the conventional asymptotic representation $(P_\alpha(z) \sim z^\alpha)$ does not hold good in this region. But it has been shown by several authors that if the Regge asymptotic form holds nearby it may be established also in the questionable region.

In the case of π-N scattering Freedman and Wang[24] have shown that high energy asymptotic Regge behaviour holds throughout the backward region. We shall not go into detail of their analysis (e.g. daughter trajectories etc.) but assume their results to hold good in the questionable region.

6. Khuri modification.

The original Regge representation (Equation 2.5) was

$$f(s,z) = i/2 \int_{-1/2-i\omega}^{-1/2+i\omega} \frac{(2l+1)}{\sin \pi l} a(l,s)\, p(l,-z)\, dl$$

$$- \pi \sum_i \frac{(2\alpha_i+1)}{\sin \pi \alpha_i} \beta_i(s)\, p(\alpha_i, -z) \qquad (2.25)$$

In the last section we discussed the high energy behaviour with large values of z (= $\cos\theta$) in the channels in which the background integral (the first term on the r.h.s of Equation (2.25)) was small compared to the dominant second

term and hence could be neglected. Also in dealing with large z behaviour it did not matter that the sum over Regge poles had a wrong cut in the z plane (the cut in $p(\alpha_i, -z)$ starts at $z = 1$ instead of the starting at $z_0 = 1 + m_0^2/2s$). Also the P.W.A.+ of the Regge pole terms in the second term on the r.h.s. of (2.25) does not have the correct threshold behaviour.

These deficiencies of the original Regge representation were removed by Khuri[7].

In the discussion below we follow Khuri's method to get the 'full' contribution of the Regge pole which has got the correct branch points in complex z plane.

Now putting $\lambda = \ell + 1/2$, $\lambda_i = \alpha_i + 1/2$ (2.25) can be written as

$$f(s,z) = -i \int_{-i\infty}^{i\infty} \frac{\lambda\, d\lambda}{\cos n\lambda}\, P(\lambda - 1/2, -z)\, a(\lambda - 1/2, s) + 2\pi \sum_i \frac{\beta_i(s)\,\lambda_i}{\cos n\lambda_i}\, P_{\lambda_i - 1/2}(-z) \qquad (2.26)$$

Now[25]

$$\frac{\pi P_{\lambda-1/2}(z)}{\cos \pi\lambda} = \sqrt{2} \int_0^\infty \frac{\cosh \lambda x}{(\cosh x + z)^{1/2}}\, dx$$

$$= \frac{1}{\sqrt{2}} \int_{-\infty}^{\infty} \frac{e^{\lambda x}}{(\cosh x + z)^{1/2}}\, dx \qquad (2.27)$$

* m_0 = masses of the particles (eg mass scattering)

\+ P.W.A = Partial Wave Amplitude

The last term is obtained by using

$$e^{\lambda x} = \cosh\lambda x + \sinh\lambda x \quad \text{((2.27) holds only for } -\tfrac{1}{2} < \mathrm{Re}\,\lambda < 1/2)$$

Hence (2.26) can be written as

$$f(s,z) = \frac{1}{\sqrt{2}} \int_{-\infty}^{\infty} \frac{B(x,s)\sinh x}{(\cosh x - z)^{3/2}}\, dx$$

$$+ 2\pi \sum_i \frac{\beta_i(s)\lambda_i}{\cos\pi\lambda_i} P_{\lambda_i,-1/2}(-z) \tag{2.28}$$

where

$$B(x,s) = \frac{1}{2\pi i} \int_{-i\infty}^{i\infty} d\lambda\, e^{\lambda x} a(\lambda - 1/2, s) \tag{2.29}$$

it exists for all x.

Now each term in the r.h.s. of (2.25), when continued to unphysical or complex values of z will have a cut starting at $z = 1$. Evidently some cancellation must occur between the two terms in the region $1 \le z < \cosh\zeta$ to ensure that the amplitude has the correct cut which starts at $z = \cosh\zeta$ ($\cosh\zeta = 1 + m_0^2/2s$). To see how it happens we decompose $B(x,s,)$ in to two parts,

$$B(x,s) = B_1(x,s)\,\theta(x-\zeta) + B_2(x,s)\,\theta(\zeta - x) \tag{2.30}$$

and

$$\int_{-\infty}^{\infty} \frac{B(x,s)\sinh x}{(\cosh x - z)^{3/2}}\, dx = \int_{-\infty}^{\zeta} I\, dx + \int_{\zeta}^{\infty} I\, dx \tag{2.31}$$

where

$$I = \frac{B(x,s)\sinh x}{(\cosh x - z)^{3/2}}$$

Now for $x < \xi$ we can write a simple expression for $B(x,s)$

In fact using the result that

$$a(\ell, s) \sim c(s)\ \frac{e^{-\ell \xi}}{\sqrt{\ell}} \qquad \text{when } \ell \to \infty$$

we can close the contour in (2.2) on the right and

get $B(\lambda, s) = -\sum \beta_i(s)\, e^{\lambda_i x} = B_2(x, s)$ for $x < \xi$ (2.32)

To get (2.32) we have used equation (2.27), and changed the order of integration in (2.25) (we also took $a(\lambda - 1/2, s)$ to be meromorphic in the right half λ plane)

Now (2.28) can be written as

$$f(s,z) = \sum_i R_1(s,z,\alpha_i) + \frac{1}{\sqrt{2}} \int_{-\xi}^{\infty} \frac{B_1(x,s)\sinh x\, dx}{(\cosh x - z)^{3/2}} \qquad (2.33)$$

where

$$R_1(s,z,\alpha_i) = -\beta_i(s)\left[\frac{\pi(2\alpha_i+1)}{\sin \pi\alpha_i} P_{\alpha_i}(-z) + \frac{1}{\sqrt{2}} \int_{-\infty}^{\xi} \frac{e^{(\alpha_i+1/2)x}}{(\cosh x - z)}\, dx\right] \qquad (2.34)$$

where $\alpha_i = \lambda_i - 1/2$ (2.35)

For Re $\lambda_i > 0$ i.e. for Re $\alpha_i > -1/2$ $R_1(s,z,\alpha_i)$ is the full contribution to $f(s,z)$ of each Regge pole in the

right half λ plane.

If we denote the full Regge pole contribution to the amplitude (in both Re $\lambda_i > 0$ and Re $\lambda_i < 0$ cases) by $R(s,z,\alpha_i)$, then for $Re\,\lambda_i > 0$,

$$\left(\mathrm{Re}\,\alpha_i > -\tfrac{1}{2}\right), \quad R(s,z,\alpha_i) = R_1(s,z,\alpha_i) \qquad (2.36)$$

Now it can be shown that the cuts of the two terms in the right hand side of (2.34) cancel each other (see Appendix 1)

Case II Re $\lambda_i < 0$

The properties of $a(\ell,s)$ for Re $\ell < -1/2$ are more complicated than those for Re $\ell > -1/2$. But according to Mandelstam[26] for a sub class of potentials $a(\ell,s)$ is meromorphic for Re $\ell < -1/2$ and so for $x > \xi$ assuming that behaviour of $a(\ell,s)$ we obtain from (2.29)

$$B_1(x,\xi) = B(\lambda,\xi) = \sum_{i}^{n(L)} \beta_i(s)\, e^{\lambda_i x} + \frac{1}{2\pi i}\int_{-L-i\infty}^{-L+i\infty} d\lambda\, e^{\lambda x}\, a(\lambda - \tfrac{1}{2}, s), \quad x > \xi \qquad (2.37)$$

The sum represents the contributions of all the poles in the strip $-L < \mathrm{Re}\,\lambda < 0$. Assuming that excluding the neighbourhood of the poles, $a(\ell,s) \le \left(|c(s)| / (|\sqrt{\lambda}|)\right) e^{|\mathrm{Re}\,x|\xi}$ we close the contour for (2.29) on the left and get

$$B_1(x,\xi) = B(\lambda,\xi) = \sum_{i=1}^{\infty} \beta_i(s)\, e^{\lambda_i x} \quad \text{for } x > \xi,\ \mathrm{Re}\,\lambda_i < 0 \qquad (2.38)$$

substituting this in (2.23) we can identify the contribution of a left hand Regge pole to f(s,z) as

$$R(s,z,\alpha_i) = \frac{\beta_i(s)}{\sqrt{2}} \int_{\gamma}^{\infty} \frac{e^{(\alpha_i+1/2)x}}{(\cosh x - z)^{3/2}} \sinh x \, dx, \quad \mathrm{Re}\,\alpha_i < -1/2 \tag{2.39}$$

This has also the correct cut in the z plane. By virtue of (2.27) it is easy to see that the representations (2.34) and (2.37) are identical in the region where $-\frac{1}{2} < \mathrm{Re}\,\alpha_i < 1/2$

Also the partial wave amplitudes of $R(s,z,\alpha_i)$ turn out to be same in both (2.36) and (2.23) representations. We shall show below that the partial wave amplitude defined by

$$f_\ell(s,\alpha_i) = \frac{1}{2} \int_{-1}^{1} P_\ell(z)\, R(s,z,\alpha_i)\, dz \tag{2.40}$$

is given by

$$f_\ell(s,\alpha_i) = -\frac{\beta_i \{e^{-(\ell-\alpha_i)}\}}{\ell-\alpha_i} \tag{2.41}$$

We shall show it for the case where $\mathrm{Re}\,\alpha_i > -1/2$, the partial wave projection of the term on the r.h.s. of (2.39) then be calculated easily following the same method. Now inverting (2.27) we have

$$\frac{\sinh x}{(\cosh x - z)^{3/2}} = -i\sqrt{2} \int_{-i\infty-1/2}^{} \frac{(\ell'+1/2)\, P_{\ell'}(-z)\, e^{-(\ell'+1/2)x}}{\cos\pi(\ell'+1/2)}\, d\ell' \tag{2.42}$$

We first take the partial wave projection of the 2nd term of the r.h.s. of (2.34) and call it f_ℓ^1

Hence

$$f_\ell^1 = \frac{i\beta_i}{2}\int_{-1}^{1} dz \int_{-i\omega-1/2}^{i\omega-1/2} d\ell' \int_{-\omega}^{\omega} \frac{dx\, e^{(\alpha_i-\ell')x}(\ell'+1/2)P_{\ell'}(-z)P_\ell(z)}{\cos\pi(\ell'+1/2)} \qquad (2.43)$$

where we have used (2.42)

But[27]

$$\int_{-1}^{1} P_{\ell'}(-z)\,P_\ell(z)\,dz = -\frac{2}{\pi}\frac{\sin\pi\ell'}{(\ell-\ell')(\ell+\ell'+1)} \qquad (2.44)$$

$$\therefore \quad f_\ell^1 = -\frac{i\beta_i}{\pi}\int_{-i\omega-1/2}^{i\omega-1/2} d\ell' \int_{-\omega}^{\omega} dx\, \frac{e^{(\alpha_i-\ell')x}(\ell'+1/2)}{(\ell-\ell')(\ell+\ell'+1)} \qquad (2.45)$$

We can write

$$\int_{-\omega}^{\omega} = \int_{-\omega}^{0} + \int_{0}^{\omega} \qquad (2.46)$$

For the first integral on the r.h.s. of (2.46) where throughout the range of integration, we integrate over in (2.45) by choosing the contour on the left half of ℓ' plane including the pole at $\ell' = -\ell - 1$ as shown in Fig. (2.5(a)). For the second integral $\int_0^{\omega}$ we integrate over $d\ell'$ by choosing the contour on the right half of ℓ' plane including the pole at $\ell' = \ell$ (Fig. 2.5(b))

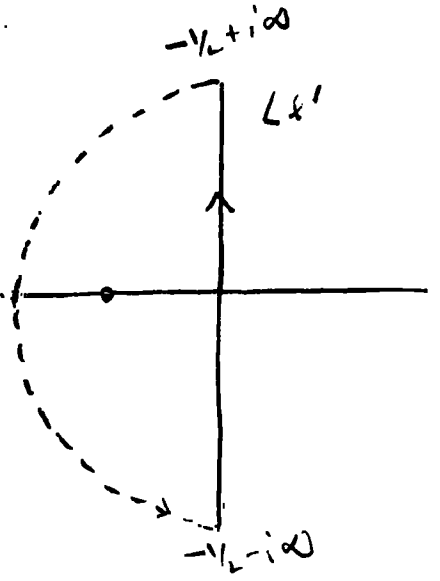

Fig.2.5(a)

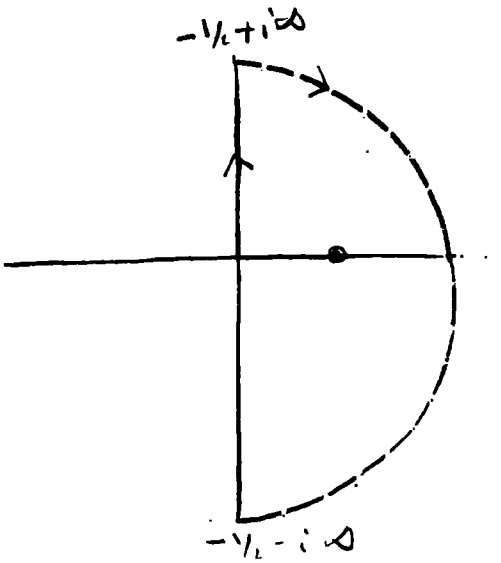

Fig.2.5(b)

thus

$$f_\ell^1 = -i\frac{\beta_i}{\pi}(2\pi i)\left[\int_{-\infty}^{0}\frac{(\ell+1/2)}{2\ell+1}e^{(\alpha_i+\ell+1)x}dx - \int_{0}^{\infty}\frac{(\ell+1/2)}{(2\ell+1)}e^{(\alpha_i-\ell)x}dx\right] \tag{2.47}$$

$$= \beta_i\left[\frac{2\alpha_i+1}{(\alpha_i+\ell+1)(\alpha_i-\ell)} - \frac{-e^{-(\ell-\alpha_i)\}}}{\alpha_i-\ell}\right] \tag{2.48}$$

Now let us take the p.w. projection of the first term of r.h.s. of eq(2.34) and call it f_ℓ^2

$$f_\ell^2 = \frac{1}{2}\beta_i \cdot \frac{2\pi(\alpha_i+1/2)}{\cos\pi(\alpha_i+1/2)}\int_{-1}^{1} P_{\alpha_i}(-z)P_\ell(z)dz$$

$$= -\frac{(2\alpha_i+1)\beta_i}{(\alpha_i-\ell)(\ell+\alpha_i+1)} \tag{2.49}$$

using (2.44)

$$\therefore\ f_\ell(s,\alpha_i) = f_\ell^1 + f_\ell^2 = -\beta_i\ \frac{e^{-(\ell-\alpha_i)}}{\alpha_i - \ell} \qquad (2.50)$$

$f(s, \alpha_i)$ has the same analytic properties as the full P.W. amplitude for physical ℓ. Also for Re $\alpha_i > 0$ it has the correct threshold behaviour as $s \to 0$.

7. Finite energy sum rule.

Finite energy sum rules follow from the consistency imposed by analyticity on functions that can be expanded at high energies say $s > N$ as a sum of Regge poles. The derivation of sum rules is as follows. If there is an analytic function f(s) satisfying a dispersion relation

$$f(s) = \frac{1}{\pi} \int \frac{\mathrm{Im}\, f(s')\, ds'}{s' - s} \qquad (2.51)$$

and subject to the asymptotic bound, for $s \to \infty$

$$|f(s)| < s^\beta,\ \beta < 1$$

then it must satisfy the condition

$$\int \mathrm{Im}\, f(s)\, ds = 0 \qquad (2.52)$$

(If we multiply both sides of (2.51) by s and take the limit $s \to \infty$, we get (2.52))

Now if f(s) represents the scattering amplitude for some process and f(s) can be represented by the Regge expansion at a fixed momentum transfer t

$$f(s) = \sum \left(\frac{1 - e^{-i\pi\alpha(t)}}{\sin \pi \alpha(t)\, \Gamma(\alpha+1)} \right) \beta \, s^{\alpha(t)}, \quad s \geq N \qquad (2.53)$$

then the following finite energy sum rule follows from (2.51) (using Cauchy's theorem)

$$\int_0^N \mathrm{Im}\, f(s)\, ds = \sum \frac{\beta N^{\alpha+1}}{(\alpha+1)\Gamma(\alpha+1)} \qquad (2.54)$$

Thus F.E.S.R. provides a link between the low energy and the asymptotic high energy regions of a scattering process. Some authors[28] used this link to determine parameters of the s channel resonances from the information about the Regge terms inferred from high energy data. Others[29] used the low energy data alone as an input to predict the exchanged Regge pole parameters. But it is obvious that a finite set of resonances which we may write as a B.W. form

$$f = \sum_i \frac{\beta_i}{s - M_i^2 + i\Gamma} P_{J_i}(\cos\theta) \qquad (2.55)$$

will not give a Regge asymptotic behaviour, but rather a fixed pole behaviour at high energy and on the other hand a Regge amplitude, such as (2.53) will not give s channel poles as usually associated with resonances. Only an infinite number of s channel resonances yield an asymptotic Regge behaviour at large s and only an infinite set of Regge trajectories may lead to a second sheet pole.

Nevertheless some authors[30] have proposed that the two descriptions have a large overlap so that many features readily interpreted in terms of Regge poles exchange can also

be analysed as cumulative effect of direct channel resonances and conversely the properties usually associated with resonance dominance can be interpreted as due to relations among Regge trajectories (such as exchange degeneracy).

8. Duality and Veneziano model

Following the same arguements just mentioned, one may introduce the idea of duality between the resonance and Regge pole description of hadron collisions. The so called average or ~~local~~ weak duality implies that the Regge amplitude when extrapolated down to low energy region gives the average behaviour of the experimentally observed cross sections as a functions of energy.

Duality in a stricter sense (local or strong duality) means that Regge poles inferred from high energy data already contain all direct channel resonances and hence when projected out give rise to partial wave amplitudes, which generate loops in argond diagram, which correspond to the physical resonances[31]. Hence supporters of strong duality seriously object to the idea of interference model[6], which writes the amplitude as the sum of Regge plus resonance amplitude,

$$f = f_{\text{Regge}} + f_{\text{res.}} \qquad (2.56)$$

as double counting.

Several authors[32] have discussed about the possible connection

between the loops (Schmid loops) generated by Regge amplitude and legitimate resonances in s channel.
In the last chapter we shall remark about the relevance of local duality with respect to the results we obtained.

However one can say that there is not yet agreement in how far duality can be used, since no precise definitation for it is yet available.

Recently Veneziano[33] has proposed a model for invariant amplitudes which offers solutions exhibiting duality properties. It incorporates crossing symmetry, resonance behaviour in the narrow width approximation and asymptotic Regge behaviour for rising linear trajectories and automatically satisfies the usual finite energy sum rule. Veneziano amplitude for say π-π scattering is of the form

$$V_{xy}(s,t) = -\lambda \frac{\Gamma(1-\alpha_x(s))\,\Gamma(1-\alpha_y(t))}{\Gamma(1-\alpha_x(s)-\alpha_y(t))} \qquad (2.57)$$

where x and y label the trajectories exchanged in the s and t channel respectively.
The amplitude (2. 57) has no double poles since each pole should correspond to a particle.
When written in terms of Legendre polynomial it will correspond to a sum of parent and daughter contributions.

The main drawback of Veneziano model is its inconsistency with unitarity. If one introduces an analytic structure compatible with unitarity, for ex, introducing non linear trajectory,

$$\alpha(t) = \alpha(0) + \alpha'(t) + \frac{t^2}{\pi}\int_{t_0}^{\infty} \frac{\mathrm{Im}\,\alpha(t')}{t'^2(t'-(t+i\epsilon))}\,dt'$$

$$\mathrm{Im}\,\alpha(t) \neq 0, \text{ for } t > t_0$$

which preserves crossing symmetry, one also introduces ancestors since the residue at one pole will no longer be a polynomial in the crossed variable.

Much work has been done using a leading Veneziano term, to explore its application in hadron scattering. It is clear that any finite set of resonance widths can be fitted with a finite number of Veneziano terms and that an infinite set can also be fitted so long as the required infinite sum of Veneziano terms preserve the Regge behaviour of the individual term. Almost all applications of Veneziano model however have been in pion - pion scattering (or interactions which can be treated on the same footing as the pion - pion scattering). Extension of Veneziano model in πN scattering introduces some problems because of spin. However simple Veneziano type form (taking more than one term) has been explored by a few authors[34] in the case of πN scattering. The result is far from conclusive.

The model itself, nevertheless, provides scopes for

further interesting investigations in many cases including that of pion - nucleon scattering.

CHAPTER III

REGGE POLES IN PION-NUCLEON SCATTERING

REGGE POLE IN PION-NUCLEON SCATTERING

Introduction:

In this chapter we shall present the form of the exact Regge amplitude for pion-nucleon scattering in direct channel, there by deriving u channel Regge amplitudes. We shall also obtain the t channel Regge amplitudes.

1. We write the total amplitude $F(s,t,u)$ as

$$F(s,t,u) = F_p(s,t,u) + F_R(s,t,u) \qquad (3.1)$$

where F_R represents the Regge amplitude.
We can split up F_R in to two parts

$$F_R(s,t,u) = F_t(s,t) + F_u(s,u)$$

F_t and F_u being the Regge pole contributions from t channel and u channel respectively. We start with the partial wave expansions of the amplitudes f_1 and f_2

$$f_1 = \sum_J a_-^J P'_{J+\frac{1}{2}}(z) - \sum_J a_+^J P'_{J-\frac{1}{2}}(z)$$
$$f_2 = \sum_J a_+^J P'_{J+\frac{1}{2}}(z) - \sum_J a_-^J P'_{J+\frac{1}{2}}(z) \qquad (3.2)$$

One can check that these equations are identical with those in (1.36)

where

$$a^J_- = f_{\not 0} + \qquad (3.3)$$

$$a^J_+ = f_{\not 2} -$$

$$z = \cos\theta = 1 + (2m^2 + 2\mu^2 - s - u)/\,2q^2 \qquad (3.4)$$

The quantities in the 2nd term on the r.h.s. of (3.4) are the same as defined in Chapter I.

Now if we make an S.W. transformation of (3.2) in terms of even ($J = 1/2, 5/2, 9/2\ldots$) and odd ($J = 3/2, 7/2\ldots.$) J parity and use the superscripts e and ϕ for odd and even respectively to $a^J_\pm$, we get, following V. Singh[35]

$$\begin{aligned} f_{1,2}(\sqrt{s},u) = {} & \mp i/4 \int_c \frac{dJ}{\cos\pi J}\, a^e_-(J,\sqrt{s})\left[P'_{J\pm 1/2}(-z) \pm P'^{(z)}_{J\pm 1/2}\right] \\ & \pm i/4 \int_c \frac{dJ}{\cos\pi J}\, a^\phi_-(J,\sqrt{s})\left[P'_{J\pm 1/2}(-z) \mp P'^{(z)}_{J\pm 1/2}\right] \\ & \mp i/4 \int_c \frac{dJ}{\cos\pi J}\, a^e_+(J,\sqrt{s})\left[P'_{J\mp 1/2}(-z) \mp P'^{(z)}_{J\mp 1/2}\right] \\ & \mp i/4 \int_c \frac{dJ}{\cos\pi J}\, a^\phi_+(J,\sqrt{s})\left[P'_{J\mp 1/2}(-z) \pm P'^{(z)}_{J\mp 1/2}\right] \end{aligned} \qquad (3.5)$$

where $a_{\pm}^{e,\phi}(J, \sqrt{s})$ are the analytical continuation of $a_{\pm}^{Je,\phi}$ in the complex J plane, obtained in the same manner as discussed in Chapter II. Now we straighten out the contour C to go along the imaginary axis and we get for a typical fermion Regge pole at $J = \alpha(\sqrt{s})$ with signature $\tau = (-1)^{J-1/2}$ and parity $P = (-1)^{\ell+1}$

$$
\begin{aligned}
f_1(\sqrt{s},u) = {} & i/4 \int_{-i\infty}^{i\infty} \frac{dJ}{\cos\pi J} \cdot a_\nu(J,\sqrt{s})\left[P'_+(-z) + \tau P'_+(z)\right] \\
& - i/4 \int_{-i\infty}^{i\infty} \frac{dJ}{\cos\pi J} \cdot a_\nu(J,\sqrt{s})\left[P'_-(-z) - \tau P'_-(z)\right] \\
& + \frac{(E_s+m)}{\sqrt{s}} \frac{\beta(\pm\sqrt{s})}{\cos\pi\alpha(\pm\sqrt{s})} \left(\frac{q^2}{s_0}\right)^{\alpha(\pm\sqrt{s})-1/2} \left[P'_{\alpha(\pm\sqrt{s})+1/2}(-z) \right. \\
& \left. + \tau P'_{\alpha(\pm\sqrt{s})+1/2}(z)\right] \\
& - \frac{(E_s+m)}{\sqrt{s}} \frac{\beta(\mp\sqrt{s})}{\cos\pi\alpha(\mp\sqrt{s})} \left(\frac{q^2}{s_0}\right)^{\alpha(\mp\sqrt{s})-1/2} \left[P'_{\alpha(\mp\sqrt{s})-1/2}(z)\right]
\end{aligned}
\tag{3.6}
$$

where $P'^{\pm}(z) \equiv P'_{J\pm 1/2,}(z)$, s_0 is a scale factor,

$E_s = (s + m^2 - u^2)/2\sqrt{s}$

ν = + or - according to whether $\ell = J + 1/2$ or

$\ell = J - 1/2$

Upper sign in the argument of α and β is for $\tau P = -1$ while the lower sign is to be taken for $\tau P = +1$, also we have made use of Macdowells symmetry (1.39) viz

$a_\gamma (J, \sqrt{s}) = -a_{-\gamma} (J, -\sqrt{s})$

so that for every pole in $a_\gamma (J, \sqrt{s})$ there is a pole in $a_{-\gamma} (J, \sqrt{s})$, also we have

$$f_2(\sqrt{s}, u) = - f_1(-\sqrt{s}, u) \qquad (3.7)$$

and hence knowing f_1 one can obtain f_2.

$\beta(\sqrt{s})$ is the residue of the pole and defined by

$$\beta(\sqrt{s}) = \lim_{J \to \alpha} \frac{\Pi \sqrt{s} (J-\alpha) a_\gamma (J, \sqrt{s})}{2 (E_0 + m) \left(q^2/s_0\right)^{\frac{J(\sqrt{s})-1/2}{2}}} \qquad (3.8)$$

Here $\beta(\sqrt{s})$ is so defined as to avoid any kinematic singularity.

2. U channel Regge Amplitude

Since u channel in π N scattering is the crossed s channel, the Regge pole formalism in u channel is similar to that of s channel.

$$\pi^+ + P \longleftrightarrow \pi^+ + P \qquad \overset{s \longleftrightarrow u}{\longleftrightarrow} \qquad \pi^- + P \longrightarrow \pi^- + P$$

$$\pi^- + P \longrightarrow \pi^- + P \qquad \overset{s \longleftrightarrow u}{\longleftrightarrow} \qquad \pi^+ + P \longrightarrow \pi^+ + P$$

and the C.E. process

$$\pi^- + p \to \pi^0 n \quad \underset{s \longleftrightarrow u}{\longleftrightarrow} \quad \pi^0 + p \to \pi^+ + n$$

We define amplitudes $f_1^u(\sqrt{u},s)$ $f_2^u(\sqrt{u},s)$ as follows

$$f_u(\sqrt{u},s) = f_1^u(\sqrt{u},s) + f_2^u(\sqrt{u},s)\cos\theta + i\sin\theta\ \vec{\sigma}\cdot\hat{n}\, f_2(\sqrt{u},s) \tag{3.9}$$

Now in (3.6) replacing $\sqrt{s}$ by $\sqrt{u}$ and neglecting the background integral, we get the contribution to the amplitude $f^u_{1,2}(\sqrt{u},s)$ for a fermion pole in u channel with signature $\zeta = (-1)^{J-1/2}$, Parity $P = (-1)^{\ell+1}$ as

$$f^u_{1,2}(\sqrt{u},s) = \frac{K(\pm\sqrt{u})}{\cos\pi\alpha(\pm\sqrt{u})}\left[P'_{\alpha(\pm\sqrt{u})+1/2}(-z_u) + P'_{\alpha(\pm\sqrt{u})+1/2}(z_u)\right]$$

$$- \frac{K(\mp\sqrt{s})}{\cos\pi\alpha(\mp\sqrt{u})}\left[P'_{\alpha(\mp\sqrt{u})-1/2}(-z_u) + P'_{\alpha(\mp\sqrt{u})-1/2}(z_u)\right] \tag{3.10}$$

where z in (3.6) is replaced by z_u, the cosine of the scattering angle in u channel.

$$z_u = -\left(s - m^2 - \mu^2 + \frac{u}{2} - \frac{(m^2-\mu^2)}{2u}\right) / 2q_u^2 \tag{3.11}$$

q_u^2 = c.m. momentum in u channel

$$= (u - 2m^2 - 2\mu^2 + (m^2 - \mu^2)^2/u)/4 \qquad (3.12)$$

and $$K(\sqrt{u}) = \frac{E_u + m}{\sqrt{u}} \frac{\beta(\sqrt{u})}{\cos\pi\alpha(\sqrt{u})} \left(\frac{q_u^2}{s_0}\right)^{\alpha(\sqrt{u})-1/2} \qquad (3.13)$$

where $$E_u = (u + m^2 - \mu^2)/(2\sqrt{u}) \qquad (3.14)$$

The upper sign in the arguments of α and β in the r.h.s. of (3.10) is to be taken for $\tau P = -1$ and the lower sign for $\tau P = +1$.

From the crossing of s and u channels (see Appendix II) we get

$$f_1^u(\sqrt{s},u) = \frac{(E_s+m)}{2\sqrt{s}}\left[(\sqrt{u}-\sqrt{s}+2m) f_1^u(\sqrt{u},s)\frac{}{E_u+m}\right.$$

$$\left. + (\sqrt{u}+\sqrt{s}-2m) \frac{f_1^u(-\sqrt{u},s)}{E_u-m}\right] \qquad (3.15)$$

where $f_1^u(\sqrt{s}, u)$ denotes the contribution to the amplitude $f_1(\sqrt{s}, u)$ as defined in (1.31) from u channel only.

Using the Macdowell symmetry[8] $f_1(\sqrt{u}, s) = -f_2(-\sqrt{u}, s)$ we obtain from (3.10) and (3.15)

$$f_1^n(\sqrt{s},n) = \left[\frac{(E_n+m)}{2\sqrt{s}}\left[\frac{(\sqrt{n}-\sqrt{s}+2m)}{\sqrt{n}}\right]\left[\frac{\beta(\pm\sqrt{n})}{\cos n\alpha(\pm\sqrt{n})}\left(\frac{q_n^2}{s_0}\right)^{\alpha(\pm\sqrt{n})-1/2}\right.\right.$$

$$\left.\times\left[\left(1+\tau e^{-in(\alpha(\pm\sqrt{n})-1/2)}\right)P'^{(-z)}_{\alpha(\pm\sqrt{n})+1/2}\right]\right.$$

$$\left.-\frac{(E_n-m)}{(E_n+m)}\frac{\beta(\mp\sqrt{n})}{\cos n\alpha(\mp\sqrt{n})}\left(\frac{q_n^2}{s_0}\right)^{\alpha(\mp\sqrt{n})-1/2}\left(1+\tau e^{-in(\alpha(\mp\sqrt{n})-1/2)}\right)P'^{(-z)}_{\alpha(\mp\sqrt{n})+1/2}\right]$$

$$+\frac{(E_n+m)}{2\sqrt{s}}\frac{(\sqrt{n}+\sqrt{s}-2m)}{\sqrt{n}}\left[\frac{\beta(-\tau\sqrt{n})}{\cos n\alpha(\mp\sqrt{n})}\left(\frac{q_n^2}{s_0}\right)^{\alpha(\mp\sqrt{n})-1/2}\left(1+\tau e^{-in(\alpha(\mp\sqrt{n})-1/2)}\right)P'^{(-z)}_{\alpha(\mp\sqrt{n})+1/2}\right.$$

$$\left.-\frac{(E_n+m)}{(E_n-m)}\frac{\beta(\mp\sqrt{n})}{\cos n\alpha(\mp\sqrt{n})}\left(\frac{q_n^2}{s_0}\right)^{\alpha-1/2}\left(1+\tau e^{-in(\alpha-1/2)}\right)P'^{(-z)}_{\alpha-1/2}\right] \qquad (3.16)$$

we took

$$\alpha \equiv \alpha(\pm\sqrt{n}) \qquad \bar{\alpha} \equiv \alpha(\mp\sqrt{n})$$

$$\beta \equiv \beta(\pm\sqrt{n}) \qquad \bar{\beta} \equiv \beta(\mp\sqrt{n}) \qquad (3.17)$$

Also we have used

$$P'_{\alpha+1/2}(+z) = e^{-in(\alpha+1/2)}P'_{\alpha+1/2}(-z)$$

$$P'_{\alpha-1/2}(+z) = -e^{-in(\alpha-1/2)}P'_{\alpha-1/2}(-z) \qquad (3.18)$$

neglecting the term with $P'_{\alpha - 1/2}(-z)$, which is small compared with $P'_{\alpha + 1/2}(-z)$ we get [36]

$$f_1^{\mu}(\sqrt{s},u) = \frac{(E_s+m)(\sqrt{u}-\sqrt{s}+2m)}{2\sqrt{su}} \frac{\beta}{\cos n\alpha} \left(\frac{q_u^2}{s_0}\right)^{\alpha-1/2} \left(1+\tau e^{-in(\alpha-1/2)}\right) \cdot P'_{\alpha+1/2}(-z)$$

$$+ \frac{(E_s+m)}{2\sqrt{su}} \frac{(\sqrt{u}+\sqrt{s}-2m)}{\cos n\bar{\alpha}} \left(\frac{q_u^2}{s_0}\right)^{\bar{\alpha}-1/2} \left(1+\tau e^{-in(\bar{\alpha}-1/2)}\right) \cdot P'_{\bar{\alpha}+1/2}(-z) \qquad (3.19)$$

Now if we assume that the asymptotic behaviour of Legendre functions for large values of the argument holds in this case, we have [37]

$$P'_{\alpha+1/2}(z_u) \sim \frac{2\Gamma(\alpha+1)}{\Gamma(1/2)\Gamma(\alpha+1/2)} (2z_u)^{\alpha-1/2}$$

$$z_u \sim \left(-\frac{s-m^2-\mu^2}{2q_u^2}\right)$$

$$\therefore P'_{\alpha+1/2}(-z_u) \sim \frac{2\Gamma(\alpha+1)}{\Gamma(1/2)\Gamma(\alpha+1/2)} \left(\frac{s}{q_u^2}\right)^{\alpha-1/2} \qquad (3.20)$$

Now the factor $1/\Gamma(\alpha+1/2)$ produces zeroes at $\alpha = -1/2, -3/2..$ and $\Gamma(\alpha+1)$ has unphysical poles at $\alpha = -1, -2.....$ which must be cancelled by β. We define, following Berger and Cline[6] a reduced residue function $\gamma(\sqrt{u})$ as

follows

$$\gamma(\sqrt{u}) = 2\beta(\sqrt{u})\,\Gamma\left(\left(\alpha(\sqrt{u})+1\right)\right) / \Gamma(1/2)\,\Gamma\left(\alpha(\sqrt{u})+1/2\right) \tag{3.21}$$

replacing $\beta(\sqrt{u})$ in (3.19) with the help of the equation (3.21) and using (3.20)we get

$$f_1^u(\sqrt{s},u) = \left[\frac{\left((\sqrt{s}+m)^2-\mu^2\right)\left[\sqrt{u}-\sqrt{s}+2m\right]}{4\,s\sqrt{u}\,\cos\pi\alpha(\sqrt{u})}\,\gamma(\sqrt{u})\cdot\left(\frac{s}{s_0}\right)^{\alpha(\sqrt{u})-1/2}\left(1+\tau e^{-i\pi\left(\alpha(\sqrt{u})-1/2\right)}\right)\right.$$

$$\left. + \frac{\left((\sqrt{s}+m)^2-\mu^2\right)\left(\sqrt{u}+\sqrt{s}-2m\right)}{4\,s\sqrt{u}\,\cos\pi\alpha(-\sqrt{u})}\,\gamma(-\sqrt{u})\left(\frac{s}{s_0}\right)^{\alpha(-\sqrt{u})-1/2}\left(1+\tau e^{-i\pi\left(\alpha(\sqrt{u})-1/2\right)}\right)\right] \tag{3.22}$$

We kept only one sign in the argument of γ and β because the formula (3.22) is valid both for poles at

$\alpha(\sqrt{u}) = J$ and $\alpha(-\sqrt{u}) = J$

Now in pion - nucleon scattering three trajectories can be exchanged (viz. N_α , N_γ and Δ_δ) in the backward region. We took only N_α and $\Delta\delta$ which proved sufficient[39] to explain high energy backward π N scattering.

Parameterization of α and γ

A linear parameterization for $\alpha_{\Delta\delta}$ produces a

dip in π^- P backward scattering at high energy at about u = - 1.8. No such dip was observed in the experimental data[40]. So like Barger and Cline[41] we took nonlinear trajectories both for Δ_δ and N_α for negative values of u. We actually chose to take

$$\alpha_i(\sqrt{u}) = \alpha_i(0) + b_i\sqrt{u} + c_i u, \quad u > 0$$
$$= \frac{\alpha_i(0) + c_i u + e_i u^3}{1 + d_i u^2}, \quad u < 0 \qquad (3.23)$$

In addition $\alpha_{\Delta_\delta}(\sqrt{u})$ was constrained to pass through values of 3/2 and 7/2 at $\sqrt{u}$ = 1.236 and 1.946 respectively in order to guarantee the well established $\Delta_\delta(1236)$ and $\Delta_\delta(1946)$ resonances. $\alpha_{N_\alpha}(\sqrt{u})$ was similarly constrained to pass through 1/2 and 5/2 at $\sqrt{u} = -0.939$ and -1.692 respectively because of the nucleon and the N_α (1692). resonance.

The residue functions $\gamma_{\Delta,N}(\sqrt{u})$ were taken to be of the form $\gamma_{\Delta,N}(\sqrt{u}) = A_{\Delta,N}(\sqrt{u})\,\gamma'_{\Delta,N}(\sqrt{u})$

where

$$A_{\Delta,N}(\sqrt{u}) = \left(\alpha_{\Delta,N}(\sqrt{u}) + 1/2\right)\left(\alpha_{\Delta,N}(\sqrt{u}) + 3/2\right), \quad \alpha_{\Delta,N} \geq -3/2$$
$$= \frac{1}{\pi}\cos\pi\alpha_{\Delta,N}(\sqrt{u}), \quad \alpha_{\Delta,N} \leq -3/2 \qquad (3.24)$$

we write further $\overline{\beta}_\Delta(\sqrt{u}) = \gamma'_\Delta(\sqrt{u})$

and

$$\overline{\beta}_N(\sqrt{u})\,(\sqrt{u} - \sqrt{u_0}) = \gamma'_N(\sqrt{u})$$

where u_0 is defined by $\alpha_N(\sqrt{u_0}) = \frac{1}{2}$. Both residues of an exponential type and those represented by polynomial expressions were investigated and solutions obtained. In continuation to lower energies the polynomial expressions appeared to be superior and we finally employed the forms

$$\bar{\beta}_{\Delta,N}(\sqrt{u}) = a'_{\Delta,N}\left(1 + b'_{\Delta,N}\sqrt{u} + c'_{\Delta,N}u\right) \tag{3.25}$$

In the fits we constrained the N_α residue parameters by requiring that

$$\gamma_N(-0.939) = \frac{3\pi}{4} g^2 \left.\frac{d\alpha_N}{d\sqrt{u}}\right|_{\sqrt{u}=-0.939} \tag{3.26}$$

where g^2 is the renormalised πNN coupling constant. We fitted the latest data[40] available (at the time the work was being done) with $P_{Lab} \geq 5.9$ GeV/c and $|u| < 3.0$ GeV^2. The Δ_δ parameters were obtained first by fitting the near backward π^- P data alone, after which they were held fixed and the N_α parameters obtained by fitting the near backward π^+ P data.

The final fits to the data are shown in figs 2(a-c) and the Δ_δ and N_α trajectories predicted are shown in figs 3a and 3b.

The values obtained for the independent parameters are shown in table 3.

TABLE 3

$\alpha_\Delta(0) = 0.187$	$\alpha_N(0) = 0.366$
$d_\Delta = 0.539$ GeV^{-4}	$d_N = 0.044$ GeV^{-4}
$e_\Delta = 0.087$ GeV^{-6}	$e_N = 0.005$ GeV^{-6}
$a'_\Delta = 2.278$ $\mu b^{1/2}$	$a'_N = 293.2$ $\mu b^{1/2}$ GeV^{-1}
$b'_\Delta = 2.642$ GeV^{-1}	$b'_N = -0.159$ GeV^{-1}
$c'_\Delta = -1.662$ GeV^{-2}	

3. 't' channel amplitudes

The Regge poles in t channel are dominant in the high energy forward elastic pion-nucleon scattering.

We shall derive the contributions of t channel Regge poles to the full amplitude f(s,z) by making use of the fact that A(s,t,u) and B(s,t,u), the amplitudes defined in (1.10) are invariant.

Hence we make partial wave decomposition of $A^{\pm}$, $B^{\pm}$ (as defined in (1.25))in t channel as follows

$$A^{\pm}(s,u,t) = \frac{8\pi}{p_t^2} \sum (J+\tfrac{1}{2}) (p_t q_t)^J \left[\frac{m \cos\theta_t}{(J(J+1))^{1/2}} P'_J(\cos\theta_t) f_-^{\pm J}(t) - P_J(\cos\theta_t) f_+^{\pm J}(t) \right]$$

$$B^{\pm}(s,u,t) = 8\pi \sum \frac{(J+\tfrac{1}{2})}{[J(J+1)]^{1/2}} (p_t q_t)^{J-1/2} P'_J(\cos\theta_t) f_-^{\pm J}(t)$$

(3.27)

where P_t, q_t and $\cos\theta_t$ are the same as defined in (2.21) and the amplitudes $f_{\pm}^{\pm J}$ are related to the partial wave amplitudes in the following way[42]

$$f_+^{\pm J}(t) = \frac{1}{8\pi} \left(-\frac{p_t^2}{(p_t q_t)^J} A_J^{\pm} + \frac{m}{(2J+1)(p_t q_t)^{J-1}} \times \left[(J+1) B_{J+1}^{\pm} + J B_{J-1}^{\pm} \right] \right)$$

$$f_-^{\pm J}(t) = -\frac{1}{8\pi} \left[\left(\frac{(J(J+1))^{1/2}}{(2J+1)} \right) \frac{1}{(p_t q_t)^{J-1}} \left(B_{J-1}^{\pm} - B_{J+1}^{\pm} \right) \right] \qquad (3.28)$$

$$(A_J^{\pm}, B_J^{\pm}) = \int_{-1}^{1} d\lambda P_J(\lambda) (A^{\pm}, B^{\pm}) \qquad (3.29)$$

The sums over J run through J = 0,2,4.... for A^+ and B^+ (i.e. I = 0 in t channel) and J = 1,3.. for A^-, B^- (I = 1)

One can avoid the fixed branch points of $f_{-}^{\pm J}(t)$ at J = 0 and J = -1 by using a new amplitude $f_{n-}^{\pm J}$ defined by

$$f_{n-}^{\pm(J)} = \frac{(J + 1/2)}{[(J(J+1)]} 1/2 \; f_{-}^{\pm(J)} \qquad (3.30)$$

Then we consider the analytical continuation of $f_{+}^{\pm J}$ and $f_{n-}^{\pm(J)}$ instead of $f_{\pm}^{\pm(J)}$ in the complex J plane.

Using equation (3.28)

$$f_{n-}^{\pm(J)} = \frac{B_{J-1}^{(\pm)} - B_{J+1}^{(\pm)}}{16 \; \pi (p_t q_t)^{J-1}} \qquad (3.31)$$

Using Mandelstam representations for $A^{\pm}$, $B^{\pm}$ we can write the fixed energy dispersion relations of the type

$$A^{\pm}(s,u,t) = \frac{1}{\pi}\int \frac{A_s^{\pm}(s',t)\,ds'}{s'-s} + \frac{1}{\pi}\int \frac{A_u^{\pm}(u',t)}{u'-u}\,du'$$

$$B^{\pm}(s,u,t) = \frac{1}{\pi}\int \frac{B_s^{\pm}(s',t)}{s'-s}\,ds' + \frac{1}{\pi}\int \frac{B_u^{\pm}(u',t)}{u'-u}\,du' \qquad (3.32)$$

Now $A^{\pm}_{J} = \int_{-1}^{1} dx \; A^{\pm}(s,u,t) \; P_J(x)$

Using (3.32)

$$= \int_{-1}^{1} \int \frac{A_s^{\pm}(s',t)}{(s'-s)} P_J(x)\, dx\, ds' + \cdots$$

Interchanging the order of integration and writing

$$x = \frac{s + p_t^2 + q_t^2}{2 p_t q_t}$$

$$A^{\pm}_{J} = -\int\int_{-1}^{1} \frac{A_s^{\pm}(s',t)\, P_J(x)\, dx}{2 p_t q_t \left(x - \frac{(s' + p_t^2 + q_t^2)}{2 p_t q_t}\right)} ds' + \cdots$$

since

$$-\frac{1}{2}\int_{-1}^{1} \frac{P_n(x)}{x - x_1} = Q_n(x_1)$$

$$A^{\pm}_{J} = \frac{1}{q_t p_t} \int A^{\pm}_{s}(s',t)\, Q_J\left(\frac{s' + p_t^2 + q_t^2}{2 p_t q_t}\right)\left(1 \pm (-1)^J\right) ds'$$

Similarly

$$B^{\pm}_{J} = \frac{1}{q_t p_t} \int B_s^{\pm}(s',t)\, Q_J\left(\frac{s' + p_t^2 + q_t^2}{2 p_t q_t}\right)\left(1 \mp (-1)^J\right)$$

(3.33)

To derive (3.33) we have used the crossing relations viz $A^{\pm}(s,u,t) = \pm A^{\pm}(u,s,t)$ and $B^{\pm}(s,u,t) = \mp B(u,s,t)$ and the fact that when $s \to u$ $\cos\theta \to -\cos\theta$ which explains the term $(-1)^J$ in (3.33) ($P_J(-\cos\theta) = (-1)^J P_J(\cos\theta)$)

Hence the crossing relations imply that

$$\text{for J even} \qquad A_J^- = B_J^+ = 0$$

$$\text{for J odd} \qquad A_J^+ = B_J^- = 0$$

Now from equation (3.33) we can see that apart from the factor $(1 \pm (-1)^J)$ $f_+^{\pm}(J)$, $f_{\eta-}^{\pm}(J)$ define analytic continuations which are suitable for Sommerfield - Watson transformation.

Thus as in Chapter II we define the even and odd J parity continuations by replacing $(-1)^J$ by $+1$ (for J = even) and -1 (J = odd)

This makes the odd J parity continuation for I = 0 and the even J parity continuation for I = 1 vanish identically. So only one of the J parity continuation for each isospin amplitude is non zero.

Now we Reggeise the amplitudes A and B.

Following Singh[35] and subsequent authors we define an amplitude

$$A' = A + \frac{\omega + t/4m}{1 - t/4m^2} B \qquad (3.34)$$

where $\omega = \frac{(s - m^2 - \mu^2)}{2m}$ = the pion laboratory energy.

From (3.27) A' can be calculated

$$A'^{\pm}(s,t) = -\frac{8\pi}{p_t^2}\sum_J (p_t q_t)^J (J+1/2) f_+^{(\pm)J} P_{J-1}(\cos\theta_t)$$
$$B^{\pm}(s,t) = 8\pi \sum_J (p_t q_t)^{J-1} f_{n-}^{(\pm)J} P'_J(\cos\theta_t) \qquad (3.35)$$

as in Chapter II we can make an S.W. transformation and write

$$A'^{\pm}(s,t) = -\frac{2\pi i}{p_t^2}\int_C \frac{(p_t q_t)^J (J+1/2)}{\sin\pi J} f_+^{(\pm)J}\left(1 \pm (-1)^J\right) P_J(\cos\theta_t)\, dJ$$
$$B^{\pm}(s,t) = 2\pi i \int_C \frac{(p_t q_t)^{J-1}(J+1/2)}{(J+1/2)\sin\pi J} f_{n-}^{(\pm)J}\left(1 \mp (-1)^J\right) P'_J(\cos\theta_t)\, dJ \qquad (3.36)$$

as usual deforming the contour so as to include Regge poles and assuming that high energy forward scattering (i.e. for large cos θ_t values) is dominated by t channel Regge poles we get for a typical t channel Regge pole

$$A'^{\pm}(s,t) = \frac{4\pi^2}{p_t^2} \beta_+^{\pm} \frac{(p_t q_t)^{\alpha^{\pm}(t)}(\alpha^{\pm}+1/2)}{\sin\pi\alpha^{\pm}(t)} \left[P_{\alpha^{\pm}}(-z_t) \pm P_{\alpha^{\pm}}(z_t)\right]$$
$$B^{\pm}(s,t) = -4\pi^2 \left(\frac{p_t q_t}{m}\right)^{\alpha^{\pm}(t)-1} \beta_-^{\pm} \frac{\left[P'_{\alpha^{\pm}}(-z_t) \mp P'_{\alpha^{\pm}}(z_t)\right]}{\sin\pi\alpha^{\pm}(t)} \qquad (3.37)$$

where α_+ and α_- are Regge trajectories that are most important for the isospin zero $\pi + \pi \to N + \bar{N}$ channel and for the isospin one $\pi + \pi \to N + \bar{N}$ channel respectively. The residues $b_+^{\pm}(t)$, $b_-^{\pm}(t)$ are defined by

$$b_+^{\pm}(t) = \lim_{J \to \alpha_\pm(t)} \left\{ m^J f_+^{(\pm)J}(t) [J - \alpha_\pm(t)] \right\}$$

$$b_-^{\pm}(t) = \lim_{J \to \alpha_\pm(t)} \left\{ m^{J-1} (f_-^{\pm(J)}(t) [J - \alpha_\pm(t)] \right\} \tag{3.38}$$

For high energy, $\cos\theta_t$ is large and we can use the Regge asymptotic behaviour

$$P_\alpha(z) \sim z^\alpha$$

Since

$$\cos\theta_t = \frac{s + p_t^2 + q_t^2}{2 p_t q_t} = \frac{s + t/2 - (m^2 + \mu^2)}{2\sqrt{(t/4 - m^2)(t/4 - \mu^2)}} \tag{3.39}$$

for $s \gg 1$, $\cos\theta_t \sim \frac{s - m^2}{2 p_t q_t} \sim \frac{2m\omega}{2 p_t q_t} = \frac{m\omega}{p_t q_t}$

where ω is the pion lab en.

Using the property of Legendre functions

$$P_\alpha(-z) \sim e^{-i\pi\alpha} P_\alpha(z)$$

we can write (3.37) as

$$A'^{\pm} = c^{\pm}(t)\left(\frac{\omega}{\omega_0}\right)^{\alpha^{\pm}(t)}\left[\frac{\pm 1 \mp e^{-in\alpha^{\pm}(t)}}{\sin n\alpha^{\pm}(t)}\right]$$

$$B^{\pm} = D^{\pm}(t)\left(\frac{\omega}{\omega_0}\right)^{\alpha^{\pm}(t)}\left[\frac{\pm 1 \mp e^{in\alpha^{\pm}(t)}}{\sin n\alpha^{\pm}(t)}\right] \qquad (3.40)$$

where $c^{\pm}$ and $D^{\pm}$ are linearly related to $b_+^{\pm}$ and $b_-^{\pm}$ respectively and ω_0 is a scale factor which we choose to be equal to 1 GeV.

In case of π N scattering the contribution of each t channel Regge pole i to A' and B is taken to be

$$A'_i = -c_i(t)\left[\left(e^{in\alpha_i} \pm 1\right)/\sin n\alpha_i\right]\left(\frac{\omega}{\omega_0}\right)^{\alpha_i}$$

$$B_i = -D_i(t)\left[\left(e^{-in\alpha_i} \pm 1\right)/\sin n\alpha_i\right]\left(\frac{\omega}{\omega_0}\right)^{\alpha_i} \qquad (3.41)$$

where the + sign in the firstbracket of the r.h.s. of Equation (3.41) is to be taken for I = 0 poles and the - sign for I = 1 poles.

We assume that the usual P, P' and φ Regge poles are adequate to describe the high energy forward scattering data for the three processes $\pi^{\pm}$ P $\longrightarrow$ $\pi^{\pm}$ P and

$\pi^- + p \rightarrow \pi^0 + n$. The works of previous authors have established that this is perhaps the minimum number needed. But a model in which only P, P' and f Regge poles are retained predicts zero polarization in the charge exchange process at high energy. Experimentally polarization is observed and this has been explained in various ways, for example the contribution of another I = 1 trajectory can be added to the amplitude or the effect may be due to cuts or the background contributions from the background integral.[43]

We slightly improved our fits to the high energy pion nucleon scattering data by taking the first of the prescriptions mentioned above. The over all fits didn't change much even after adding the extra I = 1 pole though it gave the correct polarization in the charge exchange process at high energy.

The P, P' and f poles contribute to the amplitude A as follows (and similar for B)

$$A'(\pi^- + p \rightarrow \pi^- + p) = A'_P + A'_{P'} + A'_f + A'_{f'}$$

$$A'(\pi^+ + p \rightarrow \pi^+ + p) = A'_P + A'_{P'} - A'_f - A'_{f'}$$

$$A'(\pi^- + p \rightarrow \pi^0 + n) = -\sqrt{2}\left(A'_\rho + A'_{\rho'}\right) \qquad (3.42)$$

For the residue functions $C_i(t)$ $D_i(t)$ we took the parametric forms[44]

$$C_i(t) = C_0 \exp(C_1 t)\gamma_\alpha \quad , P, P'$$
$$= C_0' \{\tfrac{1}{2}(1+C_2)\exp(C_1 t) - C_2\}\gamma'_\alpha \quad , \rho$$

$$D_i(t) = D_0 \exp(D_1 t)\alpha(t)\gamma_\alpha \quad , P, P'$$
$$= D_0' \exp(D_1' t)\gamma_\alpha \quad , \rho$$

(3.43)

Also for ρ' we took

$$C_i(t) = C_0 e^{C_1 t}\gamma'_\alpha$$
$$D_i(t) = D_0 e^{D_1 t}\gamma_\alpha \qquad (3.44)$$

where γ_α contains zeroes for unphysical (γ_α and non sense values) of α i.e., $\alpha = -1, -2, \ldots$ and for a ghost state at $\alpha = 0$. We actually took

$$\gamma_\alpha = \alpha(\alpha+1) \quad , \alpha > -1$$
$$= +\frac{\sin\pi\alpha}{\pi} \quad , \alpha \leq -1$$
$$\gamma'_\alpha = \alpha+1 \quad , \quad \alpha > -1 \qquad (3.45)$$
$$= -\sin\pi\alpha/\pi \quad , \alpha \leq -1$$

We took the trajectories to be linear in t

$$\alpha_i(t) = a_i + b_i t$$

The data we fitted in order to obtain the t channel Regge poles was that for pion lab energy $P_L \geq 5.9$ GeV/c and for $|t| \leq 1$ GeV^2 and can be found in Ref.44.

We first fitted the charge exchange data alone in order to ascertain the ρ (and also ρ') parameters. Then we fitted all the $\pi^+ - P$ and $\pi^- - P$ high energy data to fix P, and P' parameters.

The best fit to the data is shown in fig 1(a - f).

The values of the parameters* are listed in Table 4.

TABLE 4

Trajectory	a	b $(GeV)^{-2}$	C_o (mb GeV)	C_1 (GeV^{-2})	C_2	D_o (mb)	D_1 $(GeV)^{-2}$
P	1.02	0.00	6.52	2.78	-	9.44	6.37
P	.78	1.4	13.66	.72	-	9.85	9.98
ρ	.577	.95	1.38	.211	15.527	27.50	.217
ρ'	-.404	1.435	-2.097	.106	-	124.97	16.06

*We got another set of solutions which was ruled out on the grounds that it failed to satisfy the finite energy sum rules of the type proposed by Barger and Phillips.[45]

CHAPTER IV

DIRECT CHANNEL AMPLITUDE.

PARAMETERISATION OF DIRECT CHANNEL AMPLITUDE

Introduction:

In this chapter we shall discuss the parameterisation of $F_p(s,t,u)$. As mentioned earlier, two ways of parameterisation $F_p(s,t\ u)$ were attempted; one based on the modified Regge pole in s channel and the other being a power series expansion in cos θ with energy dependent coefficients. Both the methods would be described in detail in the following.

1. Modified Regge pole method.

In this case $F_p(s,t,u)$ was taken to be the direct channel Regge pole contribution with Khuri modification as discussed in Chapter II.

For the sake of convenience we rewrite equation (3.6) which is a typical Regge pole contribution in s channel at $J = \alpha(\sqrt{s})$ with signature $\tau = (-1)^{J-1/2}$ and parity $P = (-1)^{\ell+1}$

$$f_1^P(\sqrt{s},u) = i/4 \int_{-i\infty}^{i\infty} \frac{dJ}{\cos\pi J} a_\nu(J,\sqrt{s}) [P'_+(-z) + \tau P'_+(z)]$$

$$-i/4 \int_{-i\infty}^{i\infty} \frac{dJ}{\cos\pi J} a_{-\nu}(J,\sqrt{s}) [P'_-(-z) - \tau P'(z)]$$

$$+ \left(\frac{E_s+m}{\sqrt{s}}\right) \frac{\beta(\pm\sqrt{s})}{\cos\pi\alpha(\pm\sqrt{s})} \left(\frac{q^2}{s_0}\right)^{\alpha(\pm\sqrt{s})-\nu_2} [P'_{\alpha(\pm\sqrt{s})+\nu_2}(-z) + \tau P'_{\alpha(\pm\sqrt{s})+\nu_2}(z)]$$

$$- \left(\frac{E_s-m}{\sqrt{s}}\right) \frac{\beta(\mp\sqrt{s})}{\cos\pi\alpha(\mp\sqrt{s})} \left(\frac{q^2}{s_0}\right)^{\alpha(\mp\sqrt{s})-\nu_2} [P'_{\alpha(\mp\sqrt{s})-\nu_2}(-z) - \tau P'_{\alpha(\mp\sqrt{s})-\nu_2}(z)] \quad (4.1)$$

where we have replaced f_1 by f_1^P and E_s, ν are same as defined in Chapter III. Also as before we get

$$f_2^P(\sqrt{s},u) = -f_1^P(-\sqrt{s},u) \quad (4.2)$$

by MacDowell symmetry.

Now let us define amplitudes F_1^P, F_2^P as follows

$$F_1^P(\sqrt{s},u) = f_1^P(\sqrt{s},u) + z f_2^P(\sqrt{s},u) \quad (4.3)$$

$$F_2^P(\sqrt{s},u) = z f_1^P(\sqrt{s},u) + f_2^P(\sqrt{s},u) \quad (4.4)$$

Now

$$F_1^P(-\sqrt{s},u) = f_1^P(-\sqrt{s},u) + z f_2^P(-\sqrt{s},u)$$

$$= -f_2^P(\sqrt{s},u) - z f_1^P(\sqrt{s},u) \quad (\text{eq. } 4.3)$$

$$= -[z f_1^P(\sqrt{s},u) + f_2^P(\sqrt{s},u)]$$

$$= -F_2^P(\sqrt{s},u)$$

$$\therefore F_2^P(+\sqrt{s},u) = -F_1^P(-\sqrt{s},u) \quad (4.5)$$

We need calculate only $F_1^P(s,u)$ in terms of $\sqrt{s}$ and z and we get back both $f_1^P(\sqrt{s},u)$ and $f_2^P(\sqrt{s},u)$ as follows

$$f_1^P(\sqrt{s},u) = (F_1 - zF_2)/(1-z^2) \qquad |z| \neq 1$$
$$f_2^P(\sqrt{s},u) = (zF_2 - F_1)/(z^2-1)$$

(4.6)

Now using (4.1), (4.3) and the well known Legendre formulae

$$P'_{J+1/2}(z) - z\,P'_{J-1/2}(z) = (J+1/2)\,P_{J-1/2}(z)$$

$$z\,P'_{J+1/2}(z) - P'_{J-1/2}(z) = (J+1/2)\,P_{J+1/2}(z)$$

(4.7)

We get

$$F_1^P(\sqrt{s},u) = i/4 \int_{-i\infty}^{i\infty} \frac{dJ\,(J+1/2)}{\cos \pi J}\, a_\nu(s,\sqrt{s}) \left[P_{J-1/2}(-z) + \tau\, P_{J-1/2}(z)\right]$$

$$+ i/4 \int_{-i\infty}^{i\infty} \frac{dJ\,(J+1/2)}{\cos \pi J}\, a_{-\nu}(s,\sqrt{s}) \left[P_{J+1/2}(-z) - \tau P_{J+1/2}(z)\right]$$

$$+ \frac{(E_\delta + m)\,\beta(\pm\sqrt{s})}{\sqrt{s}\cos \pi\alpha(\pm\sqrt{s})} \left(\frac{q^2}{s_0}\right)^{\alpha(\pm\sqrt{s})-1/2} \frac{1}{(\alpha(\pm\sqrt{s})+1/2)} \left[P^{(-z)}_{\alpha(\pm\sqrt{s})-1/2} + \tau\, P^{(z)}_{\alpha(\pm\sqrt{s})-1/2}\right]$$

$$+ \frac{(E_\delta - m)}{\sqrt{s}} \frac{\beta(\mp\sqrt{s})}{\cos \pi\alpha(\mp\sqrt{s})} \left(\frac{q^2}{s_0}\right)^{\alpha(\mp\sqrt{s})-1/2} (\alpha(\mp\sqrt{s})+1/2) \left[P^{(-z)}_{\alpha(\mp\sqrt{s})+1/2} - \left[P^{(z)}_{\alpha(\mp\sqrt{s})+1/2}\right]\right]$$

(4.8)

We can see that the last two terms in (4.8)* have cuts in the complex z plane starting at $z = \pm 1$. But we know that the correct thresholds in the z plane are given by

$$z = \cosh\zeta_1 \;, = 1 + 2\mu^2/q^2 \rightarrow \text{R.H. cut}$$

$$z = -\cosh\zeta_2 = -\left[(s-m^2-2\mu^2)/2q^2 - 1\right] \rightarrow \text{L.H. cut} \qquad (4.9)$$

Hence there must be cancellation of cuts between the first two terms and the last two terms in (4.8) in the region $1 \leq z \leq \cosh\zeta_1$ and $-\cosh\zeta_2 \leq z \leq -1$.

We apply Khuri's method to get this cancellation, which has been shown in the spinless case in Chapter II. Khuri's method in essence is to replace $P_\lambda(z)$ by $\Pi(\lambda, z)$ and $P_\lambda(-z)$ by $\Pi(\lambda, -z)$ in the last two terms of (4.8) and thus these transformed versions of the last two terms will represent the modified Regge representation with correct cuts, whence $\Pi(\lambda, z)$ and $\Pi(\lambda, -z)$ are defined by

$$\Pi^{\zeta_2}(\lambda, z) = P_\lambda(z) - \frac{\cos\pi(\lambda+1/2)}{2\sqrt{2}\,\pi(\lambda+1/2)} \int_0^\infty \frac{\exp\left((\lambda+1/2)x\right)\sinh x\,dx}{(\cosh x + z)^{3/2}}$$

$$\Pi^{\zeta_1}(\lambda, -z) = P_\lambda(-z) - \frac{\cos\pi(\lambda+1/2)}{2\sqrt{2}\,\pi(\lambda+1/2)} \int_{-\infty}^{0} \frac{\exp\left((\lambda+1/2)x\right)\sinh x\,dx}{(\cosh x - z)^{3/2}} \qquad (4.10)$$

[* This can be seen from equation (2.34), the r.h.s. being proportional to $\Pi^{3}_{\lambda}(-z)$]

Now we write $F_1^P(\sqrt{s},u)$ as this full "Regge pole contribution" in s channel to the exact amplitude $F_1(s,t,u)$ as follows. ($F_1^P(\sqrt{s},u)$ in this case represents the amplitude $F_1^P(s,t,u)$ mentioned earlier).

$$F_1^P(\sqrt{s},u) = \frac{K(\sqrt{s})(\alpha+V_2)}{\cos\pi\alpha}\left[\Pi^{3}_{1}((\alpha-V_2),-z)+\tau\,\Pi^{3}_{2}((\alpha-V_2),z)\right]$$

$$+\frac{K(-\sqrt{s})(\bar{\alpha}+V_2)}{\cos\pi\bar{\alpha}}\left[\Pi^{3}_{1}((\bar{\alpha}+V_2),-z)-\tau\,\Pi^{3}_{2}((\bar{\alpha}+V_2),z)\right] \qquad (4.11)$$

where $\bar{\alpha} \equiv \alpha(-\sqrt{s})$, $\alpha \equiv \alpha(+\sqrt{s})$

and

$$K(\sqrt{s}) = \frac{(E_1+m)}{\sqrt{s}}\,\beta(+\sqrt{s})\left(\frac{q^2}{s_0}\right)^{\alpha(+\sqrt{s})-V_2} \qquad (4.12)$$

We define the partial wave amplitude of $\Pi^{3}_{\ell}(z)$ as

$$\Pi^{3}_{\ell}(\lambda,s) = \frac{1}{2}\int_{-1}^{1}\Pi(\lambda,-z)\,P_\ell(z)\,dz \qquad (4.13)$$

We can evaluate the integral in (4.13) as in Chapter II (see Section 6 of Chapter II) and see that

$$\Pi^{3}_{\ell}(\lambda,s) = \frac{\sin\pi\lambda}{2\pi(\lambda+V_2)}\,\frac{\exp\left(-(\ell-\lambda)\xi\right)}{(\lambda-\ell)} \qquad (4.14)$$

Now by defination

$$\pi^{\}}(\lambda,-z) = \sum (2l+1)\, \pi_l^{\}}(\lambda, s)\, P_l(z) \tag{4.15}$$

Using (4.13)

$$\pi^{\}}(\lambda,-z) = \sum \frac{(2l+1)\sin\pi\lambda}{2\pi(\lambda+\nu_L)} \frac{\exp\{-(l-\lambda)\}}{(\lambda-l)} P_l(z)$$

$$\pi^{\}}(\lambda,+z) = \sum \frac{(-1)^l (2l+1)\sin\pi\lambda}{2\pi(\lambda+\nu_L)} \times \frac{\exp\{-(l-\lambda)\}}{(\lambda-l)} P_l(z) \tag{4.16}$$

[The last equation is obtained as follows

$$\pi^{\}}(\lambda,z) = \sum (2l+1)\left(\tfrac{1}{2}\int_{-1}^{1} \pi^{\}}(\lambda,z')\, P_l(z')\, dz'\right) P_l(z)$$

$$= \sum (2l+1)\left(\tfrac{1}{2}(-1)^l \int_{-1}^{1} \pi^{\}}(\lambda,-z')\, P_l(z')\, dz'\right) P_l(z)$$

$$= \sum \frac{(-1)^l (2l+1)\sin\pi\lambda}{2\pi(\lambda+\nu_L)} \frac{\exp\{-(l-\lambda)\}}{(\lambda-l)} P_l(z)\Big]$$

Hence from (4.11) and (4.16) we finally obtain

$$F_1^p(\sqrt{s},u) = \frac{K(\sqrt{s})(\alpha+\nu_L)}{2\pi\alpha} \sum_l \Phi_l(\alpha-\nu_L)\left[e^{-(l-\alpha+\nu_L)\}_1} + [(-1)^l e^{-(l-\alpha+\nu_L)\}_L}\right]$$

$$- \frac{K(-\sqrt{s})(\bar{\alpha}+\nu_L)}{2\pi(\bar{\alpha}+1)} \sum_l \Phi_l(\bar{\alpha}+\nu_L)\left[e^{-(l-\bar{\alpha}-\nu_L)\}_1} - [(-1)^l e^{-(l-\bar{\alpha}-\nu_L)\}_L}\right] \tag{4.17}$$

where

$$\Phi_\ell(\lambda) = \frac{(2\ell+1)}{(\ell-\lambda)} P_\ell(z) \qquad (4.18)$$

2. Parameterisation of Regge functions.

Now the problem is to find suitable form for β and α. The threshold behaviour of $\mathrm{Im}\,\alpha$ is[5]

$$\mathrm{Im}\,\alpha(\sqrt{s}) \sim (s-s_1)^{\alpha(0)+1/2} \qquad (4.19)$$

Also in Pion nucleon scattering we can exchange Δ σ, N_α, N_γ trajectories both in s and u channels. All the known resonances seem to lie on these three (or possibly more), Regge trajectories. We give a list[6] of these resonances together with the predicted higher resonances on those trajectories.

TABLE 5

Resonances (mass in MeV)	Spin-parity	Width (BeV)	Elasticity (from phase shifts)
$\Delta\delta(1236)$	$(3/2)^+$	.12	1.0
$\Delta\delta(1924)$	$(7/2)^+$	.17	.50
$\Delta\delta(2450)$	$(11/2)^+$	.28	-
$\Delta\delta(2840)$	$(15/2)^+$	.40	-
$\Delta\delta(3220)$	$(19/2)^+$	.44	-

Resonances (mass in MeV)	Spin-parity	Width(BeV)	Elasticity (from phase shifts)
N_α (938)	$(1/2)^+$	-	-
N_α (1688)	$(5/2)^+$	.10	.66
N_α (2220)	$(9/2)^+$	.20	-
N_γ (2610)	$(13/2)^+$	.30	-
N_γ (1512)	$(3/2)^-$	.12	.50 - .71
N_γ (2210)	$(7/2)^-$	.24	-
N_γ (2640)	$(11/2)^-$	.40	-
N_γ (3020)	$(15/2)^-$	.40	-
N_γ (3350)	$(19/2)^-$	.10	-

In Table 5 the spin parity assignments are based on the Chew-Frautschi plot of Regge recurrences.

The trajectories Re α_i are fixed by fitting the high backward data with proper constrains. We parameterise Im α_i and β_i in the following way.

$$\mathrm{Im}\,\alpha_i(\sqrt{s}) = \frac{a_i' s + b_i' \sqrt{s} + c_i'}{a_i^2 s + b_i^2 \sqrt{s} + c_i^2} (s - s_i)^{\alpha_{i0} + V_L} \tag{4.20}$$

$$\beta_i(\sqrt{s}) = \mathrm{Re}\,\beta_i \; e^{i\,\delta_i(\sqrt{s})} \tag{4.21}$$

$$\mathrm{Re}\,\beta_i(\sqrt{s}) = \frac{a_i s + b_i \sqrt{s} + c_i}{a_i' s + b_i' \sqrt{s} + c_i'}$$

$$\delta_i(\sqrt{s}) = \frac{A_i + B_i \sqrt{s}}{A_i' + B_i' \sqrt{s}} \qquad (4.22)$$

With the following constraints (see Appendix III)

$$\text{(I)} \qquad \mathrm{Im}\,\alpha_i(\sqrt{s}) = \frac{\Gamma_{tot}}{2} \frac{d\lambda_i}{d\sqrt{s}}\Big|_{\pm M_R} \qquad (4.23)$$

$$\text{(II)} \qquad \beta_i(\sqrt{s}) = \frac{n\sqrt{s}\,\Gamma_{el}}{4(E_R \mp M) R^{2l+1}} \frac{d\lambda_i}{d\sqrt{s}}\Big|_{\pm M_R}$$

at resonance position, M_R being the mass of the resonance and the upper and lower sign being for Δ and N_α trajectory respectively.

We constrain the Δ_δ and N_α trajectories to pass through the resonances ($\Delta_\delta(1236)$, $\Delta_\delta(1924)$) for Δ_δ and ($N_\alpha(938)$, $N_\alpha(1688)$) for N_α trajectory.
Now defining

$$\frac{a_i^1 s_{i1} + b_i^1 \sqrt{s_{i1}} + c_i^1}{a_i^2 s_{i1} + b_i^2 \sqrt{s_{i1}} + c_i^2} = A_1 \qquad (4.24)$$

and

$$\frac{a_i^1 s_{i2} + b_i^1 \sqrt{s_{i2}} + c_i^1}{a_i^2 s_{i2} + b_i^2 \sqrt{s_{i2}} + c_i^2} = A_2$$

where $\sqrt{s}_{i1}$, $\sqrt{s}_{i2}$ are the first two resonance positions on the trajectory α_i ,

and

$$A_1 = \frac{\tau_1}{2(s_{i1}-s_0)^{\alpha_{i0}+1/2}} \left.\frac{d\alpha_i}{d\sqrt{s}}\right|_{\sqrt{s}_{i1}}$$

$$A_2 = \frac{\tau_2}{2(s_{i2}-s)^{\alpha_{i0}+1/2}} \left.\frac{d\alpha_i}{d\sqrt{s}}\right|_{\sqrt{s}_{i2}} \qquad (4.25)$$

τ_1 , τ_2 being the widths of the resonances; we get after some algebraical manipulations

$$a_i^1 = \frac{\lambda_i \gamma_i' - \gamma_i \lambda_i'}{\eta_i \lambda_i' - \eta_i' \lambda_i}$$

$$a_i^2 = \frac{\gamma_i \eta_i' - \eta_i \gamma_i'}{\eta_i \lambda_i' - \eta_i' \lambda_i} \qquad (4.26)$$

where

$$\eta_i = s_{i1}, \quad \eta_i' = s_{i2}$$

$$\lambda_i = -A_1 s_{i1}, \quad \lambda_i' = -A_2 s_{i2}$$

$$\gamma_i' = (\ell_i^1 \sqrt{s}_{i1} + c_i^1) - A_1(\ell_i^2 \sqrt{s}_{i1} + c_i^2)$$

$$\gamma_i' = (\ell_i^1 \sqrt{s}_{i2} + c_i^1) - A_2(\ell_i^2 \sqrt{s}_{i2} + c_i^2) \qquad (4.27)$$

so that only four parameters out of six in (4.20) are varied. The remaining being determined from the constraints (4.26).

First we attempted to fit all $\pi^+ P$ data from 2 to 5 GeV/c allowing only 4δ trajectory to be exchanged in s channel.

The fit was not very successful, for though the forward and backward direction data were fitted well, the predicted cross sections apart from those regions were very small compared with rather large experimental results.

This clearly demonstrates the fact that the simple model of one trajectory exchange in s channel can't explain pion-nucleon scattering in the intermediate energy region. There may be two or more trajectories which are involved implying the presence of resonance structures in many higher order angular momentum states. But unless we get at least a rough idea about the partial waves for large ℓ in this region it will be difficult to decide which trajectories to be exchanged in s channel. Clearly, for this, Phase shift analysis is necessary in this region. But as we mentioned earlier conventional phase shift analysis becomes increasingly difficult in this energy region. Hence we tried the alternative approach in which we simply expressed $F_p(s,t,u)$ as a polynomial in z with energy

dependent coefficients which were parameterised without using any detailed dynamical model. We discuss this approach in the following.

3. The Parametric form of $F_p(s,t,u)$

In this work we assumed that $F_p(s,t,u)$ can be parameterised in the form

$$F_p(s,t,u) = \sum_{n=0}^{N} a_n(s) z^n \qquad (4.28)$$

where $z = \cos\theta$ and the cut-off parameter N is to be selected to give the best fit to the data. It proved more convenient in practice to parameterise the amplitudes f_1 and f_2 in this fashion. The parametric forms $f_{1,2I}^{P}$, $f_{2,2I}^{P}$ (I denoting the isospin) finally adopted were as follows

T = 3/2 amplitudes

$$\mathrm{Re}\, f_{1,3}^{P} = \sum_{n=1}^{5} R_n(z)\, a_{n,1}(s), \quad \mathrm{Re}\, f_{L,3}^{P} = \sum_{n=1}^{5} R_n'(z)\, a_{n,3}(s)$$

$$\mathrm{Im}\, f_{1,3}^{P} = \sum_{n=1}^{5} R_n(z)\, a_{n,L}(s), \quad \mathrm{Im}\, f_{L,3}^{P} = \sum_{n=1}^{5} R_n'(z)\, a_{n,4}(s) \qquad (4.29)$$

$$R_1(z) = \sum_{l=0}^{4} A_l z^l, \quad R_2(z) = \sum_{l=0}^{5} B_l z^l$$

$$R_1'(z) = \sum_{l=0}^{4} A_l' z^l, \quad R_L'(z) = \sum_{l=0}^{5} B_l' z^l \qquad (4.30)$$

$$R_3(z) = \sum_{\ell=1}^{5} c_\ell z^\ell \,, \qquad R_3'(z) = \sum_{\ell=0}^{4} c_\ell' z^\ell$$

$$R_4(z) = z^6 + D z^7 \qquad R_4'(z) = z^6 + D' z^7$$

$$R_5(z) = \sum_{\ell=0}^{3} h_\ell z^{2\ell+1} \qquad R_5'(z) = \sum_{\ell=0}^{3} h_\ell' z^{2\ell}$$

and also

$$a_{nm}(s) = \frac{\lambda_{nm} s^2 + \mu_{nm} s + \nu_{nm}}{\alpha_{nm} s^4 + \beta_{nm} s^3 + \gamma_{nm} s^2 + \delta_{nm} s + \varepsilon_{nm}} \quad \text{for } n=1$$

$$a_{nm}(s) = \frac{\mu_{nm} s + \nu_{nm}}{\gamma_{nm} s^2 + \delta_{nm} s + \varepsilon_{nm}} \,, \quad n = 2,3,4$$

(4.31)

T = 1/2 amplitude

$$\mathrm{Re}\, t_{1,1}^{P} = \sum_{n=1}^{5} R_n(z)\, a_{n4}(s), \qquad \mathrm{Re}\, t_{2,1}^{P} = \sum_{n=1}^{5} R_n'(z)\, a_{n3}(s)$$

$$\mathrm{Im}\, t_{1,1}^{P} = \sum_{n=1}^{5} R_n(z)\, a_{n2}(s) \qquad \mathrm{Im}\, t_{2,1}^{P} = \sum_{n=1}^{5} R_n'(z)\, a_{n4}(s)$$

(4.32)

and

$$R_1(z) = \sum_{l=0}^{4} A_l z^l, \quad R_2(z) = \sum_{l=0}^{5} B_l z^l$$

$$R_1'(z) = \sum_{l=0}^{4} A_l' z^l, \quad R_2'(z) = \sum_{l=0}^{5} B_l' z^l$$

$$R_3(z) = \sum_{l=0}^{4} C_l z^l, \quad R_4(z) = \sum_{l=0}^{6} D_l z^l$$

$$R_3'(z) = \sum_{l=0}^{3} C_l' z^l, \quad R_4'(z) = \sum_{l=0}^{6} D_l' z^l$$

$$R_5(z) = \sum_{l=0}^{3} h_l z^{2l}, \quad R_5'(z) = \sum_{l=0}^{2} h_l' z^{2l+1} \qquad (4.33)$$

$A_{nm}(s)$'s are of the same form as in (4.31)

The parameters used in constructing $R_n(z)$'s were constrained so that $R_n(z)$'s give small contributions to the forward and backward regions, ∴ hence the number of parameters actually varied was much less than what appears in the equations above.

The values of the parameters appearing in equations as found in the best fit to the data are listed in Appendix IV.

4. Fit to the data

Using the formulas described in the previous section and holding the Regge pole parameters fixed at those values determined from high energy fit, we first fitted all the available $\pi^{\pm}p$ data in the laboratory momentum range 2 - 5 GeV/c to get the $T = 3/2$ parameters.

Then T = $^3/_2$ parameters were held at these fixed values and all the available π^-P and C. E. data were fitted to get T = $^1/_2$ parameters.

The details of the fits are described in the following (the data is listed under Reference 46).

1) π^+P Here our best fit gave a normalised χ^2 of 1.2 when 48 parameters were utilised. The best fit to the data is shown in figs. 4(a, ..m).

The fits to the observed experimental data is quite good overall. Specially the comparatively recent data of Busza et al. are explained very well by this fit.

A normalisation error of 5% was allowed for all the data and in some cases it was necessary to increase the quoted experimental errors beyond this. This was particularly true for the data at 2.0 GeV/c, where two independent groups have obtained results which are in rather poor agreement with each other at certain points

The only serious discrepancy between the fitted curve and the data lies in the fact that at a number of energies in the range 2 - 3 GeV/c the predicted cross sections show a substantial dip near the backward direction, which the data does exhibit to some extent. The dip is very well established in the data of J. Banaigs et al. from 2.85 to 3.55 GeV/c but the 2.7 GeV/c data of Coffin et al. shows no dip in this region. This is by far the most serious

case and at other energies only the occasional data disagreeing with the predicted cross section near the region of the backward dip.

2) π^--P and charge exchanges. π^--P differential cross section has got even more structures than π^+P. Our fit explains all the structures viz bumps and dips in the large angular region.

Much more data were available in this case and the parametric fit was very sensitive due to the presence of charge exchange and quite a good polarization data.

Here also the predicted cross section show a dip near the backward region in the energy range 2 to 3 GeV/c. The dip is present in the data near 2 GeV/c region but here again at near 2.8 GeV/c the dip is present in the data of Banaigs et al. (at 2.85 and 3.55 GeV/c), but the data of Coffin et al. are rather inconsistent with the data of Banaigs et al. near the backward region and it is not very clear whether it is present in the data of Busza et al. due to rather large experimental error in their data near 180°.

The overall fit is quite excellent including that of π^--P polarization but that of K.E. in the energy region 2.27 to 2.5 is not so good, though it shows the main feature of the data that were available. The representative selection of the best fit to

the data is shown in figs. 7(a, e), 8(a, e), 9(a, c)

5. Phase shifts.

We define the phase shift δ_ℓ and the elasticity parameter η_ℓ in the usual way by

$$f_{\ell\pm} = \frac{\eta_{\ell\pm}\exp(2i\delta_{\ell\pm}) - 1}{2iq}$$

One way to parameterise [47] the amplitude $A_{\ell\pm} = q f_{\ell\pm}$ in low energy phase shift analysis is to write it as a sum of resonance and non resonance amplitudes.

$$A_{\ell\pm} = \frac{\frac{1}{2}\Gamma_{\ell\pm}}{(W^R_{\ell\pm} - W) - \frac{1}{2}i\Gamma_{\ell\pm}} + (\xi_{\ell\pm} e^{2i\delta_{\ell\pm}} - 1)/2i$$

and then parameterise $\xi_{\ell\pm}$, $\delta_{\ell\pm}$ as polynomials in momentum.

In some other works[1] the analytic properties of the partial wave scattering amplitude were fully utilised.

π - N phase shift analysis has been done by several groups in the energy regions which extend up to 2 GeV[48].

We investigated phase shifts and elasticities over the laboratory momentum range 1.8 to 5.0 GeV/c and $\ell \leq 16$. We exhibit our results for $\ell \leq 6$ in figures and give all the numbers for $\ell \leq 16$ (the phase shifts for $\ell > 6$ are very small and structure less) in Appendix V.

Since phase shifts, at the lower end of the energy region we investigated, already exist, we compared our results with those. We find that although the present results agree with those in their main features,* there are some quantitative disagreements.

The positions of possible resonances** in the range 2.0 to 5.0 GeV/c are indicated on the figs. 6(a-g) and 10(a-g) and in Table 6.

*(Our S_{31}, S_{11} phase shift parameters are quite different)

TABLE 6

$T = 3/2$ resonances

Position (W in GeV)	Partial Wave	Associated Regge trajectory.
2.1	S_{31}	Daughter of Δ_β (?)
2.2	D_{33}	Degenerate with Δ_β (?)
2.2	D_{35}	Δ_β ($P = -$ $\tau = +$)
2.4	F_{35}	Δ_α ($P = +$ $\tau = +$)
2.4	H_3 11	Δ_δ ($P = +$ $\tau = -$)
2.6	P_{33}	Daughter of Δ_α (?)

Here Δ_δ is the established Regge trajectory through $\Delta(1236)$ and $\Delta(1940)$ and the existence of $H_{3,11}$ is also confirmed.[49]

** See p 41A for further details.

Also Δ_β, Δ_α are the trajectories considered by Crittenden et al.[50] and whose lowest mass states are supposed to be

Δ (1630, $^1/_2$ -), Δ(1930, $^1/_2$ +) respectively.[49]

$T = {}^1/_2$ resonances.

Position (W in GeV)	Partial Wave	Associated Regge trajectory.
2.16	G_{17}	N_γ (P = - τ = -)
2.1	G_{19}	N_β (P = - τ = +)
2.59	$H_{1,9}$	Daughter of N_α (P = + τ = +) ?
2.2	P_{11}	Daughter of N_α (P = + τ = +)
2.16	F_{15}	N_α (P = + τ = +)
2.52	S_{11}	?

Among the above mentioned $T = {}^1/_2$ resonances G_{17} is well established.

In view of the large background at these energies it is difficult to identify a resonance, and Table 5 must be considered as a list of possibilities. For the same reason no attempt has been made to estimate the widths and elasticities of these tentative resonances.

5A. Resonances

We consider resonances as poles in the scattering amplitude on the first unphysical sheet above the elastic threshold. It is worth noting that only poles that are allowed on the physical sheet are the bound state poles which occur on the positive real axis below the lowest threshold. (Poles on the real axis above threshold violate unitarity).

Now let us consider a resonance of spin ℓ associated with a second sheet pole at the position p which is denoted by $S_p = S_R - i\,\gamma$ where γ is real and positive.

To consider the physical effect of this pole let us expand the function $f(s)$ defined by

$$f(s) = (s - s_R)\, a_\ell(s) \qquad (5A.1)$$

($a_\ell(S)$ is the partial wave amplitude as defined in 2.1) in a power series about the pole position $s = s_p$

$$f(s) = f(S_p) + (S - S_p)\, f'(S_p) + \ldots. \qquad (5A.2)$$

This series converges in the circle centred on S_p and passing through the next nearest singularity of $a_\ell(S)$. Now if we assume that for small γ $f(s) \simeq f(s_p)$ near $s = s_R$

then

$$a_\ell(S) \simeq -\frac{f(S_p)}{S_R - S - i\,\gamma} \qquad (5A.3)$$

which is the Breit-Wigner form of a resonance with width $\tau = \gamma/\sqrt{S_R}$.

Now if we define the phase shift δ_ℓ and for elasticity parameter η by

$$a_\ell(S) = \eta_\ell \frac{e^{2i\delta_\ell}-1}{2iq}$$

then.

$$\delta_\ell = \tfrac{1}{2} \tan^{-1}\left(\frac{q \operatorname{Re} a_\ell(S)}{\tfrac{1}{2}-q \operatorname{Im} f_\ell(S)}\right) \qquad (SA.4)$$

So the narrow Breit-Wigner resonance of (SA.3) corresponds to the phase shift increasing rapidly through $\pi/2$ (for elasticity >.5) or through 0 (for elasiticty <.5) as increases through S_R.

In our model poles in $F_p(s,t)$ term can only appear in $a_{nm}(S)$ as defined in (4.31), the second sheet poles that were found in $a_{nm}(S)$ indicated possible resonance positions and then each partial wave was examined for possible resonance behaviour in the Argand diagram. The resonances found in this way are listed in Table 6.

6. Conclusion:

In our work we found that in order to get a good fit to the pion - nucleon scattering data from 2 to 5 GeV/c, some higher resonance terms are needed along side with the large Regge background from t and u channels.

Regge amplitude alone can explain at least qualitatively the forward and backward peaks in the energy region mentioned above, but very prominent structures such as dips and bumps in large angular region in the differential cross section $d\sigma/d\Omega$ as a function of cos θ imply the presence of some high spin resonances in this region. Moreover these resonance terms are contained in $F_p(z)$ term, which is the difference between the exact amplitude and the Regge amplitude. Hence our model is very much consistent with generalised interference model as opposed to the duality model discussed in Chapter II (strong duality).

It will be rather interesting to see whether finite energy sum rule is well satisfied using our results for the phase shifts from 2 to 5 GeV/c together with the already existent phase shifts up to 2 GeV/c. (Assuming of course that the Regge behaviour sets in above about 5 GeV/c).

APPENDICES

Appendix I

It will be shown here that $R_1(s,z,\alpha i)$ as defined in (2.34) has no right hand cut in the region $1 \leq z < \cosh\}$ for the case $R_e\,\alpha i > 0$

We have from (2.34)

$$R_1(s,z,\alpha_i) = -\beta_i(s)\left[\frac{\pi(2\alpha_i+1)}{\sin\pi\alpha_i} P_{\alpha_i}(-z) + \frac{1}{\sqrt{2}}\int_{-\infty}^{\}} \frac{\exp((\alpha_i+\nu_L)x)}{(\cosh x - z)^{3/2}}\,dx\right.$$

(A.I.1)

We shall show that

$$\Delta R(s,z,\alpha_i) = 0$$

Now $\Delta P_{\alpha i}(-z)$

$$= \frac{1}{2i}\left[P_{\alpha_i}(-z-i\epsilon) - P_{\alpha_i}(-z+i\epsilon)\right]$$

$$= -\frac{2}{\pi}\sin\pi\alpha_i\, \Delta Q_{\alpha_i}$$

$$= -\sin\pi\alpha_i\, P_{\alpha_i}(z), \quad 1 \leq z < \cosh\}$$

(A.I.2)

Hence

$$\Delta\left(\beta_i \frac{\pi (2\alpha_i+1) P_{\alpha_i}(-z)}{\sin \pi \alpha_i}\right) = -\pi (2\alpha_i+1) P_{\alpha_i}(-z), \quad z \geq 1$$

(AI.3)

Using the integral representation for Legendre function

$$P_{\alpha_i}(-z) = \frac{\sqrt{2}}{\pi} \int_0^{\cosh^{-1} z} \frac{\cosh(\alpha_i + 1/2)x}{(z - \cosh x)^{1/2}} dx, \quad z > 1$$

we have

$$\Delta\left(\pi \frac{\beta_i (2\alpha_i+1) P_{\alpha_i}(-z)}{\sin \pi \alpha_i}\right)$$

$$= -\sqrt{2}\, \beta_i (2\alpha_i+1) \int_0^a \frac{\cosh(\alpha_i+1/2)x}{(z-\cosh x)^{1/2}} dx$$

(AI.4)

where $a = \cosh^{-1} z$

Next we deal with the integral terms in (AI.1).

Denoting the integral by I we have

$$I(s,z,\alpha_i) = \frac{\beta_i}{\sqrt{2}} \int_{-\infty}^{\infty} \frac{\exp((\alpha_i+1/2)x)}{(\cosh x - z)^{3/2}}\,dx$$

$$= -\sqrt{2}\,\beta_i \frac{\exp(3(\alpha_i+1/2))}{(\cosh 3 - z)^{1/2}} + \frac{\beta}{\sqrt{2}}(2\alpha_i+1)\int_{-\infty}^{\infty} \frac{\exp((\alpha_i+1/2)x)}{(\cosh x - z)^{1/2}}\,dx, \quad (A.II.5)$$

(integrating by parts)

$1 \le z < \cosh 3$

Hence

$$\Delta\,(I(s,z,\alpha_i)) = \Delta\left(\frac{\beta}{\sqrt{2}}(2\alpha_i+1)\int_{-\infty}^{\infty} \frac{\exp((\alpha_i+1/2)x)}{(\cosh x - z)^{1/2}}\,dx\right) \quad (A.I.6)$$

for $1 \le z < \cosh 3$

We use

$$(\cosh x - z \mp i\epsilon)^{1/2} = \mp i\,(z - \cosh x)^{1/2}$$

and we get from (A.II.6)

$$\Delta\,(I(s,z,\alpha_i)) = \frac{\beta_i(2\alpha_i+1)}{\sqrt{2}} \int_{-a}^{a} \frac{\exp((\alpha_i+1/2)x)}{(z-\cosh x)^{1/2}}\,dx$$

$$= \sqrt{2}\,\beta_i(2\alpha_i+1)\int_0^a \frac{\cosh((\alpha_i+1/2)x)}{(z-\cosh x)^{1/2}}\,dx$$

$$= -\Delta\left(\pi\frac{\beta_i(2\alpha_i+1)P_{\alpha_i}(-z)}{\sin\pi\alpha_i}\right)$$

(from (A.I.4))

and finally we have

$$\Delta\,(R_i(s,z,\alpha_i)) = 0, \qquad 1 \le z < \cosh 3$$

Q.E.D.

Appendix II

Crossing.

The invarient amplitude T (see equation 1.10) is of the form,

$$T = -A + i\,(\gamma\cdot Q)\,B \qquad \text{(A.II.1)}$$

Now under crossing i.e. $s \leftrightarrow u$ A, B change as follows

$$A(s,u,t) \longleftrightarrow A(u,s,t)$$
$$B(s,u,t) \longleftrightarrow -B(u,s,t) \qquad \text{(A.II.2)}$$

(The amplitude B changes sign due to the fact that $(\gamma\cdot Q)$ changes sign under crossing $(\gamma\cdot Q) \to -(\gamma\cdot Q)$ (A.II.3)

Now from (1.30) we can write

$$A(s,u,t) = 4\pi\left[\frac{\sqrt{s}+m}{E_s+m}f_1(\sqrt{s},u) - \left(\frac{\sqrt{s}-m}{E_s-m}\right)f_2\right]$$

$$B(s,u,t) = 4\pi\left[\frac{1}{E_s+m}f_1(\sqrt{s},u) + \frac{1}{(E_s-m)}f_2(\sqrt{s},u)\right] \qquad \text{(A.II.4)}$$

and

$$A(u,s,t) = 4\pi\left[\frac{\sqrt{u}+m}{E_u+m} f_1(\sqrt{u},s) - \frac{(\sqrt{u}-m)}{E_u-m} f_2(\sqrt{u},s)\right]$$

(A.II.5)

$$B(u,s,t) = 4\pi\left[-\frac{1}{E_u+m} f_1(\sqrt{u},s) + \frac{1}{(E_u-m)} f_2(\sqrt{u},s)\right]$$

where

$$E_s = \frac{s+m^2-\mu^2}{2\sqrt{s}}, \quad E_u = \frac{u+m^2-\mu^2}{2\sqrt{u}}$$

Hence from A.II.3, A.II.4 and A.II.5 , we can write

$$\frac{\sqrt{s}+m}{E_s+m} f_1(\sqrt{s},u) - \frac{(\sqrt{s}-m)}{E_s-m} f_2(\sqrt{s},u)$$

$$= \frac{\sqrt{u}+m}{E_u+m} f_1(\sqrt{u},s) - \frac{(\sqrt{u}-m)}{E_u-m} f_2(\sqrt{u},s)$$

(A.II.6)

and

$$\frac{f_1(\sqrt{s},u)}{(E_s+m)} + \frac{f_2(\sqrt{s},u)}{(E_s-m)} = -\left[\frac{f_1(\sqrt{u},s)}{E_u+m} + \frac{f_2(\sqrt{u},s)}{E_u-m}\right]$$

solving these two equations for $f_1(\sqrt{s},u)$ and $f_2(\sqrt{s},u)$ we get (3.15).

Appendix III

We shall show here how the relations between a Regge trajectory and resonance parameters are obtained at a resonance point.

From (4.8) neglecting the integral terms we get, for a trajectory $\alpha(\sqrt{s})$ exchanged in s channel with residue $\beta(\sqrt{s})$ signature τ and parity P

$$F_1^P(\sqrt{s},u) = \frac{(E_s+m)\,\beta(\pm\sqrt{s})}{\sqrt{s}\cos\pi\alpha(\pm\sqrt{s})}\left(\frac{q^2}{s_0}\right)^{\alpha(\pm\sqrt{s})-1/2}\left(\alpha(\pm\sqrt{s})+1/2\right)\left[P^{(-z)}_{\alpha(\pm\sqrt{s})-1/2}+\tau P_{\alpha(\pm\sqrt{s})-1/2}(-z)\right]$$

$$+\frac{(E_s-m)\,\beta(\mp\sqrt{s})}{\sqrt{s}\cos\pi\alpha(\mp\sqrt{s})}\left(\frac{q^2}{s_0}\right)^{\alpha(\mp\sqrt{s})-1/2}\left(\alpha(\mp\sqrt{s})+1/2\right)\left[P^{(-z)}_{\alpha(\mp\sqrt{s})+1/2}-\tau P^{(z)}_{\alpha(\mp\sqrt{s})+1/2}\right] \qquad \text{(A.III.1)}$$

For Δ_δ trajectory P = +1, τ = -1 and the resonances occur at $\mathrm{Re}\,\alpha_\Delta = 3/2, 7/2, \ldots$

Hence at those points neglecting the 2nd term on r.h.s. of A.III.1 we get

$$F_4^P(\sqrt{s},u) = -2K\frac{(\sqrt{s})(\alpha+1/2)}{\cos\pi\alpha}P_{\alpha-1/2}(z) \qquad \text{(A.III.2)}$$

and $K(\sqrt{s}) = \frac{E_s+m}{\sqrt{s}}\beta(\sqrt{s})\left(\frac{q^2}{s_0}\right)^{\alpha(\sqrt{s})-1/2}$,

$\alpha \equiv \alpha(\sqrt{s})$

But at resonance point $\mathrm{Re}\,\alpha(\sqrt{s}) = J = \ell + 1/2$

hence

$$F_A \simeq -\frac{2K(\sqrt{s})(\ell+1)P_\ell(z)}{\cos\pi\alpha} \qquad \text{(A.III.3)}$$

For N_α trajectory

$$P = +1, \qquad \tau = +1$$

so

$$F_N = -\frac{2K(-\sqrt{s})(\bar{\ell}+1/2)}{\cos\pi\bar{\ell}}\, P_{\bar{\ell}+1/2}(z) \qquad \text{(A.III.4)}$$

here the resonances occur at

$$\mathrm{Re}\,\alpha(-\sqrt{s}) = J = \ell - 1/2$$

So we get (assuming $\mathrm{Im}\,\alpha(\sqrt{s})$ to be very small near resonance position compared with $\mathrm{Re}\,\alpha(\sqrt{s})$)

$$F_N \simeq -\frac{2K(+\sqrt{s})\ell\, P_\ell(z)}{\cos\pi\alpha} \qquad \text{(A.III.5)}$$

But near resonance position we can write α as

$$\alpha = J + i\,\mathrm{Im}\,\alpha(M_R) + (\sqrt{s}-M_R)\frac{d}{d\sqrt{s}}\mathrm{Re}\,\alpha\Big|_{M_R} + \cdots$$

assuming $\mathrm{Im}\,\alpha$ varies only slowly;

also $\cos(\pi/2+\epsilon) \simeq -\epsilon$ similarly for $5\pi/2$, $9\pi/2$, ...

$\cos(3\pi/2+\epsilon) \simeq +\epsilon$ similarly for $7\pi/2$, $11\pi/2$, ...

hence

$$F_4 = - \frac{2K(M_R)(l+1) P_l(z)}{\pi \alpha'_R \left[\sqrt{s} - M_R + i \frac{\mathrm{Im}\,\alpha}{\alpha'_R}\right]} \qquad \text{(A.III.6)}$$

where

$$\alpha'_R = \left. \frac{d\, \mathrm{Re}\,\alpha(\sqrt{s})}{d\sqrt{s}} \right|_{\sqrt{s}=M_R}$$

But using Breight-Wigner form, a resonance on $\Delta\delta$ trajectory is of the form

$$F_4 = \frac{1}{R} \frac{(J+1/2)\,\Gamma_{el}/\Gamma}{M_R - \sqrt{s} - i\,\Gamma/2} P_l(z) \qquad \text{(A.III.7)}$$

Where $W = \sqrt{s}$. comparing (A.III.6) with (A.III.7)

we get $$\frac{\Gamma}{2} \alpha'_R = \mathrm{Im}\,\alpha_R \qquad \text{(A.III.8)}$$

and $$\frac{\Gamma_{el}}{2R} = \frac{2K(M_R)}{\pi \alpha'_R} \qquad \text{(A.III.9)}$$

Writing $K(M_R) = \frac{E_R + M}{M_R} \beta(M_R) R^{2l}$ in (A.III.9)

we obtain

$$\beta(M_R) = \frac{\Gamma_{el}}{4 R^{2l+1}} \frac{\pi \alpha'_R M_R}{(E_R + M)} \qquad \text{(A.III.10)}$$

Similarly for N_ℓ trajectory we get

$$F_N = - \frac{2K(-M_R)\, \ell\, P_\ell(z)}{\pi \bar{\alpha}'_R \left[-(\sqrt{s}+M_R) + i \frac{g_m \bar{\alpha}_R}{\bar{\alpha}'_R} \right]} \qquad \text{(A.III.11)}$$

(Here $\bar{\alpha}'_R = \left. \frac{d\alpha(\sqrt{s})}{d\sqrt{s}} \right|_{\sqrt{s}=-M_R}$)

$$= \frac{2K(-M_R)\,(J+1/2)\, P_\ell(z)}{\left[M_R + W - i \frac{g_m \bar{\alpha}_R}{\bar{\alpha}'_R} \right]} \qquad \text{(A.III.12)}$$

$(J = \ell - 1/2)$

From B.W. formula

$$F_N = \frac{1}{R} \frac{(J+1/2)\, \Gamma_{el}/2}{M_R + W - i\Gamma/2} P_\ell(z) \qquad \text{(A.III.13)}$$

comparing (A.III.12) and (A.III.13)

$$g_m \bar{\alpha}_R = \frac{\Gamma}{2} \bar{\alpha}'_R \qquad \text{(A.III.14)}$$

and

$$\beta(-M_R) = \frac{\Gamma_{el}}{q_R^{2\ell+1}} \frac{\pi \alpha'_R M_R}{(E_R - M)} \qquad \text{(A.III.15)}$$

Appendix IV

The values of the T = $^3/_2$ parameters appearing in equation 4.32 found from the best fit to the data.

	A	B	C	A'	B'	C'	
0	.327	-.225		0.327	-.222	0.238	D = 2.585
1	.435	.409	.0508	.435	.221	0.0001	D' = 2.585
2	-.389	1.681	0.0	-.389	1.198	-3.333	
3	-.349	.591	-.6118	-.349	.779	0.0	
4	.0623	-1.456	0.0	.062	-.977	4.999	
5	-	-1.0	.886	-	-.10	-	

m \ n=1	λ^m_n	μ^m_n	ν^m_n	α^m_n	β^m_n	γ^m_n	δ^m_n	ε^m_n
1	.147	.243	.107	1.0	-5.708	-6.928	62.117	62.338
2	0.0	.4817	.37	0.0	0.0	1.0	-9.307	23.976
3	-1.233	-2.561	-1.233	1.0	-8.207	16.046	4.966	55.145
4	.031	.364	.262	0.0	1.0	-12.307	51.896	-71.928

m \ n=2								
1	-	.3862	-1.97	-	-	1.0	-1.46	5.738
2	-	.5573	-3.246	-	-	1.0	-13.0	44.0
3	-	.2804	.042	-	-	1.0	1.1	-0.083
4	-	-.545	.427	-	-	1.0	-13.0	44.0

Appendix IV, continued.

n =3 / m								
1	-	-0.9	5.454	-	-	1.0	-12.12	39.77
2	-	0.0	9.0	-	-	1.0	-12.12	39.77
3	-	0.061	-3.636	-	-	1.0	-12.12	39.77
4	-	0.0	-1.518	-	-	1.0	-12.12	39.77

n=4 / m								
1	-	-0.0975	.458	-	-	1.0	-9.405	22.609
2	-	-0.0107	0.0335	-	-	1.0	-9.405	22.409
3	-	-0.0072	0.0338	-	-	1.0	-9.405	22.409
4	-	-0.037	0.059	-	-	1.0	-9.405	22.409

n= 5 / m								
1	-	3.323	-25.6366	-	-	1.0	-16.909	71.5579
2	-	0.0	1.538	-	-	1.0	-16.909	71.5579
3	-	-.41634	3.5197	-	-	1.0	-16.909	71.5579
4	-	0.0	-.02085	-	-	1.0	-16.909	71.5579

$h_0 = .206$ $h_0' = .206$

$h_1 = .777$ $h_1' = 2.333$

$h_2 = -1.544$ $h_2' = -7.7227$

$h_3 = 1.0$ $h_3' = 7.0$

Appendix IV, Continued

The values of the $T = {}^{1}/_{2}$ parameters appearing in equation (4.33) found from the best fit to the data.

	A	B	C	D	H	A'	B'	C'	D'	H'
0	-.052	-.1558	-.67876	.3402	.0711	-.05	-.1558	0.0	.34	
1	1.0347	-.0893	0.6	-.346	-	1.0347	-.0893	-1.714	-.346	-4.4528
2	-.615	1.0365	-.8224	0.0	.793	-.615	1.037	0.0	0.0	-
3	-1.0346	1.0893	0.0	.371	-	-1.035	1.084	4.0	-.371	-4.304
4	.667	-.8808	1.0	0.0	-.729	.667	-.88	-	0.0	-
5	-	-1.0	-	0.0	-	-	-1.0	-	0.0	6.0
6	-	-	-	-.599	1.0	-	-	-	-.599	-
7	-	-	-	1.0	-	-	-	-	-	-

Appendix IV, continued

m \ n=1	λ_n^m	μ_n^m	ν_n^m	α_n^m	β_n^m	γ_n^m	δ_n^m	ε_n^m
1	.9476	.6713	-.2728	1.0	-11.047	40.2976	-48.548	38.2509
2	0.0	.6381	-.1797	0.0	0.0	1.0	-9.7315	26.021
3	-2.801	15.488	-4.139	1.0	-15.7455	97.9696	-287.1223	349.296
4	2.995	9.19	-2.8251	0.0	-10.0215	34.974	-67.21	159.535

m \ n=2								
1	-	2.7537	-15.0	-	-	1.0	-5.356	-.569
2	-	.509	-2.9	-	-	1.0	-13.841	48.411
3	-	.1472	-1.0186	-	-	1.0	-13.841	48.411
4	-	-.084	.1042	-	-	1.0	-13.841	48.411

Appendix IV, continued

n=3 / m	λ^m_n	μ^m_n	ν^m_n	α^m_n	β^m_n	γ^m_n	δ^m_n	ε^m_n
1	-	.3095	-1.3468	-	-	1.0	-8.702	17.658
2	-	0.0	.6718	-	-	1.0	-8.702	17.658
3	-	-4.272	1.8588	-	-	1.0	-8.702	17.658
4	-	0.0	-0.0136	-	-	1.0	-8.702	17.658

n=4 / m								
1	-	.104	-.501	-	-	1.0	-9.634	24.15
2	-	.234	.185	-	-	1.0	-9.634	24.15
3	-	-.0323	.1556	-	-	1.0	-9.634	24.15
4	-	.0742	.6663	-	-	1.0	-9.634	24.15

Appendix IV, continued

m	n=5	λ_n^m	μ_n^m	ν_n^m	α_n^m	β_n^m	γ_n^m	δ_n^m	ε_n^m
1		-	-.4178	2.4087	-	-	1.0	-11.5232	34.280
2		-	0.0	.801	-	-	1.0	-11.5232	34.280
3		-	.0672	-.3871	-	-	1.0	-11.5232	34.280
4		-	0.0	-.13353	-	-	1.0	-11.5232	34.280

Appendix V

Phase Shifts *

T = 1/2

	S_{11}		P_{11}		P_{13}		D_{13}		D_{15}		F_{15}		F_{17}	
P_{lab} † (GeV/c	η	δ	η	δ	η	δ	η	δ	η	δ	η	δ	η	δ
2.0	.42	76.0	.16	17.38	.45	15.25	.51	-2.04	.67	-10.7	.62	-3.3	.66	-2.16
2.1	.44	79.9	.14	25.17	.43	-14.5	.55	-2.85	.68	-10.03	.63	-4.26	.63	-3.65
2.2	.43	82.38	.14	28.76	.4	-14.66	.57	-3.57	.66	-9.43	.64	-4.79	.62	-5.03
2.3	.39	84.24	.15	27.86	.37	-15.5	.58	-4.20	.64	-9.11	.66	-4.94	.62	-6.08
2.4	.33	86.43	.16	23.82	.35	-17.3	.59	-4.90	.61	-9.47	.67	-4.84	.63	-6.8
2.5	.26	88.83	.19	22.34	.32	-17.4	.59	-4.38	.57	-9.41	.68	-4.61	.63	-7.28
2.6	.20	93.44	.20	19.45	.30	-18.38	.59	-4.22	.54	-10.33	.68	-4.29	.63	-7.57

* δ is in degrees. † P_{lab} = Pion laboratory momentum.

Appendix V, Continued

	G_{17}		G_{19}		H_{19}		$H_{1,11}$		$I_{1,11}$		$I_{1,13}$	
Plate GeV/c	η	δ	η	δ	η	δ	η	δ	η	δ	η	δ
2.0	.75	-.70	.75	1.31	.88	3.80	.94	-1.84	.96	1.56	.97	-.21
2.1	.75	-1.65	.75	1.46	.86	4.11	.93	-1.6	.95	1.85	.97	-.36
2.2	.74	-1.77	.74	1.28	.83	4.33	.92	-1.22	.95	2.17	.97	-.51
2.3	.73	-1.73	.73	.86	.81	4.46	.92	-.79	.95	2.5	.97	-.60
2.4	.73	-1.63	.71	.36	.79	4.52	.91	-.35	.94	2.83	.97	-.65
2.5	.72	-2.04	.70	-.72	.77	4.27	.90	-.16	.94	3.17	.92	-.60
2.6	.72	-2.12	.69	-1.42	.75	4.08	.89	0.07	.93	3.48	.96	-.48

Appendix V, continued

Plate (GeV/c)	S_{11}		P_{11}		P_{13}		D_{13}		D_{15}		F_{15}		F_{17}	
	η	δ	η	δ	η	δ	η	δ	η	δ	η	δ	η	δ
2.7	.14	101.29	.21	17.51	.29	-19.0	.58	-3.91	.52	-11.28	.68	-3.96	.63	-7.8
2.8	.11	124.53	.21	16.15	.27	-19.3	.57	-3.5	.51	-12.1	.68	-3.66	.62	-8.02
2.9	.10	132.0	.21	15.31	.26	-19.7	.55	-3.1	.49	-12.84	.69	-3.42	.61	-8.3
3.0	.12	-33.9	.20	15.07	.25	-20.2	.53	-2.70	.47	-13.53	.69	-3.18	.59	-8.66
3.1	.15	-25.5	.18	15.41	.23	-21.11	.51	-2.25	.45	-14.26	.7	-2.92	.58	-9.10
3.2	.17	-20.65	.15	15.93	.21	-22.10	.48	-1.69	.42	-14.90	.70	-2.66	.57	-9.52
3.3	.18	-17.84	.14	15.42	.2	-22.65	.46	-1.13	.41	-15.1	.69	-2.45	.56	-9.85

Appendix V, continued

	G_{17}		G_{19}		H_{19}		$H_{1,11}$		$I_{1,11}$		$I_{1,13}$	
Plab (GeV/c)	η	δ	η	δ	η	δ	η	δ	η	δ	η	δ
2.7	.72	-2.2	.68	-2.09	.73	3.76	.88	.17	.92	3.73	.96	-.34
2.8	.72	-2.34	.68	-2.64	.72	3.36	.87	.16	.90	3.92	.95	-.21
2.9	.72	-2.42	.69	- 3.08	.71	2.9	.86	.05	.88	4.03	.94	-.10
3.0	.73	-2.47	.69	-3.43	.70	2.43	.85	-.11	.86	4.06	.93	-0. 04
3.1	.74	-2.51	.70	-3.70	.69	1.93	.85	-.29	.84	4.0	.92	-. 03
3.2	.75	-2.55	.71	-3.95	.69	1.44	.85	-.48	.83	3.86	.91	-.06
3.3	.75	-2.62	.71	-4.21	.69	1.0	.84	-.68	.81	3.65	.90	-.12

Appendix V, continued

	S_{11}		P_{11}		P_{13}		D_{13}		D_{15}		F_{15}		F_{17}	
Plab (GeV/c)	η	δ	η	δ	η	δ	η	δ	η	δ	η	δ	η	δ
3.4	.19	-16.29	.14	13.45	.19	-22.35	.45	-.62	.41	-14.76	.67	-2.33	.56	-10.02
3.5	.20	-15.31	.15	10.8	.20	-21.43	.44	-.27	.41	-14.15	.65	-2.29	.56	-10.09
3.6	.21	-14.63	.17	8.48	.2	-20.3	.43	-0.078	.42	-13.50	.64	-2.30	.56	-10.09
3.7	.21	-14.02	.18	6.56	.21	-19.27	.43	.13	.42	-12.93	.62	-2.33	.56	-10.09
3.8	.22	-13.5	.19	5.05	.21	-18.35	.43	.24	.43	-12.45	.61	-2.38	.56	-10.07
3.9	.22	-13.04	.20	3.83	.22	-17.54	.43	.32	.43	- 12.05	.60	-2.42	.56	-10.06
4.0	.23	-12.62	.21	2.84	.22	-16.56	.42	.39	.43	-11.71	.59	-2.46	.55	-10.04

Appendix V, continued

	G_{17}		G_{19}		H_{19}		$HZ_{1,11}$		$I_{1,11}$		$I_{1,13}$	
Plate (GeV/c)	η	δ	η	δ	η	δ	η	δ	η	δ	η	δ
3.4	.74	-2.72	.71	-4.48	.70	.63	.83	-.86	.81	3.41	.89	-.22
3.5	.73	-2.84	.7	-4.74	.70	.35	.82	-1.02	.80	-3.18	.88	-.33
3.6	.72	-2.97	.69	-5.0	.70	.14	.81	-1.27	.80	2.96	.87	-.45
3.7	.71	-3.09	.68	-5.22	.7	-1.46	.80	-1.46	.79	2.74	.86	-.56
3.8	.70	-3.20	.67	-5.43	.7	- .18	.79	-1.66	.79	2.54	.85	-.68
3.9	.69	-3.29	.67	-5.62	.69	-.30	.78	-1.85	.78	2.36	.85	-.80
4.0	.68	-3.37	.66	-5.80	.69	-.42	.77	-2.05	.78	2.18	.84	-.91

Appendix V, continued

	S_{11}		P_{11}		P_{13}		D_{13}		D_{15}		F_{15}		F_{17}	
Plab (GeV/c)	η	δ	η	δ	η	δ	η	δ	η	δ	η	δ	η	δ
4.1	.23	-12.24	.22	2.0	.23	-16.27	.42	.44	.43	-11.41	.58	-2.5	.55	-10.02
4.2	.24	-11.90	.22	1.30	.23	-15.75	.42	.48	.43	-11.15	.57	-2.55	.54	-10.0
4.3	.24	-11.56	.23	.62	.23	-15.27	.42	.49	.43	-10.92	.57	-2.58	.54	- 9.48
4.4	.25	-11.29	.23	.09	.24	-14.86	.42	.52	.43	-10.71	.56	-2.62	.54	-9.95
4.5	.25	-11.04	.24	-.37	.24	-14.48	.42	.54	.42	-10.51	.56	-2.66	.53	-9.92
4.6	.26	-10.82	.24	-.78	.24	-14.13	.42	.54	.42	-10.33	.55	-2.70	.53	-9.88
4.7	.26	-10.59	.25	-1.19	.24	-13.80	.42	.54	.42	-10.18	.52	-2.72	.52	-9.85

Appendix V, continued

Plate (GeV/c)	G_{17}		G_{19}		H_{19}		$H_{1,11}$		$I_{1,11}$		$I_{1,13}$	
	η	δ	η	δ	η	δ	η	δ	η	δ	η	δ
4.1	.68	-3.43	.65	-5.96	.69	-.52	.76	-2.24	.77	2.02	.83	-1.02
4.2	.67	-3.49	.65	-6.10	.69	-.62	.75	-2.43	.77	1.86	.83	-1.13
4.3	.67	-3.53	.64	-6.23	.69	-.71	.74	-2.6	.77	1.70	.82	-1.24
4.4	.66	- 3.57	.64	-6.34	.68	-.79	.74	-2.78	.76	1.56	.82	-1.35
4.5	.66	-3.61	.63	-6.45	.68	-.86	.73	-2.94	.76	1.42	.81	-1.46
4.6	.65	-3.63	.63	-6.54	.68	-.93	.72	-3.10	.76	1.29	.80	-1.56
4.7	.65	-3.66	.62	-6.63	.68	-1.0	.72	-3.25	.76	1.17	.80	-1.67

Appendix V, continued

	S_{11}		P_{11}		P_{13}		D_{13}		D_{15}		F_{15}		F_{17}	
Plab (GeV/c)	η	δ	η	δ	η	δ	η	δ	η	δ	η	δ	η	δ
4.8	.26	-10.41	.25	-1.51	.25	-13.51	.42	.54	.42	-10.0	.55	-2.78	.52	-9.81
4.9	.26	-10.21	.25	-1.85	.25	-13.22	.42	.52	.42	- 9.88	.54	-2.78	.51	-9.77
5.0	.27	-10.06	.26	-2.09	.25	-12.96	.42	.51	.41	-9.74	.54	-2.82	.51	-9.72

Appendix V, continued

Plate (GeV/c)	G_{17}		G_{19}		H_{19}		$H_{1,11}$		$I_{1,11}$		$I_{1,13}$	
	η	δ	η	δ	η	δ	η	δ	η	δ	η	δ
4.8	.64	-3.68	.62	-6.71	.68	-1.06	.71	-3.39	.75	1.05	.79	-1.77
4.9	.64	-3.69	.61	- 6.78	.67	-1.12	.71	-3.53	.75	.94	.79	-1.87
5.0	.64	-3.70	.61	-6.84	.67	-1.17	.70	-3.65	.75	.83	.78	-1.96

Appendix V, continued

T = 3/2 Phase Shifts *

	S_{31}		P_{31}		P_{33}		D_{33}		D_{35}		F_{35}		F_{37}	
Plab + (GeV/c)	η	δ	η	δ	η	δ	η	δ	η	δ	η	δ	η	δ
1.9	.87	-54.4	.66	-37.7	.39	-9.46	.79	-2.42	.63	-2.4	.97	.2	.65	-5.3
2.0	.86	-55.15	.68	-35.1	.42	-9.71	.76	-3.86	.59	-4.16	1.0	-0.09	.67	-5.64
2.1	.86	-55.63	.69	-33.75	.44	-10.57	.75	-5.59	.57	-6.45	1.0	-.42	.67	-5.9
2.2	.83	-55.17	.67	-33.56	.43	-11.6	.76	-6.86	.57	-8.22	.97	-.78	.66	-6.10
2.3	.79	-54.0	.64	-33.43	.42	-12.61	.77	-7.54	.57	-9.31	.93	-1.19	.65	-6.26
2.4	.74	-53.56	.61	-32.9	.41	-13.5	.79	-7.84	.57	-10.03	.90	-1.62	.63	-6.42
2.5	.69	-51.83	.59	-31.94	.41	-14.34	.79	-7.94	.56	-10.54	.89	-2.06	.61	-6.61

* δ is in degrees + Plab = Pion laboratory momentum.

Appendix V, continued

	G_{37}		G_{39}		$H_{3,9}$		$H_{3,11}$		$I_{3,11}$		$I_{3,13}$	
Plate (GeV/c)	η	δ	η	δ	η	δ	η	δ	η	δ	η	δ
1.9	.97	-1.93	.83	0.0	1.0	.76	.90	3.17	1.0	-.27	1.0	.38
2.0	.97	-2.27	.81	-.75	1.0	.78	.86	3.12	1.0	-.24	.99	.57
2.1	.97	-2.52	.80	-1.45	.99	.72	.83	2.79	.99	-.27	.99	.72
2.2	.97	-2.58	.80	-1.88	.96	.64	.80	2.27	.98	-.35	.98	.84
2.3	.97	-2.46	.79	-2.05	.94	.55	.78	1.66	.97	-.48	.97	.90
2.4	.96	-2.27	.79	-2.08	.92	.47	.75	1.02	.96	-.64	.95	.90
2.5	.95	-2.06	.78	-2.06	.90	.31	.72	.41	.95	-.83	.94	.82

Appendix V, continued

	S_{31}		P_{31}		P_{33}		D_{33}		D_{35}		F_{35}		F_{37}	
Plate (GeV/c)	η	δ	η	δ	η	δ	η	δ	η	δ	η	δ	η	δ
2.6	.65	-49.93	.56	-30.88	.41	-15.28	.80	-8.8	.55	-11.14	.88	-2.47	.59	-6.83
2.7	.61	-48.13	.53	-30.0	.40	-16.48	.80	-7.97	.53	-11.78	.88	-2.83	.58	-7.04
2.8	.58	-46.73	.50	-29.6	.39	-18.22	.79	-8.07	.50	-12.62	.88	-3.12	.57	-7.2
2.9	.55	-44.08	.46	-29.95	.36	-20.72	.77	-8.27	.47	-13.7	.89	-3.34	.57	-7.26
3.0	.52	-45.7	.42	-30.63	.34	-23.74	.74	-8.56	.44	-14.94	.90	-3.51	.57	-7.28
3.1	.50	- 44.3	.39	-30.76	.33	-26.35	.72	-8.86	.41	-16.0	.89	-3.66	.56	-7.31
3.2	.48	-44.46	.36	-29.61	.34	-27.76	.70	-9.08	.40	-16.59	.88	-3.8	.56	-7.4

Appendix V, continued

Plate (GeV/c)	G_{37}		G_{39}		$H_{3,9}$		$H_{3,11}$		$I_{3,11}$		$I_{3,13}$	
	η	δ	η	δ	η	δ	η	δ	η	δ	η	δ
2.6	.94	-1.90	.77	-2.04	.88	-0.10	.7	-1.46	.95	-1.02	.93	.69
2.7	.93	-1.78	.76	-2.06	.87	-.84	.69	-.61	.94	-1.19	.92	.54
2.8	.93	-1.71	.75	-2.1	.86	-1.56	.70	-.97	.94	-1.34	.91	.38
2.9	.93	-1.68	.76	-2.18	.85	-1.94	.72	-1.23	.94	-1.44	.91	+.23
3.0	.94	-1.69	.76	-2.28	.85	-2.06	.74	-1.44	.93	-1.51	.90	.09
3.1	.94	-1.74	.76	-2.4	.84	-2.08	.76	-1.63	.93	-1.54	.90	-.03
3.2	.93	-1.82	.75	-2.56	.84	-2.08	.76	-1.80	.93	-1.54	.89	-.13

Appendix V, continued

	S_{31}		P_{31}		P_{33}		D_{33}		D_{35}		F_{35}		F_{37}	
Plate (GeV/c)	η	δ	η	δ	η	δ	η	δ	η	δ	η	δ	η	δ
3.3	.46	-43.29	.34	-27.24	.35	-28.26	.69	-9.24	.40	-16.76	.87	-3.94	.55	-7.52
3.4	.44	-41.99	.32	-24.03	.37	-28.49	.68	-9.37	.40	-16.71	.85	-4.05	.55	-7.70
3.5	.43	-40.76	.31	-20.1	.39	-28.9	.67	-9.5	.41	-16.57	.83	-4.13	.54	-7.92
3.6	.42	-39.65	.29	-15.12	.42	-29.68	.66	-9.62	.41	-16.42	.81	-4.15	.54	-8.21
3.7	.41	-38.67	.29	-8.62	.45	-30.9	.65	-9.75	.41	-16.23	.79	-4.09	.54	-8.6
3.8	.4	-37.76	.30	-1.0	.49	-32.66	.64	-9.82	.41	-16.15	.77	-3.93	.53	-9.02
3.9	.39	-36.93	.34	2.34	.50	-34.50	.63	-9.98	.41	-16.05	.76	-3.91	.53	-9.39

Appendix V, continued

	G_{37}		G_{39}		$H_{3,9}$		$H_{3,11}$		$I_{3,11}$		$I_{3,13}$	
Plate (GeV/c)	η	δ	η	δ	η	δ	η	δ	η	δ	η	δ
3.3	.91	-1.91	.74	-2.74	.83	-2.10	.76	-1.97	.93	-1.53	.88	-0.22
3.4	.9	-2.03	.73	-2.92	.83	-2.12	.76	-2.14	.93	-1.5	.88	-.30
3.5	.88	-2.14	.71	-3.11	.82	-2.14	.76	-2.30	.93	-1.48	.87	-.37
3.6	.87	-2.26	.70	-3.28	.82	-2.17	.75	-2.47	.93	-1.45	.87	-.45
3.7	.86	-2.37	.69	-3.45	.82	-2.20	.75	-2.63	.93	-1.43	.86	-.63
3.8	.84	-2.49	.68	-3.62	.82	-2.21	.74	-2.79	.93	-1.41	.85	-.60
3.9	.83	-2.61	.67	-3.79	.82	-2.26	.74	-2.91	.93	-1.4	.85	-.67

Appendix V, continued

	S_{31}		P_{31}		P_{33}		D_{33}		D_{35}		F_{35}		F_{37}	
Plate (GeV/c)	η	δ	η	δ	η	δ	η	δ	η	δ	η	δ	η	δ
4.0	.38	-36.15	.45	-13.4	.32	-32.03	.62	-10.08	.41	-16.0	.76	-5.18	.51	-8.1
4.1	.37	-35.4	.73	-29.2	.16	-29.15	.61	-10.18	.41	-15.87	.76	-7.43	.50	-5.34
4.2	.37	-34.69	.77	-31.91	.22	12.2	.60	-10.26	.41	-15.79	.74	-8.04	.50	-4.80
4.3	.36	-34.0	.71	-31.61	.23	6.71	.59	-10.32	.41	-15.72	.73	-7.96	.50	-5.17
4.4	.36	-33.3	.65	-30.68	.24	1.59	.58	-10.38	.41	-15.65	.72	-7.83	.50	-5.57
4.5	.35	-32.68	.65	-29.67	.25	-2.09	.58	-10.43	.41	-15.57	.71	-7.73	.50	-5.90
4.6	.35	-32.04	.57	-28.70	.25	-4.65	.57	-10.46	.41	-15.50	.70	-7.67	.49	-6.16

Appendix V, continued

	G_{37}		G_{39}		$H_{3,9}$		$H_{3,11}$		$I_{3,11}$		$I_{3,13}$	
Plate (GeV/c)	η	δ	η	δ	η	δ	η	δ	η	δ	η	δ
4.0	.82	-2.72	.66	-3.94	.82	-2.52	.73	-2.80	.93	-1.4	.84	-.75
4.1	.81	-2.84	.66	-4.10	.81	-2.95	.73	-2.51	.92	-1.39	.83	-.83
4.2	.81	-2.95	.65	-4.24	.81	-3.10	.72	-2.51	.92	-1.40	.83	-.91
4.3	.80	-3.06	.64	-4.39	.81	-3.13	.72	-2.62	.92	-1.41	.82	-1.0
4.4	.79	-3.17	.64	-4.53	.80	-3.15	.72	-2.73	.91	-1.42	.82	-1.1
4.5	.78	-3.28	.63	-4.66	.80	-3.18	.71	-2.82	.91	-1.43	.81	-1.14
4.6	.77	-3.38	.62	-4.79	.80	-3.23	.71	-2.91	.91	-1.45	.80	-1.22

Appendix V, continued

	S_{31}		P_{31}		P_{33}		D_{33}		D_{35}		F_{35}		F_{37}	
Plate (GeV/c)	η	δ	η	δ	η	δ	η	δ	η	δ	η	δ	η	δ
4.7	.34	-31.43	.55	-27.82	.26	-6.45	.57	-10.49	.41	-15.43	.69	-7.64	.49	-6.38
4.8	.34	-30.83	.53	-27.02	.27	-7.76	.56	-10.51	.41	-15.36	.68	-7.62	.49	-6.56
4.9	.33	-30.25	.51	-26.28	.27	-8.72	.56	-10.52	.41	-15.29	.67	-7.61	.49	-6.71
5.0	.33	-29.68	.50	-25.60	.28	-4.46	.55	-10.53	.41	-15.21	.67	-7.61	.48	-6.85

Appendix V, continued

	G_{37}		G_{39}		$H_{3,9}$		$H_{3,11}$		$I_{3,11}$		$J_{3,13}$	
Plate (GeV/c)	η	δ	η	δ	η	δ	η	δ	η	δ	η	δ
4.7	.77	-3.48	.62	-4.91	.80	-3.27	.70	-2.99	.90	-1.47	.80	-1.30
4.8	.76	-3.57	.61	-5.03	.79	-3.32	.70	-3.06	.90	-1.5	.79	-1.37
4.9	.76	-3.69	.61	-5.14	.79	-3.37	.69	-3.12	.90	-1.45	.79	-1.53
5.0	.75	-3.76	.60	-5.25	.79	-3.42	.69	-3.18	.89	-1.55	.78	-1.52

References

1. H. Yukawa, Proc. Phys. Math. Soc., Japan, 17 48 (1935)

2. C.D. Anderson and S.H. Neddermeyer, Phys. Rev. 51, 884 (1937)

3. C.M.G. Lattes, G.P.S. Occhialini, C.F. Powell, Nature 160, 453, 486 (1947)

4. B.H. Bransden, R.G. Moorhouse and P.J. O'Donnel, Phys. Rev. 139, B1566
   A. Donnachie, R.G. Kirsopp and C. Lovelace, Phys. Let. 26B, 161 (1968)

5. See for example
   'Regge poles in particle physics' by P.D.B. Collins and E.J.S. Squires, (Springer tracts in modern physics)

6. V. Barger and D. Cline, Phys. Rev. 155, 1792 (1968)
   R. Dolen, D. Horn and C. Schmid, Phys. Rev. 166 1768 (1968). A. Donnachie and R.G. Kirsopp, NUC. Phys. B10, 433 (1969)

7. N.N. Khuri, Phys. Rev. 130, 429 (1963)

8. For a full discussion see J. Hamilton's review article in 'Strong interactions and high energy physics' edited by R.G. Moorhouse (1963)

9. 'Strong Interaction Physics' by M. Jacob and G.F. Chew (Benjamin, (1964))

10. See M. Jacob and G.C. Wick, Ann. Phys. 115, 1741 (1959)

11. S.W. MacDowell, Phys. Rev. 116, 774 (1960)

12. S. Mandelstam, Phys. Rev. 112, 1344 (1958)

13. L.D. Roper, R.M. Wright, and B.T. Feld, Phys. Rev. 138, B190 (1965)

14. See E.C. Titchmarsh
'Theory of functions, 2nd Edition, Oxford
University Press 1939.

15. E.J. Squires, Complex angular momentum
(Benjamin

16. Sommerfield, 'Partial differential equations
in Physics' (1964) p.282

17. See reference 5 p.54-55

18. T. Regge, N.C. 14, 951 (1959)

19. S. Mandelstam, Ann. Phys. 19, 254 (1962)

20. M. Gell-man, M.L. Goldberger, F. Low, E. Marx and
F. Zachariasen, Phys. Rev. 133, B145 (1964)
Also see reference 15, p.26.

21. M. Gell-man. - lecture given at International
Conference on High-Energy Physics, CERN (1962)

22. D.A. Atkinson and V. Barger, N.C. 38, 634 (1965)

23. This can be shown easily by putting $u = o$ and
$u = u_B$ in equation (2.23)

24. D.J. Freedman and J. Wang, Phys. Rev. Lett. 17,
569 (1966)

25. Bateman manuscript project, higher transcendental
functions. Vol.I, p.156.

26. S. Mandelstam, Ann. Phys. (N.Y.) 19, 254 (1962)

27. Reference 25, Vol.II, p.315.

28. V. de Alfaro, S. Fubini, G. Furlan, G. Rossetti
Phys. Letters 21 576 (1966)

29. R. Dolen, D. Horn and C. Schmid, Phys. Rev. 166,
1768 (1968)

30. An excellent review on duality will be found in
M. Jacob's lectures given at the VIII International
Conference on Theoretical Physics at Schladming
(CERN preprint, 1969)

31. C. Schmid, Phys. Rev. Letters. 20, 689 (1968)

32. P.D.B. Collins, R.C. Johnson and E.J. Squires, Phys. Letters. 27B, 23 (1968)

33. G. Veneziano, Nuovo Cimento 57A, 190 (1968)

34. K. Igi, Phys. Letters. 28B, 330 (1968)

35. V. Singh, Phys. Rev. 129, 1889 (1963)

36. C.B. Chin and J.D. Stack, Phys. Rev. 153, 1575 (1967)

37. See reference 24 and also reference 6.

38. V. Barger and D. Cline, Phys. Rev. Letters. 21, 392 (1968)

39. Y. Nairot, M. Rimpault and Y. Saillard, Phys. Letters. 26B, 454 (1966)
K. Igi, S. Matsuda, Y. Oyanagi and Hikurasato, Phys. Rev. Lett. 21, 580 (1968)

40. D.P. Owen et al., Cornell University Preprint (1969)

41. See reference 38.

42. W.R. Frazer and J.R. Fulco, Phys. Rev. 117, 1603 (1960)

43. Mengta Chung, Karlsruhe, preprint, 1968

44. These forms are taken from the following paper; W. Rarita, R.J. Riddell, C.B. Chiu and R.J.N. Phillips, Phys. Rev. 165, 1615 (1968) and then analytically continued over the whole physical range of t.

45. See, for example reference 5.

46. V. Cork et al., Phys. Rev. 130, 762 (1963)
($\pi^{\pm}$ P Dif. cross-section 1.5, 2.0, 2.5 GeV/c);
D.E. Damouth et al., Phys. Rev. Letters. 11, 287 (1963)
($\pi^{\pm}$ P Dif. cross section 2 GeV/c);
C.T. Coffin et al., Phys. Rev. Letters. 17, 458 (1968)
($\pi^{\pm}$ P Dif. cross section 2.3 to 4.0 GeV/c);

O. Chamberlain et al. Phys. Rev. Letters. 17, 975 (1966)
($\pi^{\pm}$ P Polarization .670 to 3.75 GeV/c);
Kormanyos et al., Phys. Rev. (- P Dif. cross-section at 180°) ;
F.E. James et al., Phys. Let. 19, 72 (1965)
(π^{+} P Dif. cross section 1.76, 2.08 GeV/c);
J. Banaigs et al., Nucl. Phys. B8, 32 (1968)
($\pi^{\pm}$ P Dif. cross section 2.85, 3.30, 3.55 GeV/c);
W. Busza et al., Phys. Rev. 180, 1339 (1969)
($\pi^{\pm}$ P Dif. cross section 1.72 - 2.80 GeV/c);
P. Sonderegger et al., Phys. Letters. 20,75 (1968)
(C.E. Dif. cross section 3.07 to 18.2 GeV/c);
A.S. Carroll et al., Proc. Roy. Soc. A289,513 (1966)
(C.E. Dif. cross section 1.72 to 2.46 GeV/c);
M.L. Perl et al., Phys. Rev. 132, 1252 (1963)
(π^{+} P Dif. cross section 3 to 5 GeV/c);
R.J. Esterling et al., Phys. Rev. Letters. 21, 1410 (1968)
(π^{+} P Polarization 5.15 GeV/c);
D. Drobnis et al., Phys. Rev. Letters. 20, 274 (1968)
(C.E. Polarization 2 to 5 GeV/c).

47. For a full discussion see
A. Donnachie, 14th Intern. Conf. on High-Energy Physics, Vienna, 1968

48. P. Bareyre, C. Bricman, and G. Villet, Phys. Rev. 165, 1730 (1968), also see reference 4.

49. Particle data group, Rev. Mod. Phys. 41, 109 (1969) (pp. 123, 164, 165)

50. R.R. Crittenden et al., Indiana University pre-print (1969).

Figure Legends

Figure 1 (a), (b), (c), (d), (e), (f). Regge pole fit to π^+ , π^- elastic scattering by protons and charge exchange, in the forward direction.

Figure 2 (a), (b), (c). Regge pole fit to π^+ and π^- elastic scattering by protons in the backward direction.

Figure 3 (a), (b). The $\Delta\delta$ and N_α trajectories.

Figure 4 (a)...(j)..(m) Comparison of the experimental π^+ -p elastic scattering data and the best fit provided by the amplitudes parameterised as discussed in the text.

Figure 5 (a)-(c). Comparison of the data of Busza et al. (1969) (π^+-p) with cross sections predicted by the parameterised amplitudes.

Figure 6 (a)-(g). $T = {}^3/_2$ phase shifts determined from the parameterised amplitudes that provided the best fit to the data.

Figure 7 (a)....(e)	Comparison of the experimental $p\ \pi^-$-p elastic scattering data and the best fit provided by the amplitudes parameterised as discussed in the text.
Figure 8 (a)....(e)	Comparison of the experimental π^--p and C.E. polarization and the best fit.
Figure 9 (a)....(c)	Comparison of the experimental C.E. differential cross section data and the best fit.
Figure 10 (a)....(g)	$T = {}^1/_2$ phase shifts.

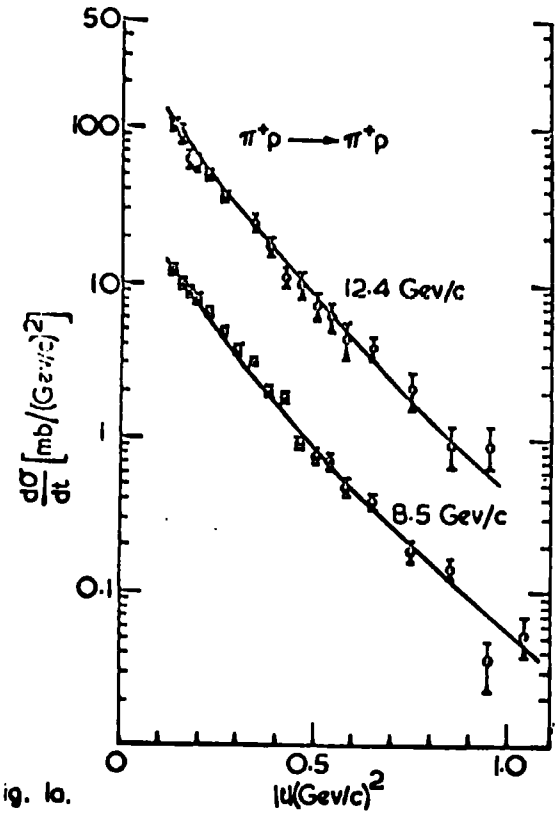

ig. Ia.

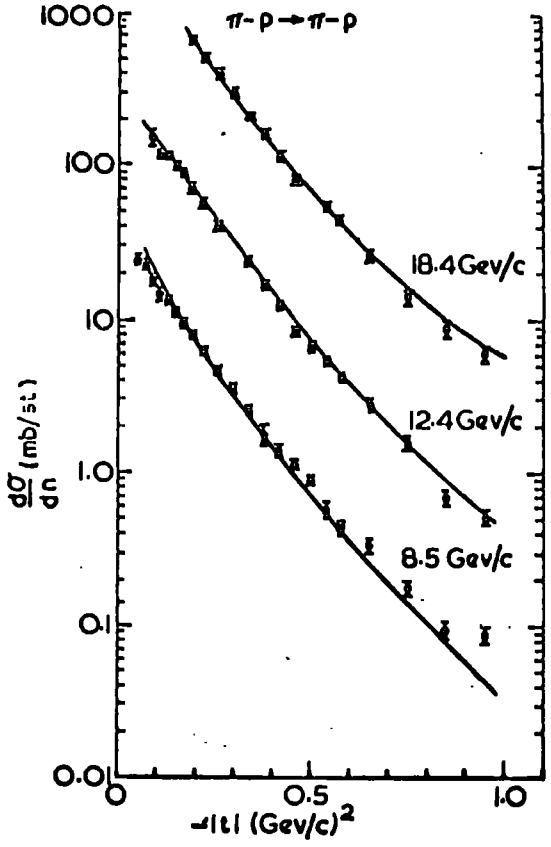

Fig.Ib.

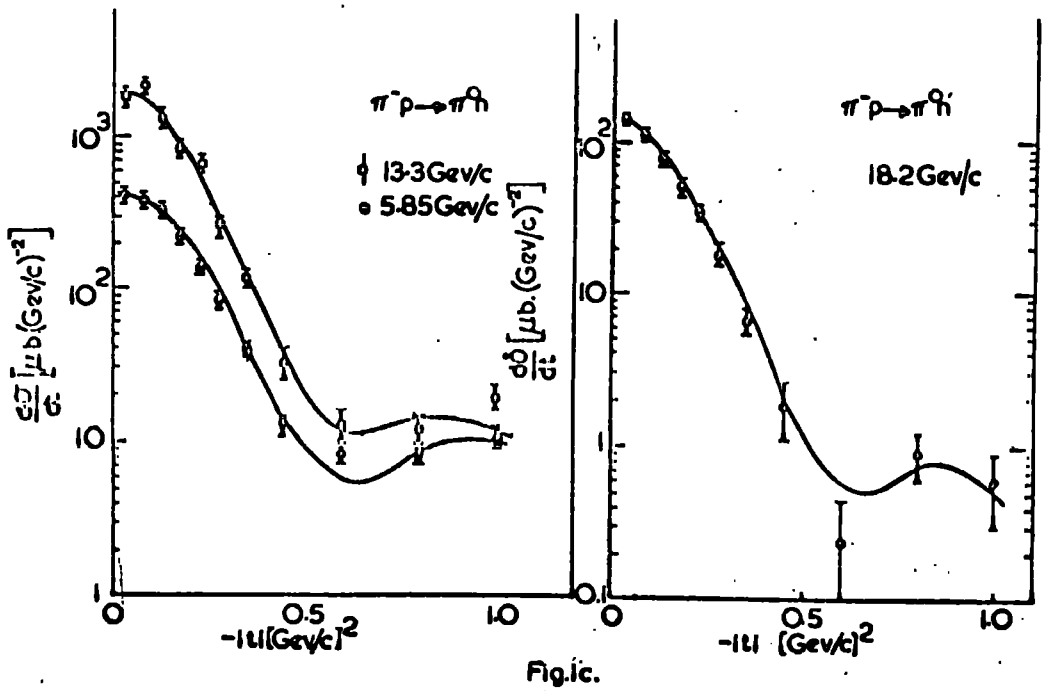

Fig.Ic.

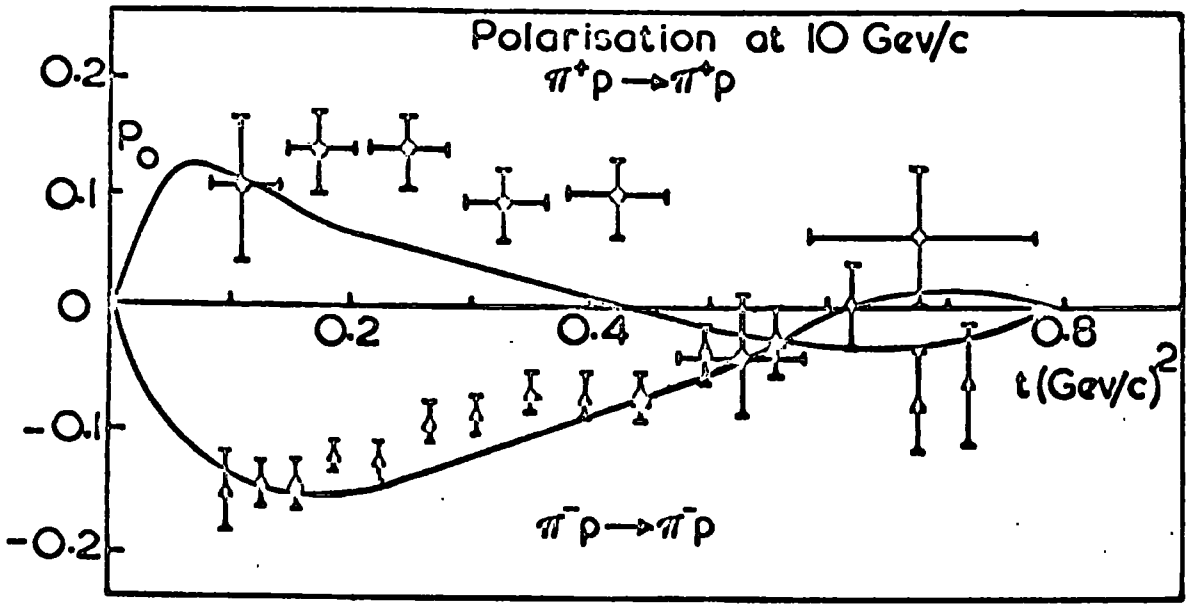
Polarisation at 10 Gev/c
$\pi^+ p \rightarrow \pi^+ p$
P_o
0.2
0.1
0
-0.1
-0.2
0.2
0.4
0.8
$t\,(Gev/c)^2$
$\pi^- p \rightarrow \pi^- p$

Fig. 1d.

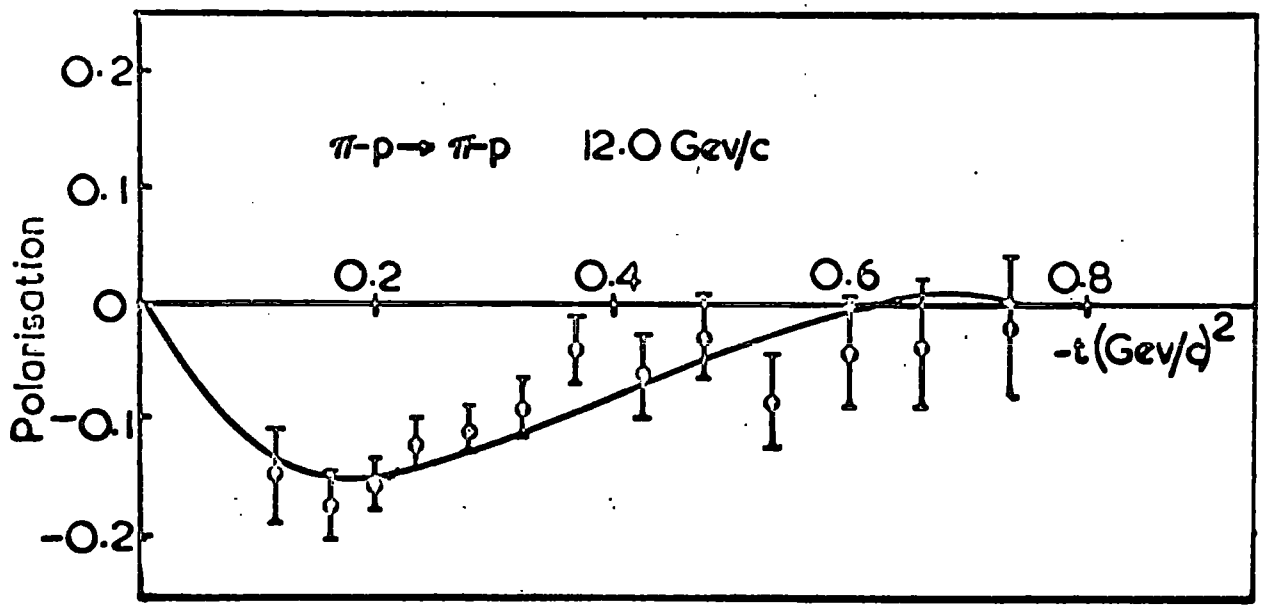
$\pi^- p \rightarrow \pi^- p$ 12.0 Gev/c
Polarisation
0·2
0·1
0
-0·1
-0·2
0·2
0·4
0·6
0·8
$-t\,(Gev/c)^2$

Fig. 1e.

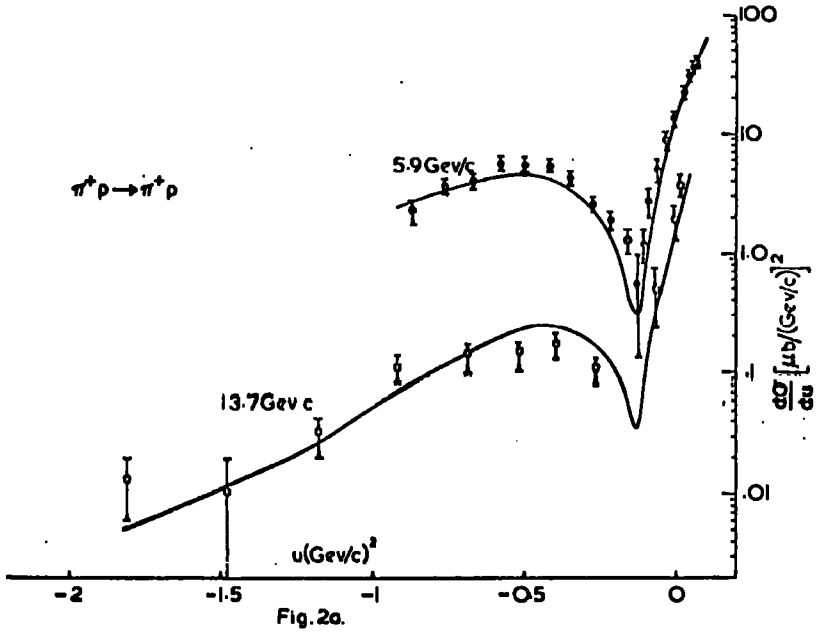

Fig. 2a.

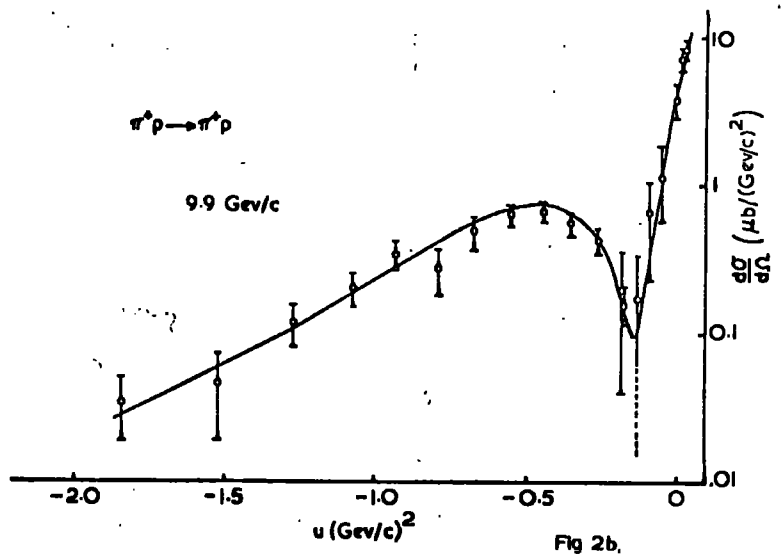

Fig 2b.

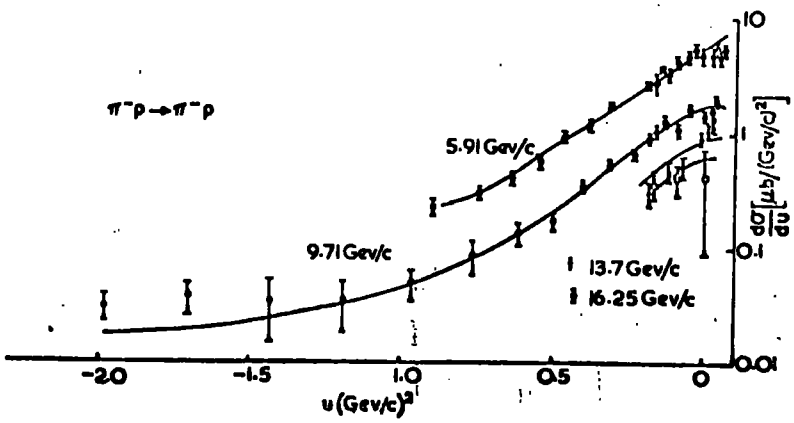

Fig. 2c.

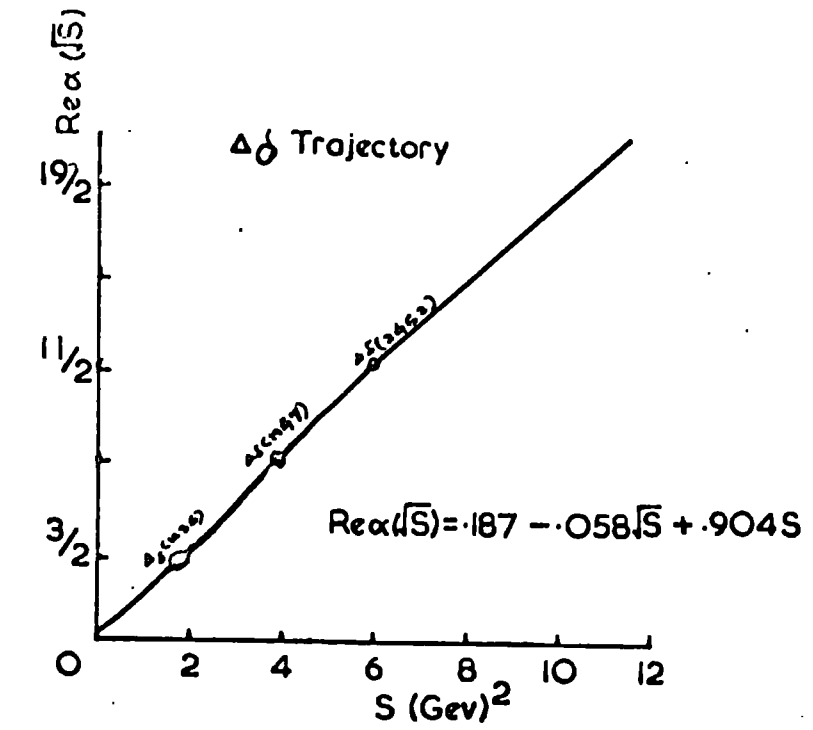
Re α (√S)
Δδ Trajectory
19/2
11/2
3/2
0
2
4
6
8
10
12
S (Gev)²
Re α(√S) = ·187 − ·058√S + ·904S

Fig. 3a.

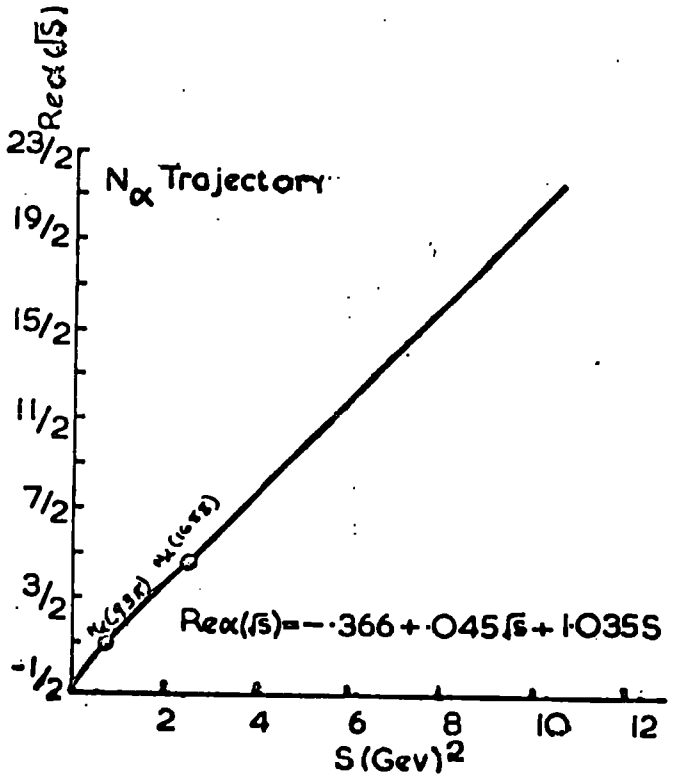
Re α (√S)
23/2
N_α Trajectory
19/2
15/2
11/2
7/2
3/2
-1/2
2
4
6
8
10
12
S (Gev)²
Re α(√S) = − ·366 + ·045√S + 1·035S

Fig. 3b.

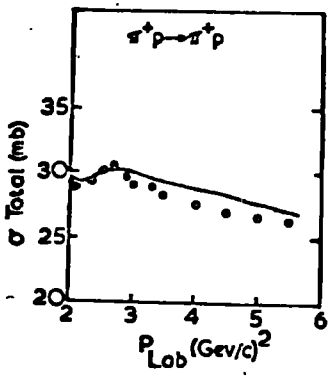

Fig.4a.

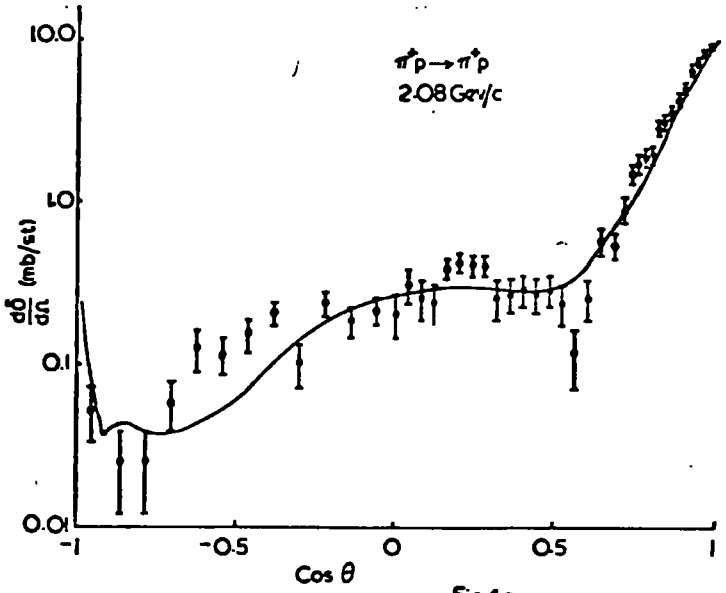

Fig.4c

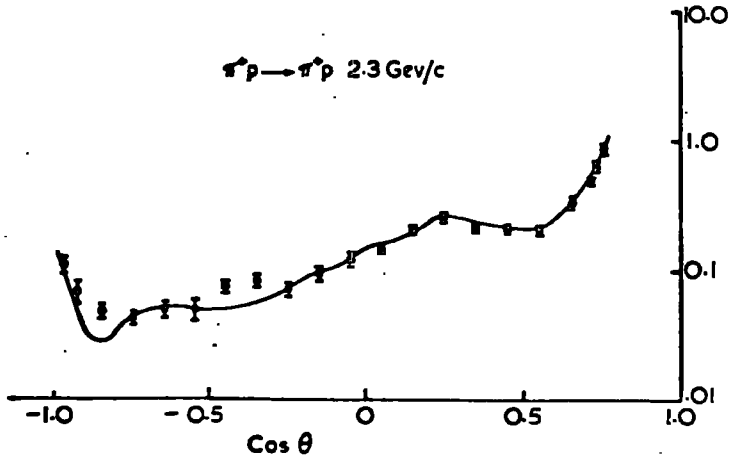

Fig. 4d.

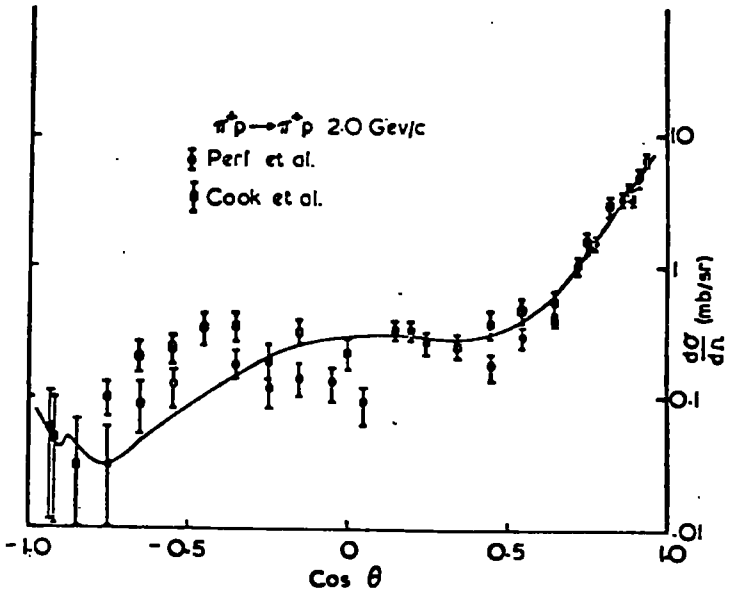

Fig. 4b.

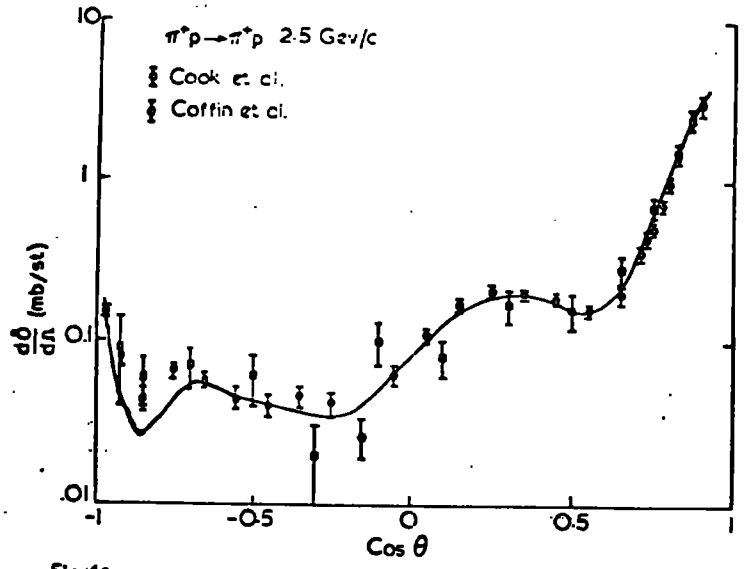

Fig.4e.

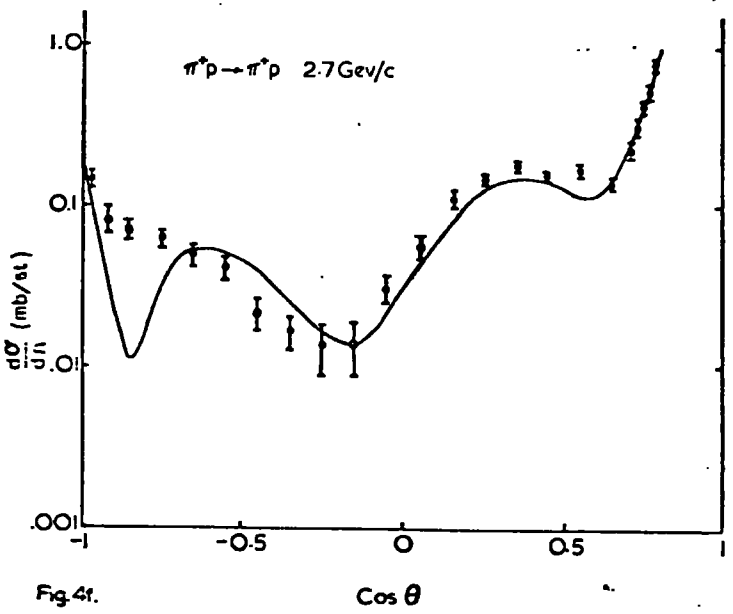

Fig.4f.

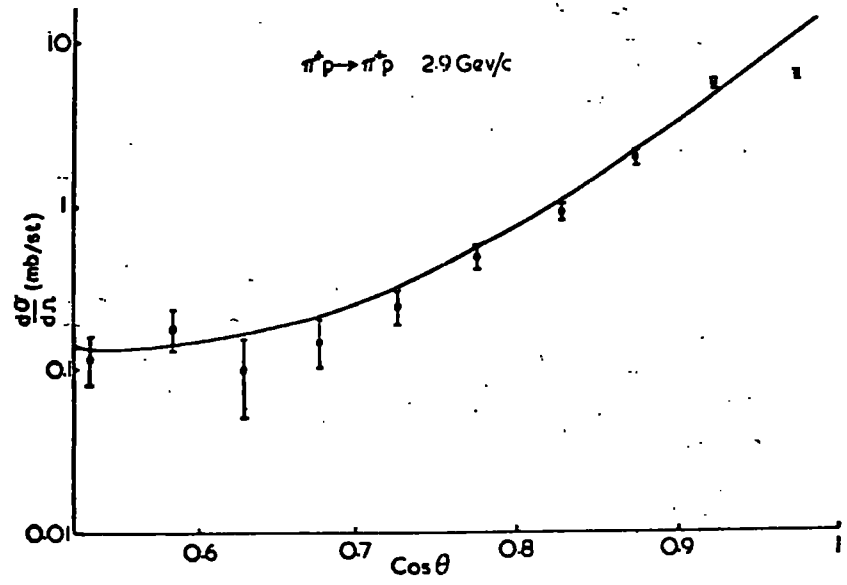

Fig.4g.

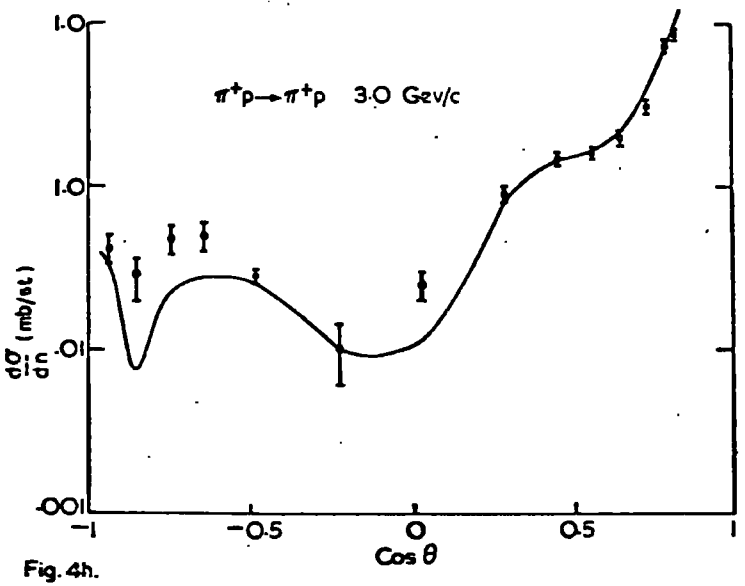

Fig. 4h.

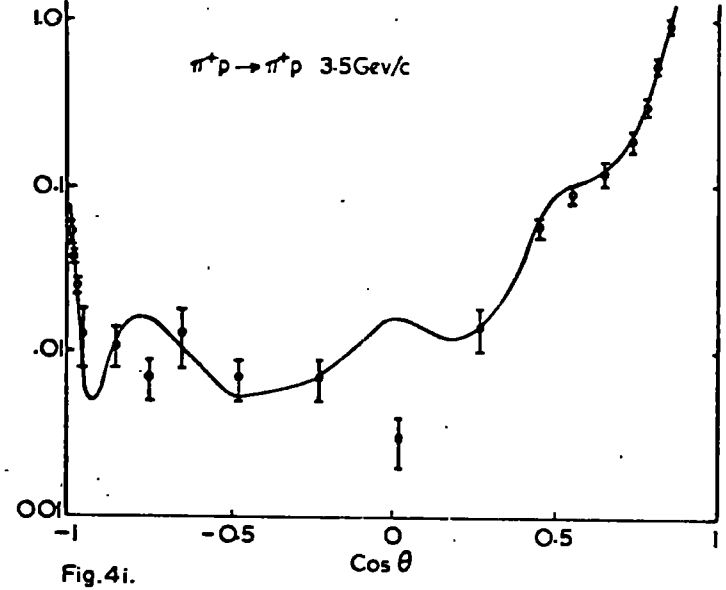

Fig. 4i.

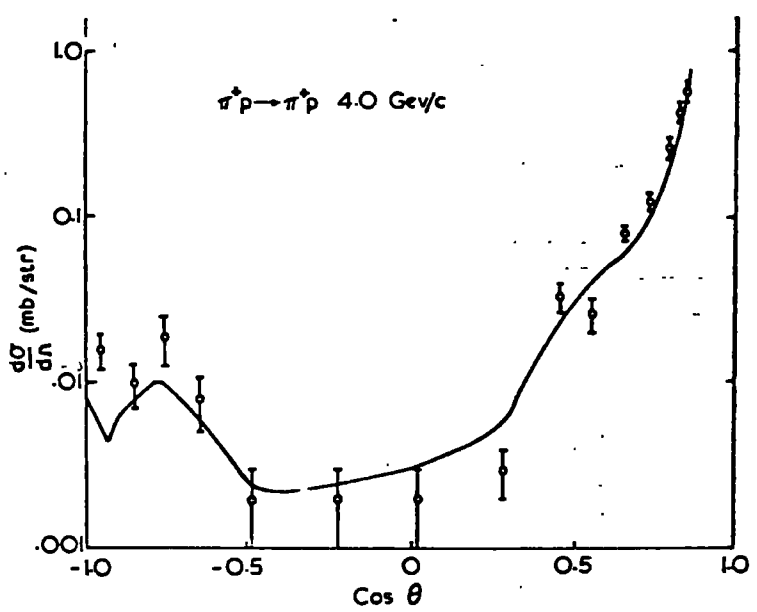

Fig. 4j

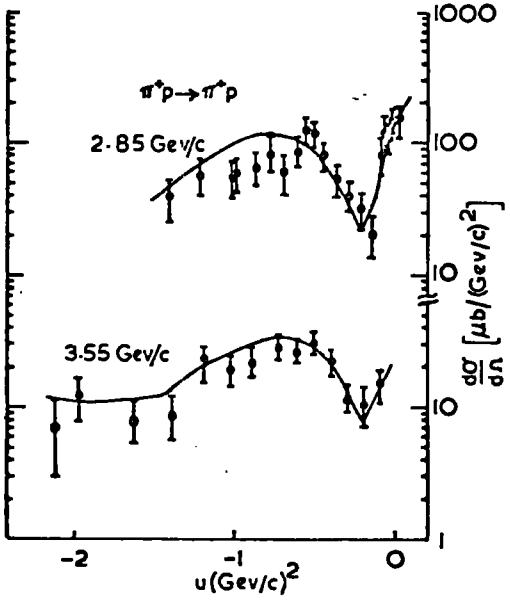

Fig. 4k.

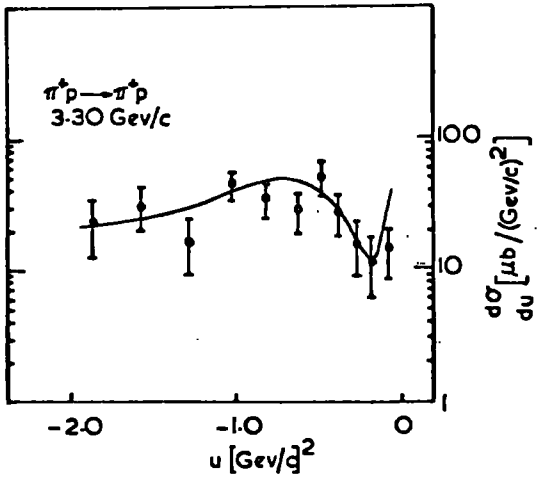

Fig. 4l.

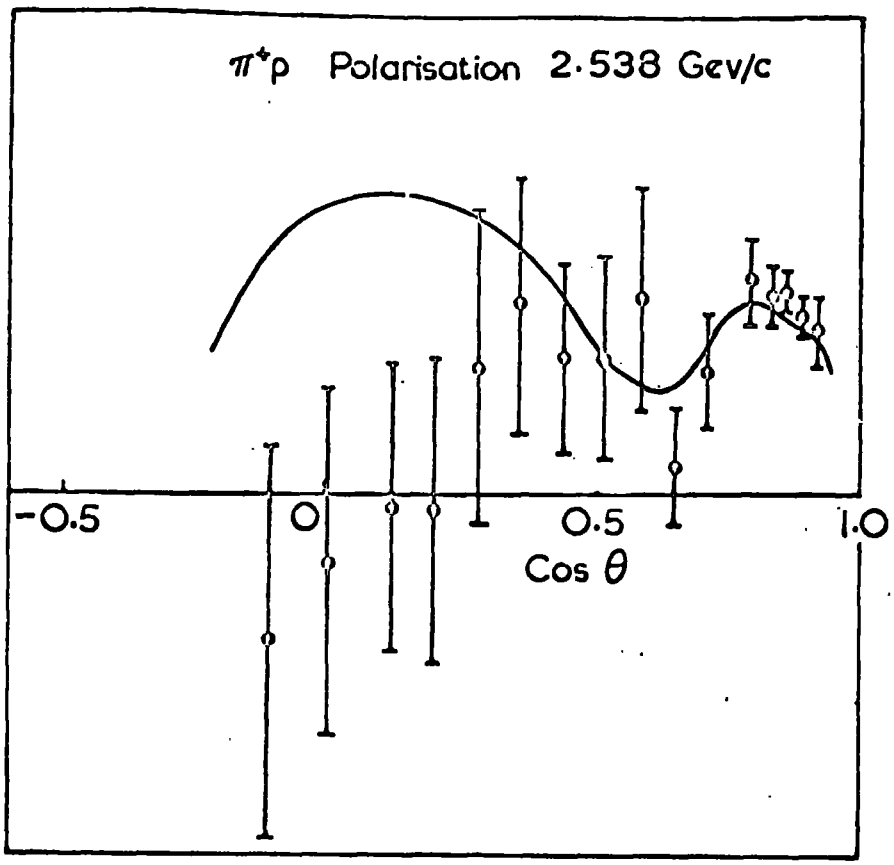
π⁺p Polarisation 2·538 Gev/c
-0.5
0
0.5
1.0
Cos θ

Fig. 4m.

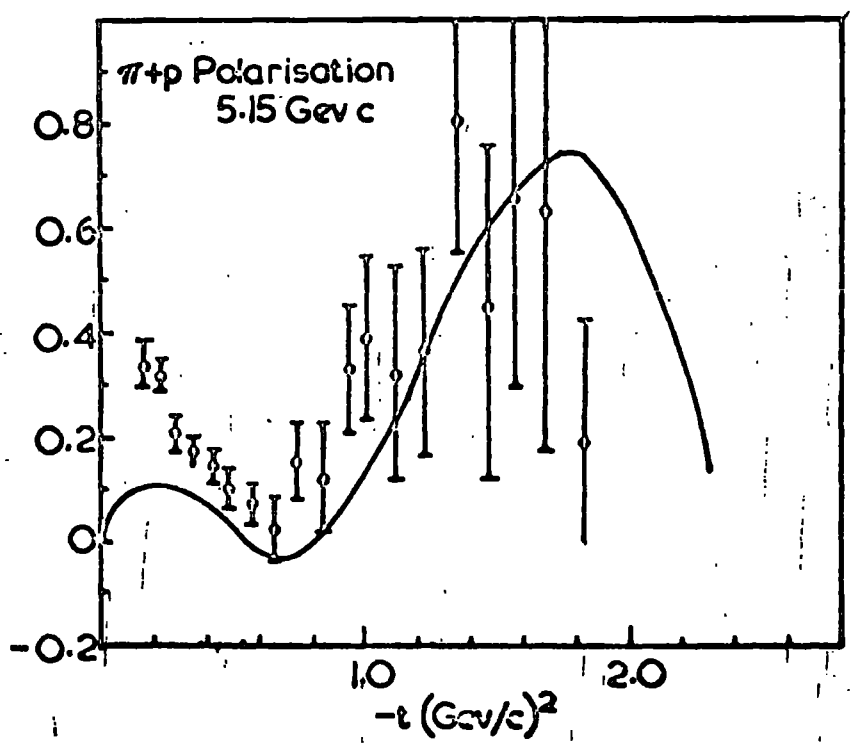
π+p Polarisation
5.15 Gev c
0.8
0.6
0.4
0.2
0
-0.2
1.0
2.0
-t (Gev/c)²

Fig An.

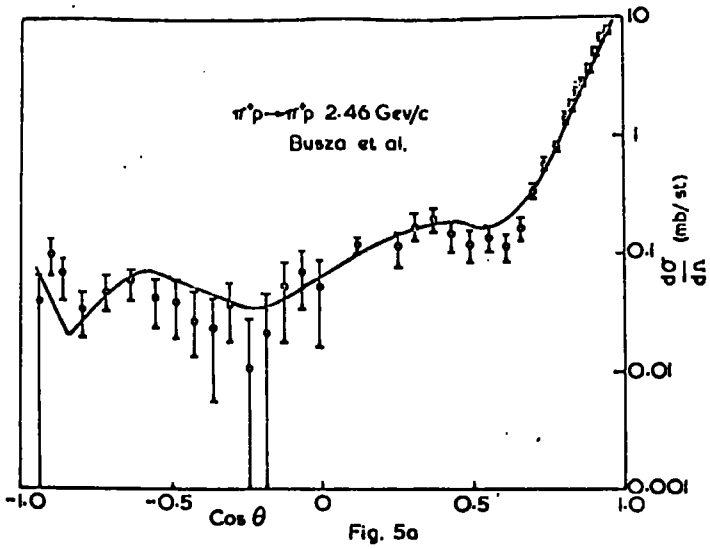

Fig. 5a

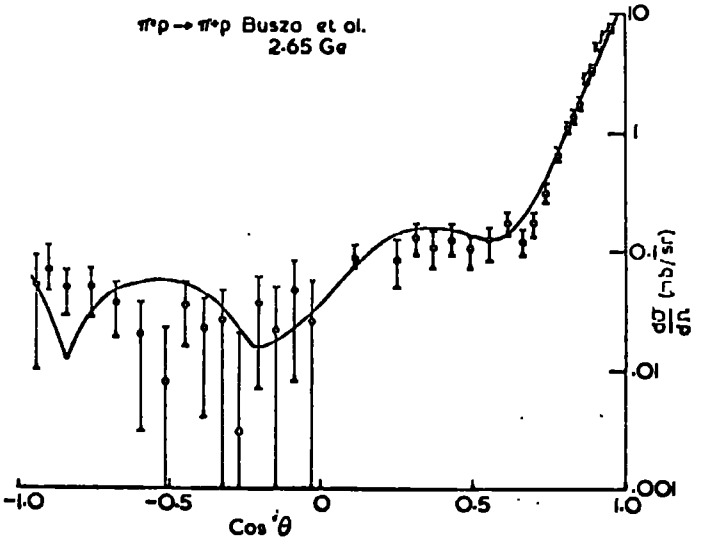

Fig. 5b

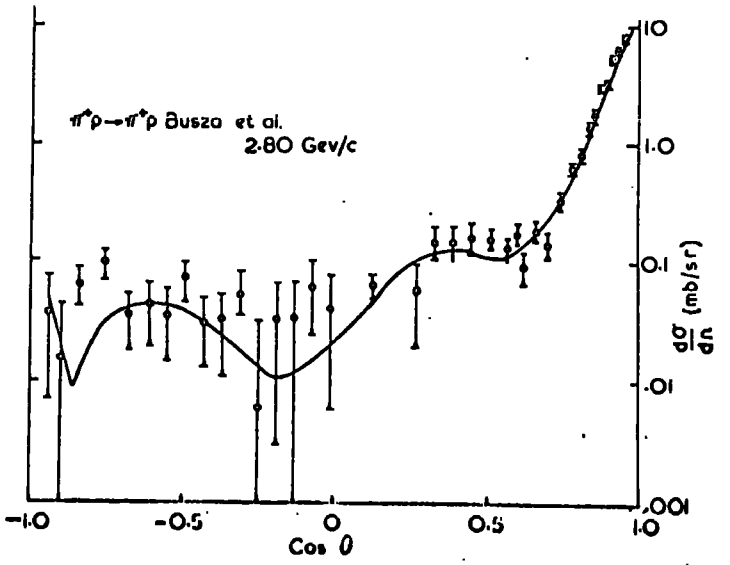

Fig. 5c.

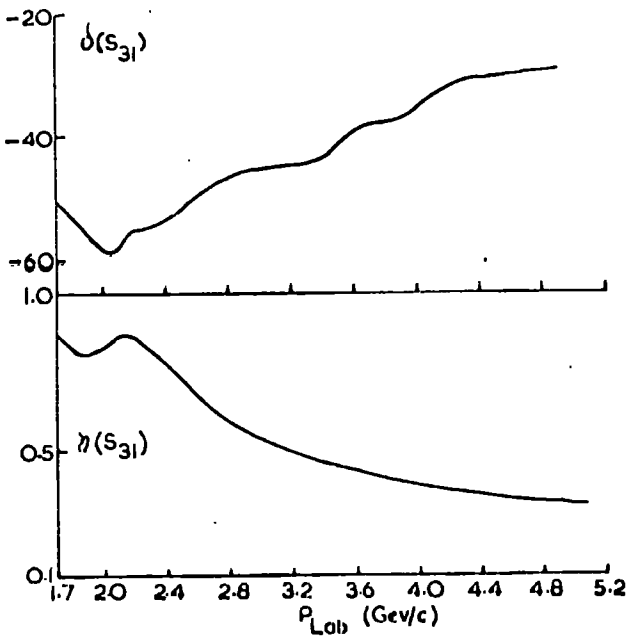

Fig. 6a.

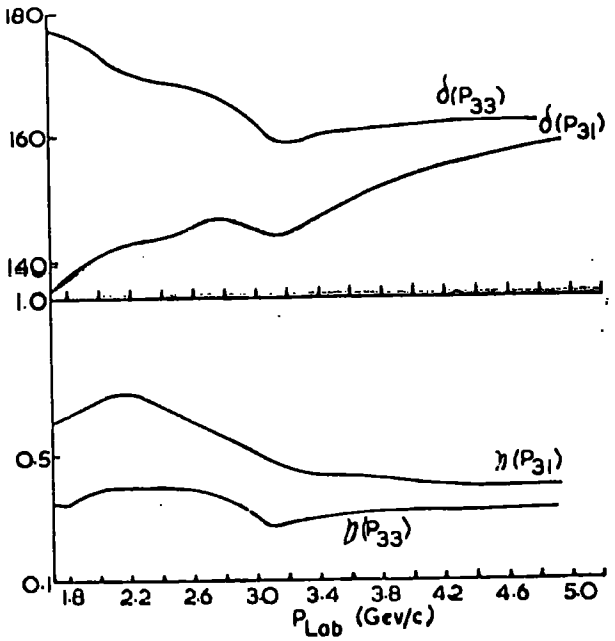

Fig. 6b.

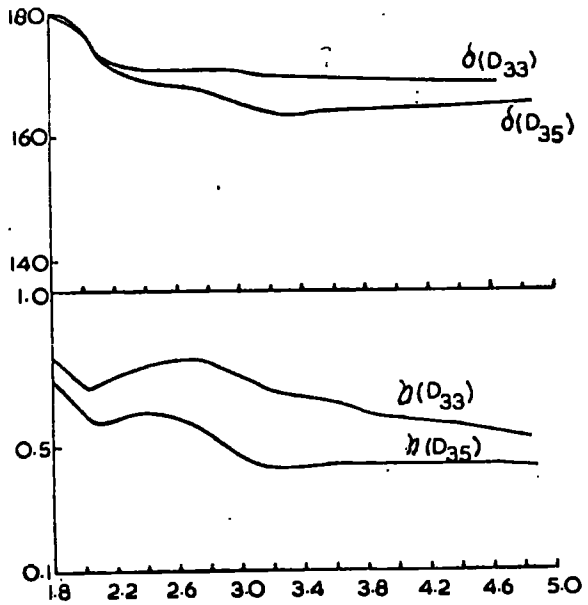

Fig. 6c.

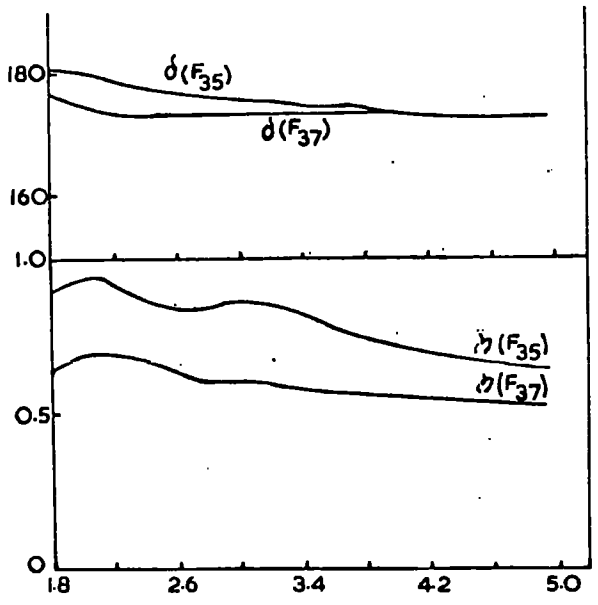

Fig. 6 d

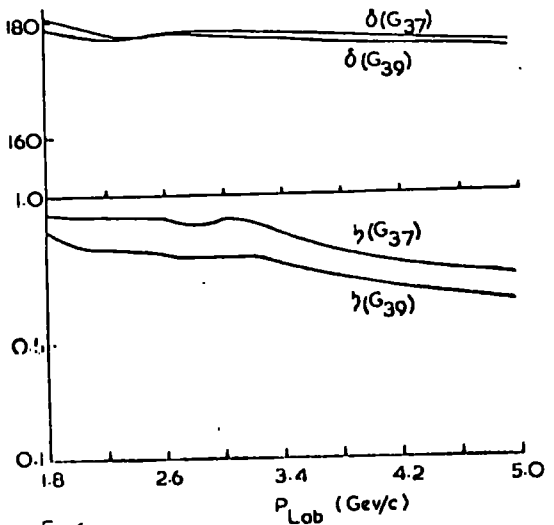

Fig.6e.

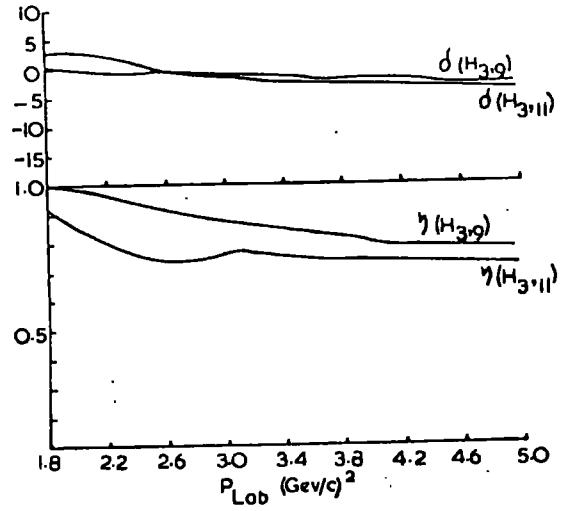

Fig. 6f.

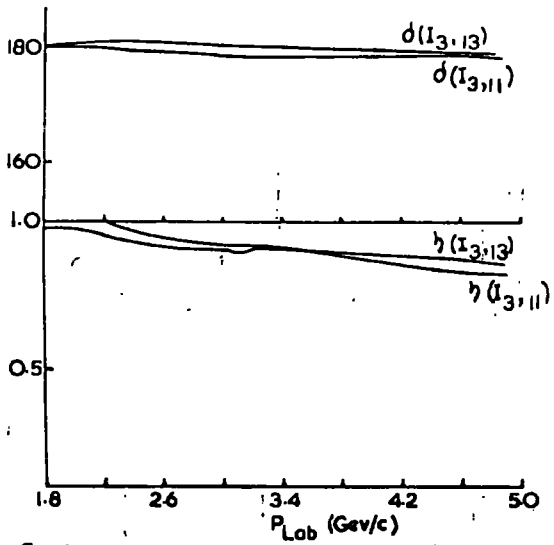

Fig. 6g.

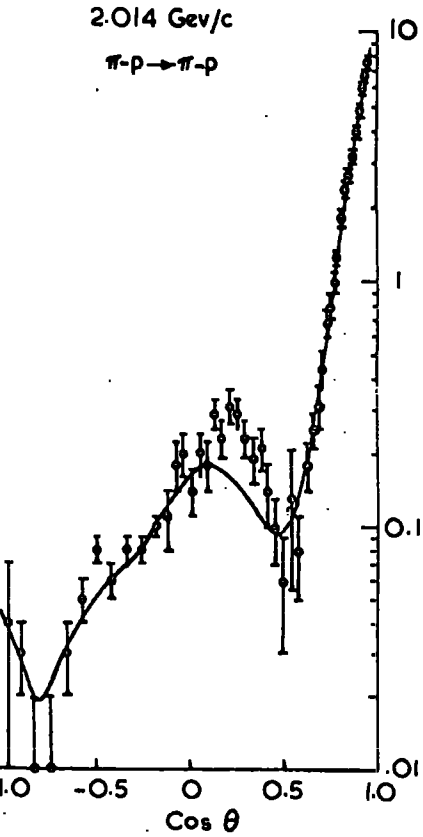

g. 7a.

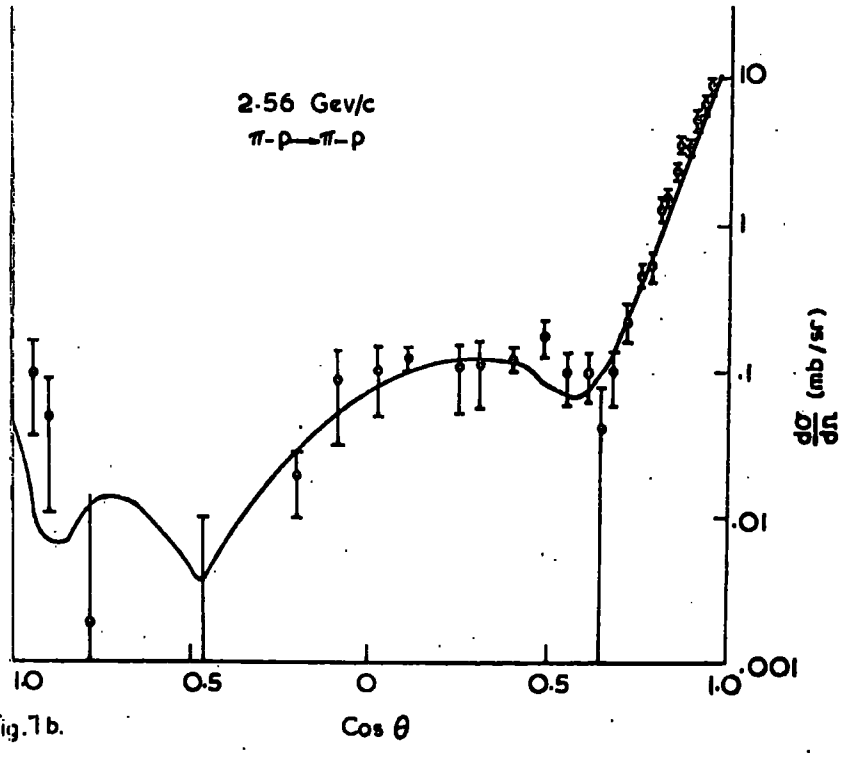

Fig. 7b.

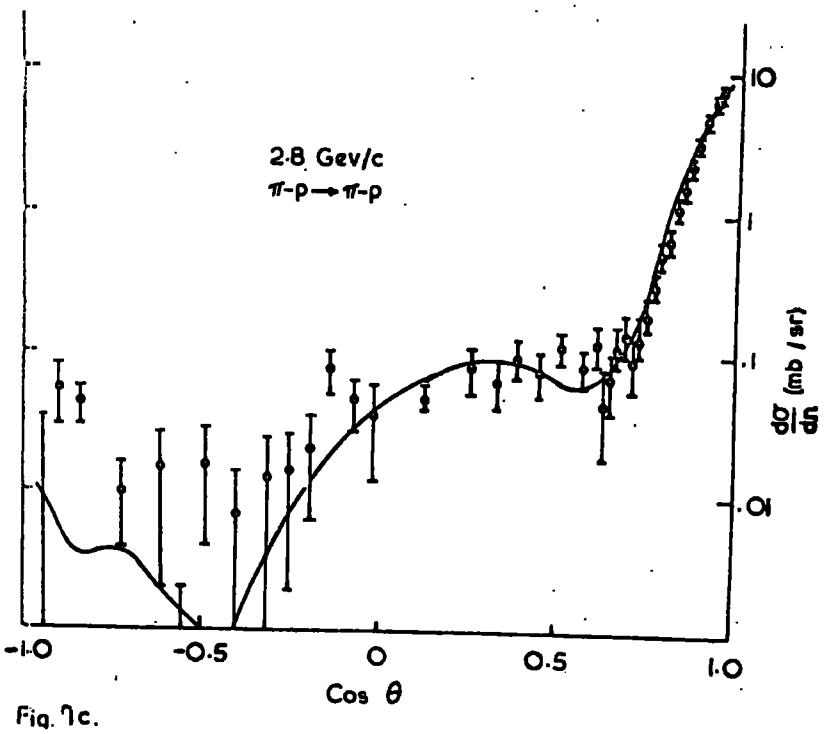

Fig. 7c.

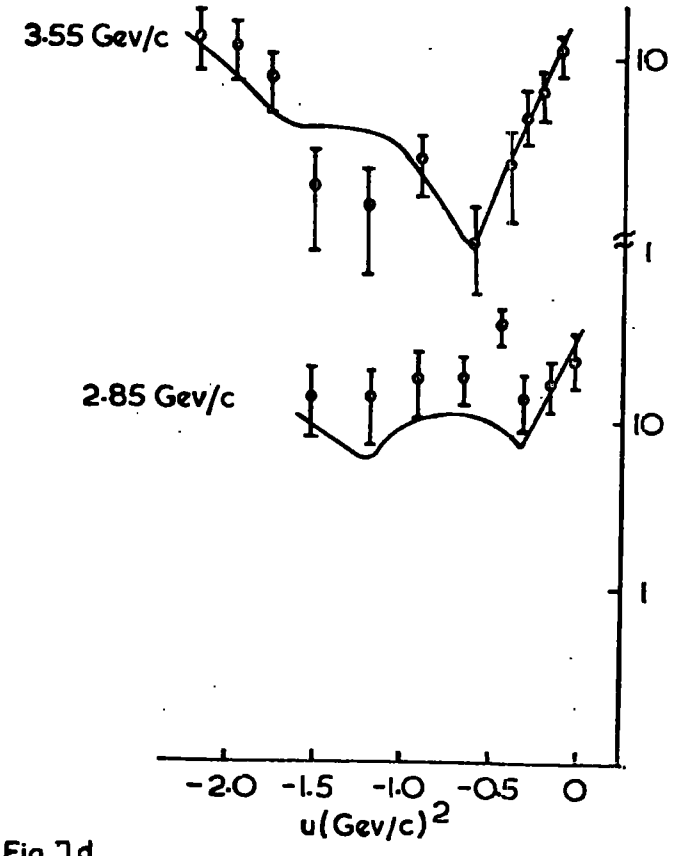
π-p→π-p
3.55 Gev/c
2.85 Gev/c
10
1
10
1
-2.0
-1.5
-1.0
-0.5
0
u(Gev/c)²

Fig. 7d.

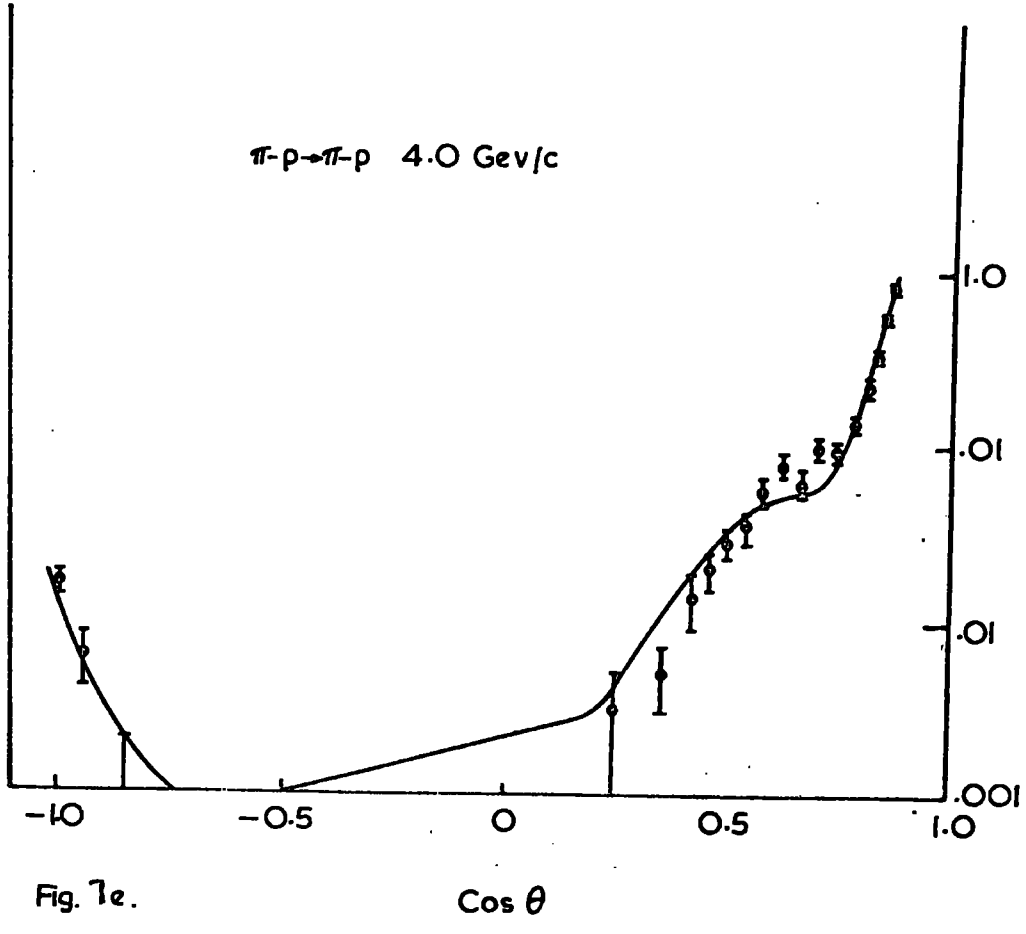
π-p→π-p 4.0 Gev/c
1.0
.01
.01
.001
-1.0
-0.5
0
0.5
1.0
Cos θ

Fig. 7e.

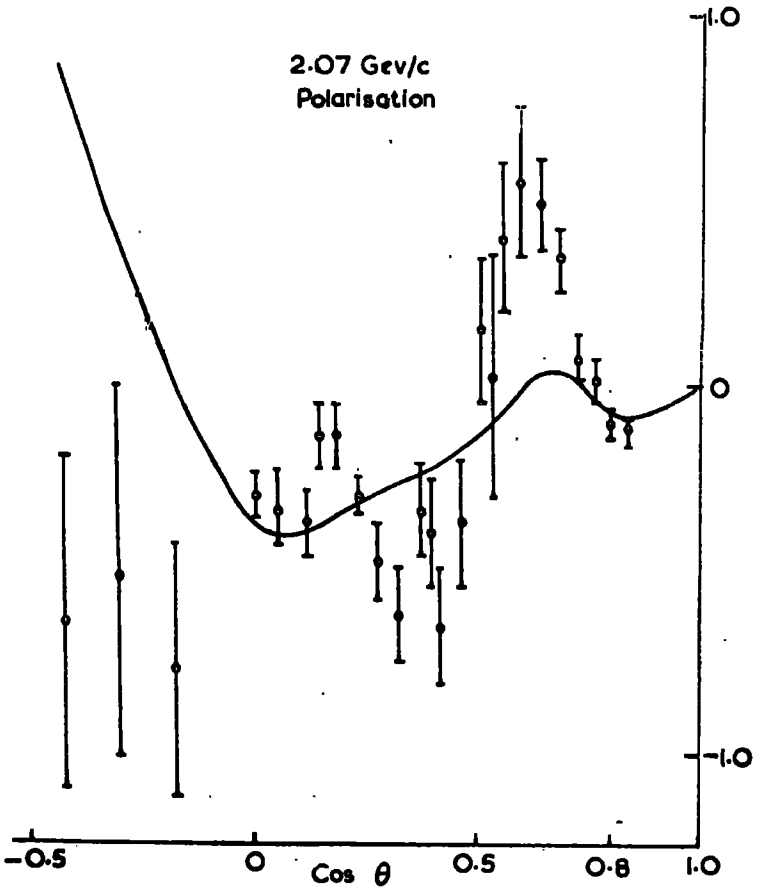

Fig. 8a

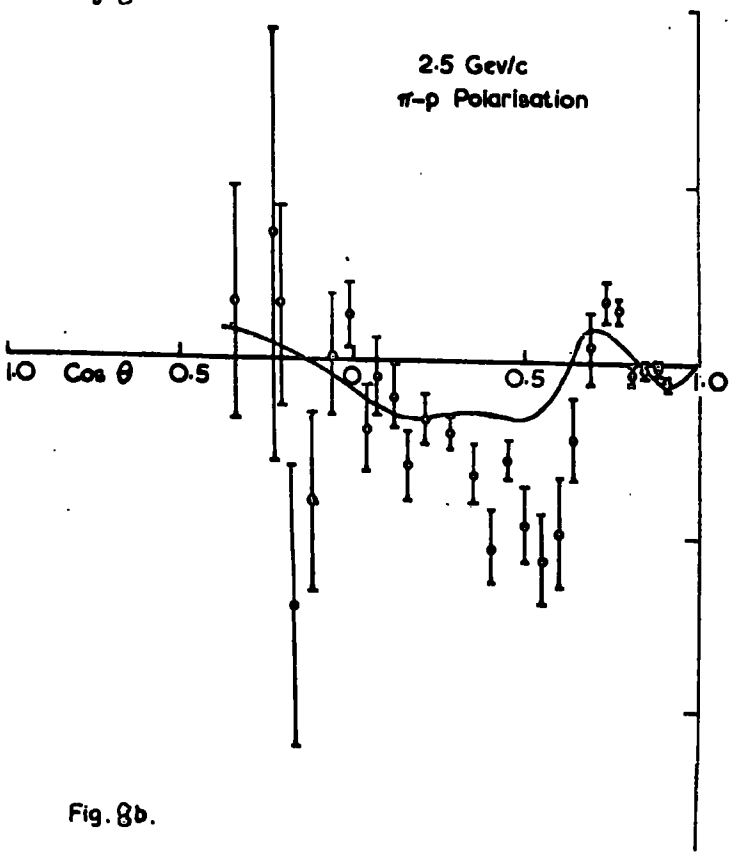

Fig. 8b.

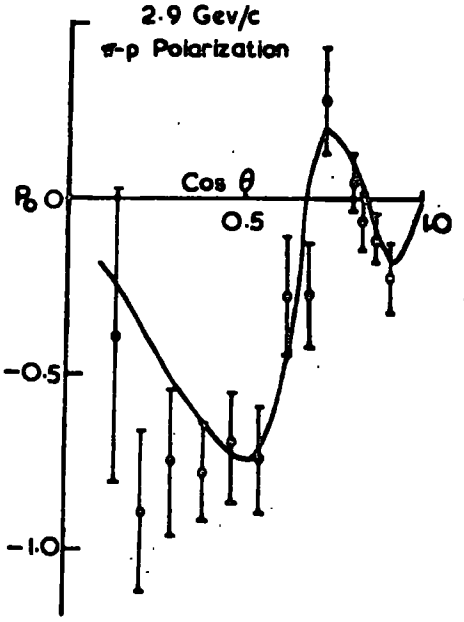

Fig. 8c.

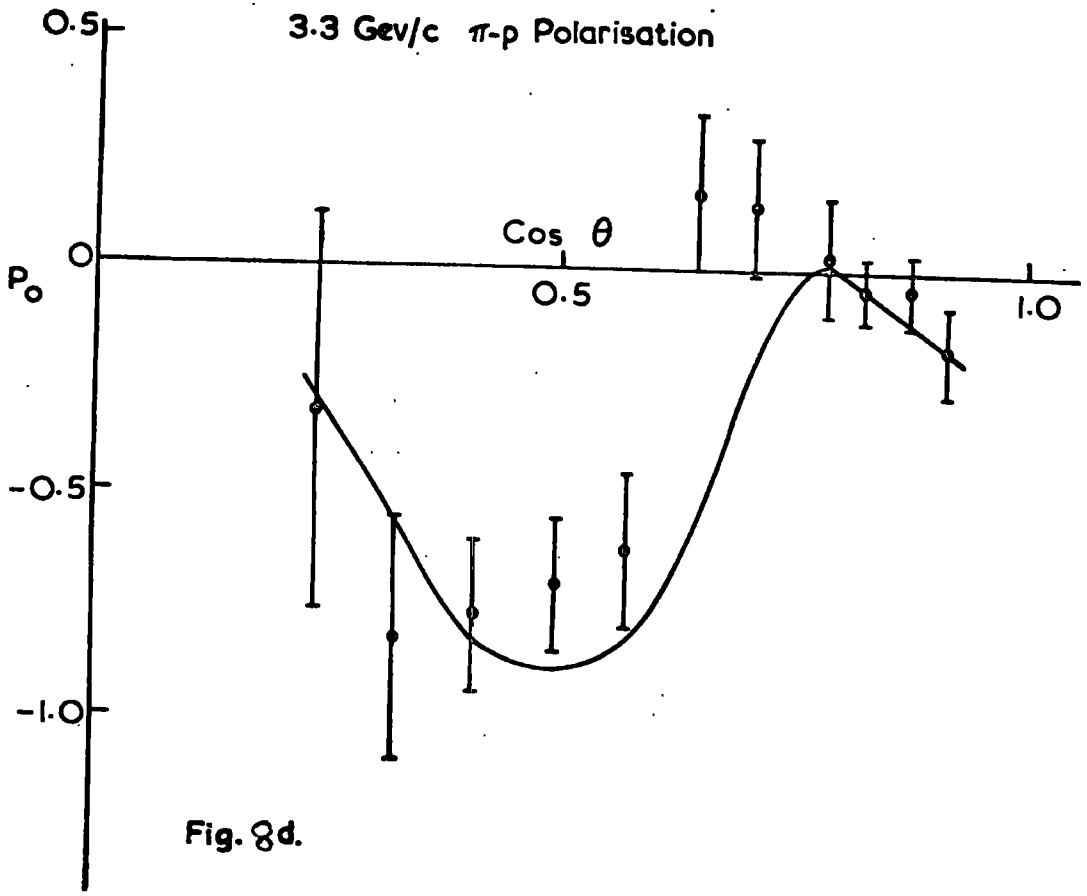
3.3 Gev/c π-p Polarisation
0.5
0
-0.5
-1.0
P_o
Cos θ
0.5
1.0

Fig. 8d.

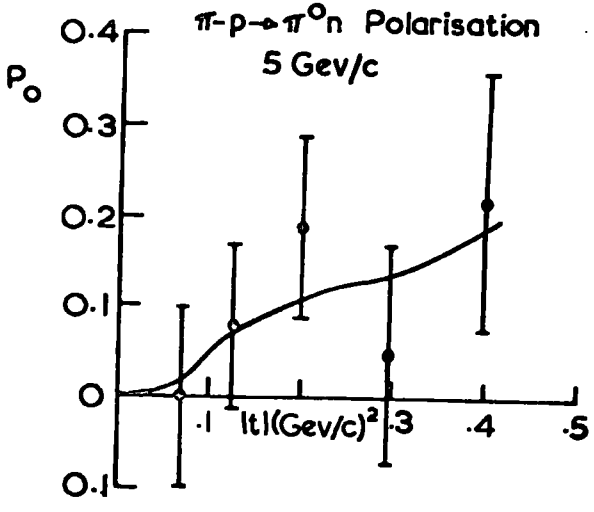
π-p→π°n Polarisation
5 Gev/c
0.4
0.3
0.2
0.1
0
0.1
P_o
.1
|t|(Gev/c)²
.3
.4
.5

Fig. 8e.

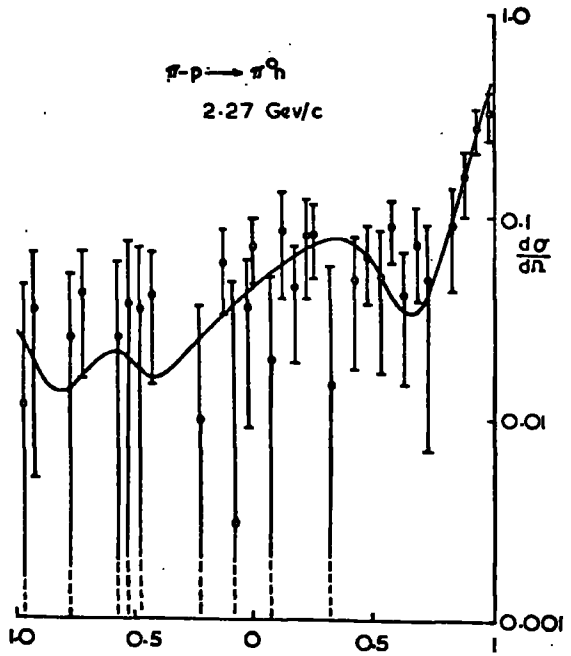

Fig 9a

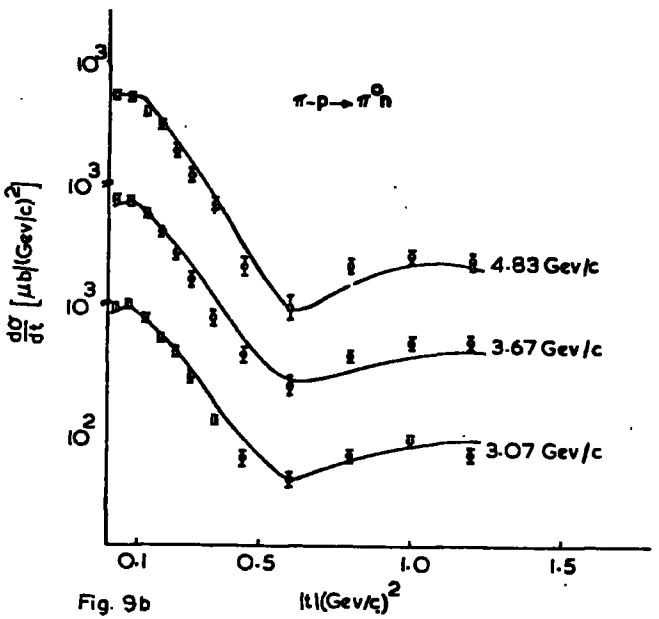

Fig. 9b

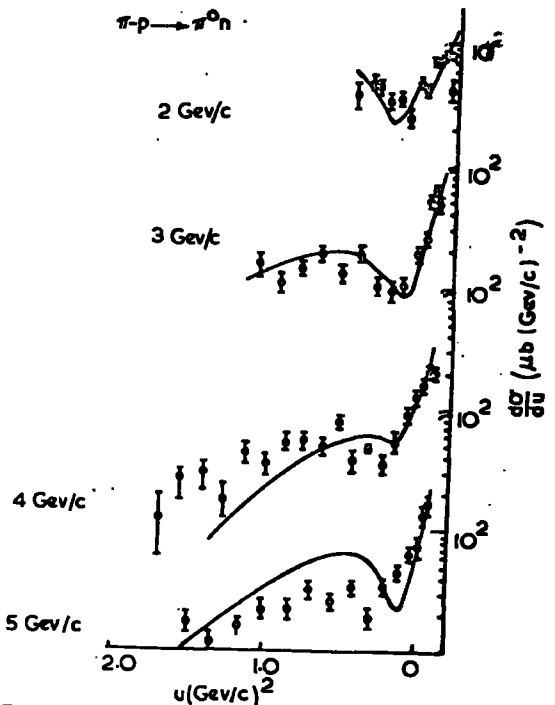

Fig. 9c.

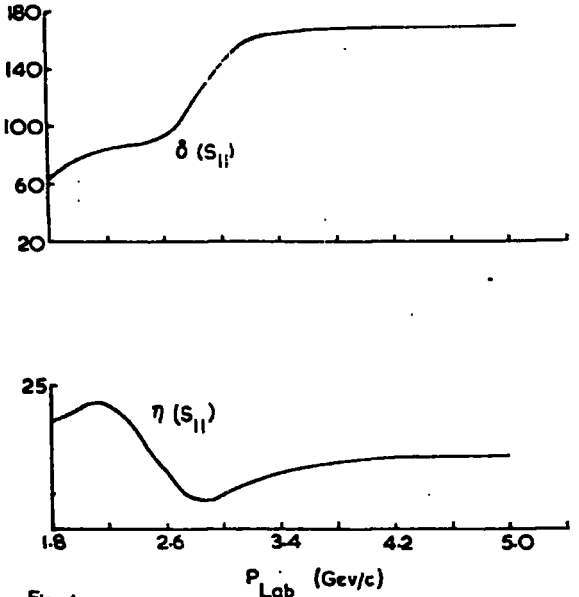

Fig 1aa.

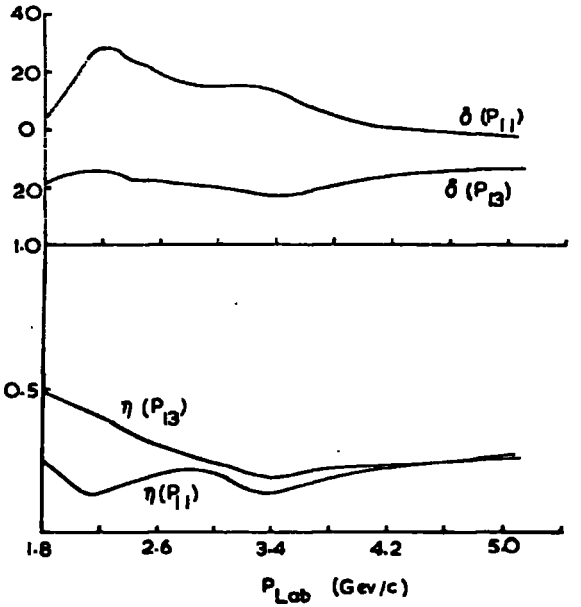

Fig. 1ab.

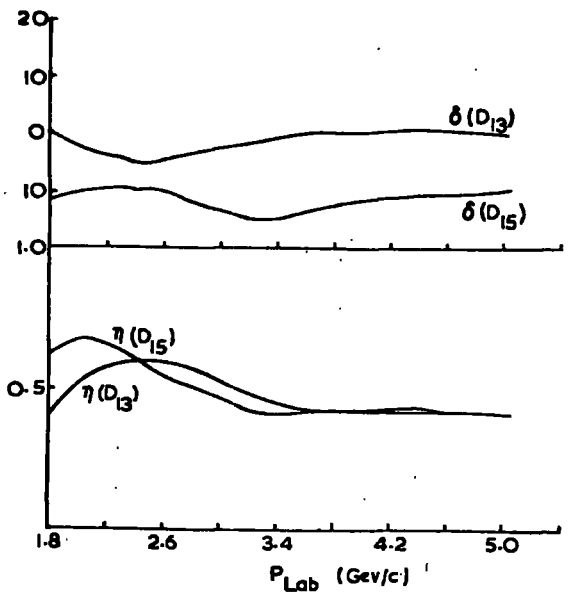

Fig. 1ac.

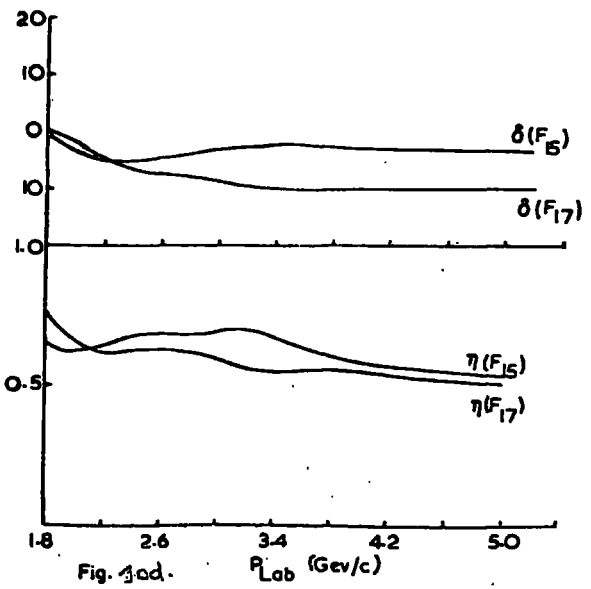

Fig. 1ad.

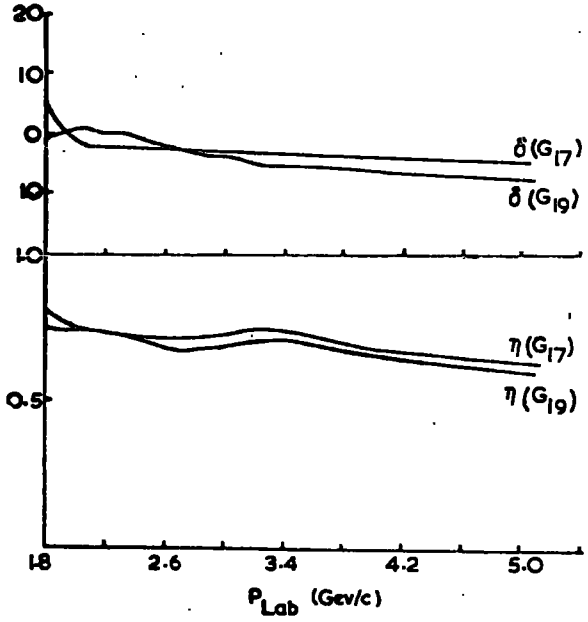

Fig. 10e.

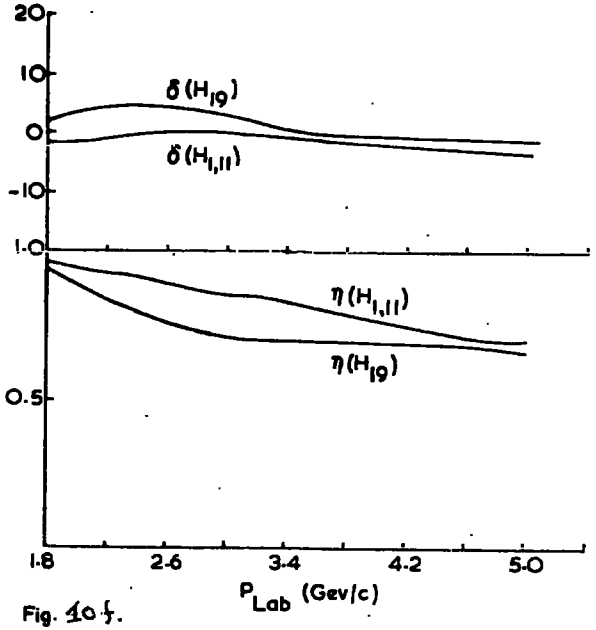

Fig. 10f.

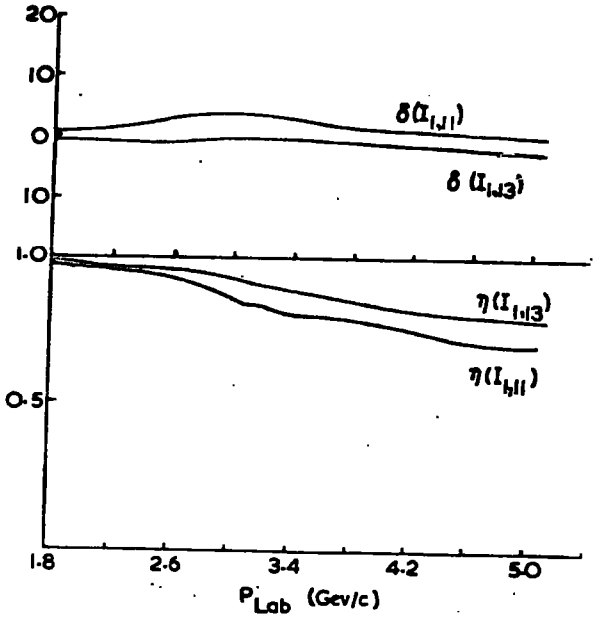

Fig. 10g.